Dissertations   Theses and Dissertations

2013

A Study of the Therapeutic Potential of AF4 Mimetic Peptides

Nisha N. Barretto
Loyola University Chicago, nibarretto@lumc.edu

LOYOLA UNIVERSITY CHICAGO

A STUDY OF THE THERAPEUTIC POTENTIAL OF AF4 MIMETIC PEPTIDES

A DISSERTATION SUBMITTED TO

THE FACULTY OF THE GRADUATE SCHOOL

IN CANDIDACY FOR THE DEGREE OF

DOCTOR OF PHILOSOPHY

MOLECULAR AND CELLULAR BIOCHEMISTRY PROGRAM

BY

NISHA BARRETTO

CHICAGO, IL

DECEMBER 2013

ACKNOWLEDGEMENTS

I would like to thank everyone who supported me through my graduate career. I am very grateful to Dr. Charles Hemenway for being a great mentor. His consistent optimism and encouragement helped me progress through the many challenges of my graduate study. I thank him for teaching me how to be patient and persistent to succeed in science. I also like to thank all the members of my committee: Nancy Zeleznik-Le Ph.D., Caroline Le Poole Ph.D., Claudia Osipo Ph.D., and William Simmons Ph.D., for all their suggestions with my dissertation project and the help offered during the preparation of this manuscript.

I would like to acknowledge Dr Jiwang Zhang and Dewen You, for lending their expertise on xenograft establishment. Thank you to Patricia and Veronica in the FACS core for the guidance with the flow cytometry experiments. Next, I would like to thank the members of the Hemenway laboratory that I worked with over the years. Amanda Winters and Ming Chang, who welcomed me, taught me laboratory skills and helped me get started. It was also a pleasure to work with Bhavana Malik and the summer student Dean Karahalios. I would also like to thank all the members of the Gene Regulation and Epigenetics group at Loyola for providing a supportive environment and sharing ideas.

I would like to acknowledge the Loyola University Chicago Biomedical Sciences Graduate School and Cellular and Molecular Biochemisty Program for providing the opportunity to earn a doctorate degree. Also, I would like to thank Dr Simmons and Dr

To my family

TABLE OF CONTENTS

LIST OF FIGURES

LIST OF ABBREVIATIONS

ALL	Acute Lymphoid Leukemia
ALL1/MLL	*Mixed lineage leukemia gene*
AF4	*ALL1*-fused gene from chromosome 4
AF9	*ALL1*-fused gene from chromosome 9
ANC-1	Actin non complementing-1
AML	Acute Myeloid Leukemia
7AAD	7-Aminoactinomycin D dye
BCoR	BCL-associated co-repressor
Brd4	Bromodomain 4
COX-1V	Cytochrome oxidase IV
DOT1	Disruptor of Telomerase-1
DMSO	Dimethyl sulphoxide
EGFP	Enhanced Green fluorescent protein
ENaCα	Epithelial Sodium channel subunit α
ENL	Eleven nineteen leukemia protein
ELL	Eleven nineteen Lysine-Rich Leukemia protein
F-actin	Filamentous actin (polymerized form)
G-actin	Globular actin (monomeric form)

HAT	histone acetyltransferase
HDAC	histone deacetylase
HMT	histone methyltransferase
HIV-LTR	HIV Long terminal repeats
HSC	Hematopoietic Stem Cell
H3	Histone 3
H3K4	Histone 3 Lysine 4
me	methylation
MLL^N	Mixed lineage leukemia N terminus
MLL^C	Mixed lineage leukemia C terminus
MLL-AF9	MLL fused to AF9
MLL-AF4	MLL fused to AF4
MLL-ENL	MLL fused to ENL
WT MLL	Wild type MLL
NAcGlu	N acetylglucosamine
PcG	Polycomb Group
PFWT	Peptide FMR2 wild type
PHD	Plant homeodomain
PTEFb	Positive transcriptional elongation factor b
PTD	Partial Tandem duplication
RPB1	RNA polymerase binding protein 1
SEC	Super elongation complex

sh	Small hairpin
TAD	Transcriptional activation domain
Tat	Transactivator of transcription protien
UB	Ubiquitin
WGA	Wheat germ agglutinin

ABSTRACT

Mixed lineage leukemias (MLL) are a group of acute and aggressive leukemias. They account for over 70% of infant leukemias, and 10% of acute adult leukemias. Pediatric ALL and therapy related MLL leukemias carry poor prognosis in spite of several advancement in the field of leukemia research. Therefore, new therapies for MLL leukemias are needed.

Majority of MLL leukemias arise due to the balanced translocations of the *MLL* gene. As a result of these translocations, chimeric MLL fusion proteins are expressed. The most frequently occurring MLL fusion proteins are known to aberrantly recruit the super elongation complex (SEC) resulting in constitutive transcription of genes that promote the development of leukemia. Hence, our strategy is to target the SEC as a means of inhibiting MLL leukemia. AF4 and AF9 proteins co-purify with components of the SEC and directly interact with each other. Our laboratory has previously identified the domain of AF4 which is required for AF9 interaction and demonstrated that inhibition of this interaction using an AF4 mimetic peptide results in decreased viability of leukemia cell lines expressing MLL fusion genes. The AF4 mimetic peptide was modified to improve its *in vivo* stability and the newly designed peptide was designated SPK111.

Here, we demonstrate that SPK111 peptide inhibits the AF4-AF9 interaction and reduces the activity of the SEC using luciferase reporter assays. Further, we show that

SPK111 selectively reduces the viability of MLL leukemic cells *in vitro*. It induces membrane permeability and necrotic cell death. In order to test the *in vivo* efficacy of SPK111, we generated mice xenografts of MOLM13 and KOPN8 MLL leukemia cells. We observed a trend toward prolonged survival of xenografted mice following SPK111 treatment. However, the increased survival of treated mice did not reach statistical significance. A larger dose or dosing at an earlier point in time during disease progression had little effect on survival. Although it was difficult to achieve efficacy *in vivo*, pretreatment of leukemic cells with SPK111 prior to tail vein injection effectively inhibited xenograft establishment. This suggests that SPK111 is effective on leukemia initiating cells and may be developed as an effective bone marrow purging agent. We also developed an ELISA for detection of serum SPK111 which can be used for future kinetic studies.

PFWT is an AF4 mimetic peptide similar to SPK111. Previous studies suggest that PFWT perturbs the actin cytoskeleton which is likely to induce cell death. However our investigations show that PFWT does not adversely affect the filamentous actin content of leukemic cells. Moreover, pretreatment with actin stabilizing drugs does not protect against PFWT induced cell death. An apparent 10 kDa increase in the molecular weight of the AF9 protein was identified on exposure to PFWT. Our analysis of probable post-translational modifications shows the absence of O-glycosylation and monoubiqutination. Interestingly, multiple phosphorylation sites and an acetylation site of AF9 were identified using mass spectroscopy.

Our studies on the AF4 mimetic peptide, suggest that inhibition of the AF4-AF9 protein-protein interaction serves as an effective therapy for MLL leukemias.

CHAPTER 1

AN INTRODUCTION TO MIXED LINEAGE LEUKEMIA

Mixed lineage leukemias (MLL) are an aggressive subset of hematological malignancies. They are characterized by translocations of chromosome 11 band q23 and involve the *MLL* gene (Ziemin-van der Poel et al., 1991). These translocations are balanced and result in an in-frame fusion of the *MLL* gene to one of over 70 different genes. The expressed chimeric MLL fusion proteins give rise to acute leukemia. The name "Mixed lineage leukemia" derives from the observation that these leukemic cells express cell surface markers of lymphoid origin, or myeloid origin, or both. (Chowdhury and Brady, 2008). Figure 1 explains the distinct hematopoietic lineages and the subsequent differentiated cells that arise from hematopoietic stem cells. The dual phenotype of MLL leukemias suggest that *MLL* translocations transform early hematopoietic precursors or reprogram cells to a more pluripotent state.

MLL leukemias represent approximately 5-10% of all leukemias, and are found in patients of all ages. However, *MLL* rearrangements are especially common in infants less than one year of age. About 70% - 80% of all infant acute lymphoid leukemia (ALL) cases and 30-35% of infant acute myeloid leukemia (AML) cases are diagnosed with MLL translocations (Krivtsov and Armstrong, 2007). The presence of *MLL* rearrangements in infant ALL is associated with a poor prognosis, while its presence in infant AML has an intermediate prognosis (Mohan et al., 2010b). Event-free survival of

infants with leukemia carrying *MLL* translocation after conventional therapy and hematopoietic stem cell transplant is less than 50% compared to greater than 80% survival of infant leukemia cases that lack the translocation (Biondi et al., 2000; Mann et al., 2010)

Another group of leukemias in which MLL translocations arise is therapy-related leukemias. They arise as a secondary condition in patients treated with topoisomerase II inhibitors, such as etoposide and daunorubicin, for unrelated malignancies such as breast, ovarian, and lung cancers (Andersen et al., 2001; Chowdhury and Brady, 2008; Super et al., 1993). They arise within 6-24 months post exposure to the inhibitors and most commonly are of the myeloid phenotype. Like infant ALL, these leukemias respond poorly to conventional therapies (Andersen et al., 2001; Felix, 1998; Super et al., 1993).

In addition, MLL leukemia also results from partial tandem duplication (PTD) of exons 5-12 within the *MLL* gene. As a result, an extra amino-terminus is added in frame to the full length MLL (Strout et al., 1998). These cases generally occur in adult or older patients and are associated with early relapse of the disease following initial remission on treatment. The gene expression pattern for PTD-carrying MLL leukemias are different compared to MLL fusion induced leukemia which suggests different molecular mechanisms may exist for this disease (Ross et al., 2004).

Significant advances have improved the overall prognosis of leukemia patients. However, in spite of the advances, MLL leukemia often has a poor prognosis and a high relapse rate. Hence, new targeted therapies need to be developed for this group of leukemias. In this thesis we explore one possible targeted therapy.
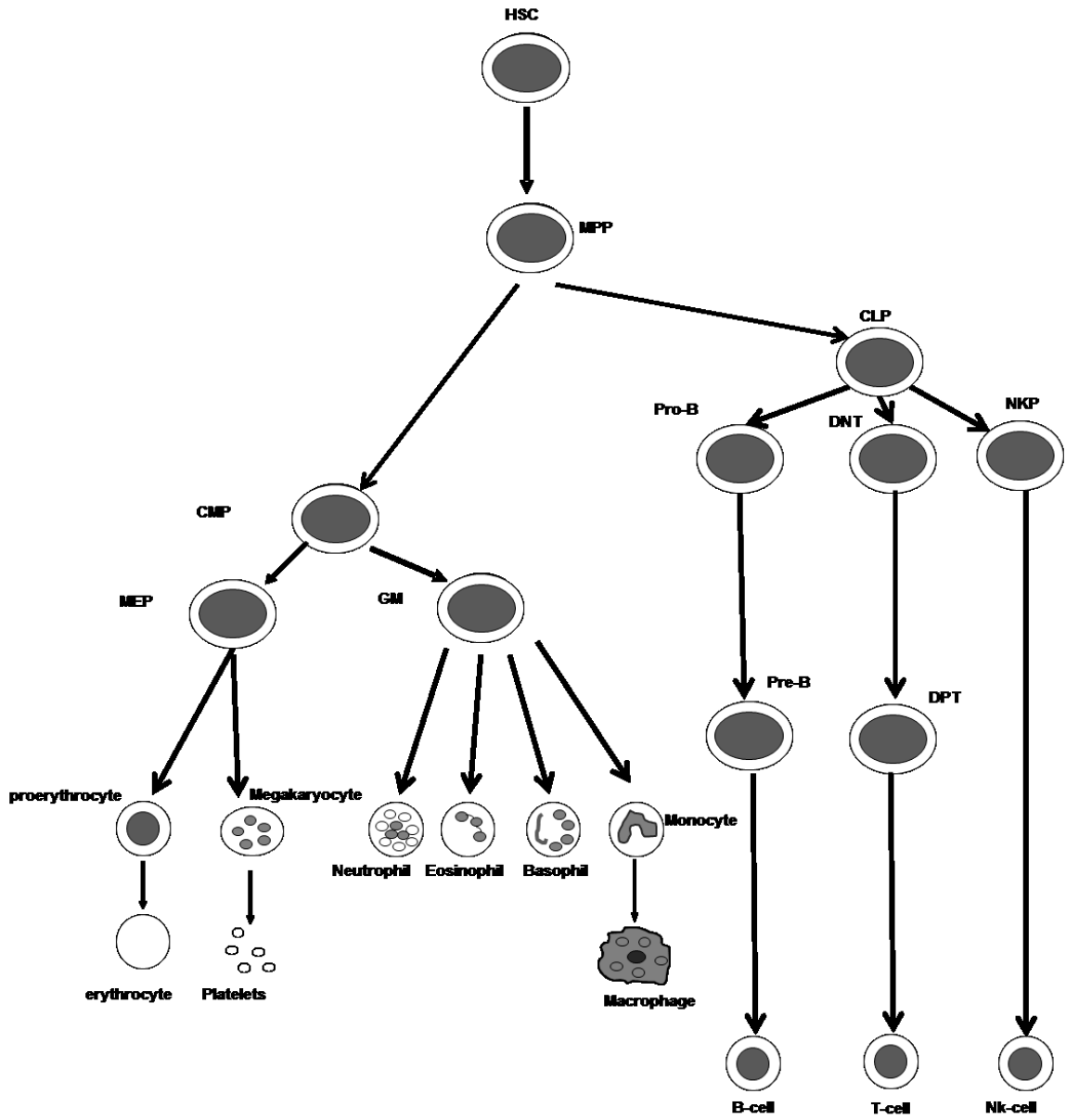
Figure 1 A schematic of hematopoiesis

HSC: Hematopoietic Stem Cells give rise to multipotent progenitor (MPP) that further branches into two lineage precursors, Common Myeloid Progenitor (CMP), and Common Lymphoid Progenitor (CLP). From the CLP, arise the B cell, the T cell and the Natural Killer NK cells. On the other hand, the CMP give rise to the Granulocyte myeloid precursors (GMP) and the myeloid erythroid precursor (MEP). GMP gives rise to macrophages and to granulocytes which include neutrophils, eosinophils and basophils. MEP differentiates into pro-erythrocytes and megakaryocytes. Terminal differentiation of pro-erythrocytes gives rise to red blood cells, and megakaryocytes give rise to platelets.

Finally, the common MLL fusion partners AF4 and AF9, epigenetic regulators and non-coding RNAs that play a role in MLL leukemias and which can be used for therapeutic targeting are introduced.

MLL

A Multidomain protein

The *MLL* gene at the chromosome locus 11q23 was identified due to its role in acute leukemias. It codes for a multi domain, 500kD protein that is 3969 amino acids in length. A schematic of its domain structure is shown in Figure 2. It is post-translationally cleaved by a threonine aspartase, Taspase1, into a 320 kD N-terminal fragment (MLL^N) and a 180kD C-terminal fragment (MLL^C) (Hsieh et al., 2003a; Hsieh et al., 2003b). The MLL^N and MLL^C fragments interact with each other via the hydrophobic residues of phenylalanine and tyrosine rich N-terminal domain (FYRN domain) and a phenylalanine and tyrosine rich C-terminal domain (FYRC domain) to give rise to a stable, functional holoenzyme that catalyzes Histone 3 Lysine4 (H3K4) methylation (Hsieh et al., 2003b; Yokoyama et al., 2011). The MLL holoenzyme localizes to the nucleus and is known to regulate the expression of *HOX* genes, among others.

At the extreme amino-terminus of the MLL^N fragment is the Menin Binding Domain (MBD). Menin functions as an adaptor and mediates the interaction of MLL with Lens Epithelium Derived Growth Factor (LEDGF) and c-Myb (Jin et al., 2010; Yokoyama and Cleary, 2008; Yokoyama et al., 2005; Yokoyama et al., 2004). LEDGF is a transcriptional co-activator, whose DNA binding domain helps mediate the binding of

MLL to DNA. c-Myb is a transcription factor belonging to the MYB family of oncogenic proteins and plays a significant role in hematopoietic regulation (Emambokus et al., 2003). *Myb* null mice die due to failure of fetal liver hematopoiesis (Mucenski et al., 1991). A distinct concentration range of c-Myb is required at every stage of hematopoiesis (Emambokus et al., 2003). Importantly, c-Myb is shown to recruit MLL to the Interleukin-13 gene locus, promoting its expression during the differentiation of memory T helper type 2 cells (Kozuka et al., 2011).

Three AT hook binding sequences are found downstream of MBD. These hooks bind to the minor groove of AT- rich DNA, giving preference to structural features over precise nucleotide sequences for DNA binding (Broeker et al., 1996). The speckled nuclear localization sequences SNL1 and SNL2 are next to the AT hooks. They direct MLL to the nucleus and cause its accumulation in distinct punctate structures which can be detected by immunofluorescence (Butler et al., 1997).

The location of breakpoints within the *MLL* gene at which translocations occur is limited to an 8.3 kb region, referred to as the breakpoint cluster region (bcr). This bcr divides the activator and repressor recruiting sequences within MLL. The repression domains one and two, are designated as RD1 and RD2, N-terminal of the bcr. Meanwhile, the atypical Bromo-domain and the transcriptional activation domain (TAD) lie toward the C- terminal and recruit co-activators.

RD1 and RD2 interact directly with histone deacetylases, polycomb group proteins, and the co-repressor C-terminal-binding protein (CTBP) (Xia et al., 2003). Paradoxically, the repression domain also facilitates the continued expression of the MLL

target genes. The cysteine rich CXXC domain within the RD1 region binds to non-methylated CpGs, and confers protection against methylation that can otherwise result in silencing (Ayton et al., 2004; Cierpicki et al., 2010; Erfurth et al., 2008). The CXXC-RD2 region binds to the polymerase-associated factor C (PAFc), which is involved in transcription initiation. This region is conserved in MLL fusions, and the association of PAFc with MLL fusion proteins has been shown to be important for leukemogenesis (Muntean et al., 2010). An open chromatin structure is facilitated by the binding of the atypical bromodomains to acetylated histone lysines, while the TAD binds to the transcriptional co-activators like Cyclic AMP-responsive element-binding protein (CREB) to promote transactivation (Jeanmougin et al., 1997), (Ernst et al., 2001). Thus, MLL functions as a dynamic hub that recruits both activator and repressor complexes.

A striking feature of MLL is that it can recognize and catalyze the histone three lysine four (H3K4) methylation mark. These recognition and catalytic domains are located in separate MLL fragments. The catalytic methyl transferase activity of MLL resides in the Su(var)3-9,enhancer of zeste, trithorax (SET) domain found in the MLL^C fragment (Milne et al., 2002). This domain is highly conserved among yeast, D*rosophil*a, and mammals, and mono-, di-, and trimethylates H3K4. The core MLL H3K4 methylating complex as illustrated in Figure 3 includes MLL, Retinoblastoma binding protein 5 (RBP5), absent small or homeotic like Drosophilla (ASH2), and WD repeat containing protein 5 (WDR5) (Dou et al., 2006). WDR5 is a chromo-domain containing protein that binds to the H3K4 methylation marks. The methylation model proposed by Dou *et al* and Wysocka *et a*l suggests that WDR5 recruits the MLL complex to the
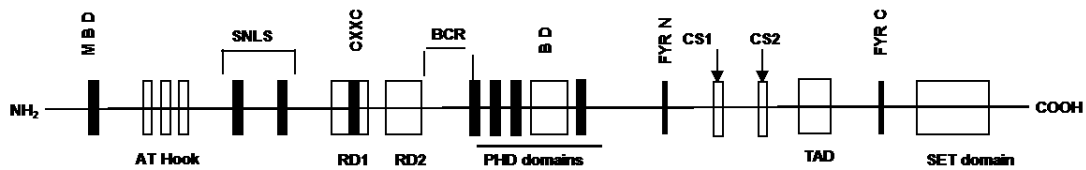
Figure 2 Domain structure of the MLL protein

The domains found in MLL from the N-terminus to the C-terminus: the Menin-Binding Domain (MBD); the AT hooks ; Speckled Nuclear Localization Signals (SNLS); Repression Domains (RD), with the CxxC domain boxed in black; Plant-homeo-domain (PHD), separated by the BromoDomain (BD); Transcriptional Activation Domain (TAD); and the H3K4 methyltransferase activity containing SET domain. Taspase-1 Cleavage Sites (CS1 and CS2), and FYRN and FYRC motifs, and Breakpoint Cluster Region (BCR) of the gene are also shown.

H3K4me2 mark allowing progression to trimethylation and promoting MLL catalyzed dimethylation on adjacent nucleosomes (Dou et al., 2006; Wysocka et al., 2005). RBP5 stabilizes the MLL core complex while both RBP5 and ASH2L participate in catalytic action performed by MLL (Cao et al., 2010).

The Plant homeo domain three (PHD3) found in the MLL^N fragment is the recognition domain. It binds to the H3K4me2 and the H3K4me3 marks and promotes gene transcription (Chang et al., 2010b). PHD3 also binds to the cyclophilin CYP33, which in turn recruits repressors to the MLL target gene. Mutually exclusive binding of PHD3 to H3K4me3 and CYP33 helps switch between activation and repression of MLL-bound genes (Chen et al., 2008a; Park et al., 2010). Overall, MLL contains four plant homeo-domain fingers named numerically in order of occurrence from the N-terminus. An isoform of the MLL^N fragment has a partial deletion of the PHD1 domain due to which it fails to interact with MLL^C and is promptly degraded. Hence, in addition to FYRN and FYRC, the MLL PHD fingers also stabilize the MLL holoenzyme (Yokoyama et al., 2011).

Biological role of MLL

MLL is known to play a role in hematopoiesis. It maintains the normal number of progenitors and is not present in differentiated lymphoid and myeloid cells (Jude et al., 2007). Inducible inactivation of *Mll* in adult mice leads to bone marrow failure. *Mll*-null hematopoietic stem cells also fail to reconstitute the hematopoietic system of syngenic lethally irradiated mice. Further investigation revealed that loss of *Mll* propels the

progenitor cells to proliferate and differentiate without replenishing the pool of quiescent stem cells, which eventually leads to bone marrow failure. Similar to the adult hematopoiesis, *in vitro* assays using *Mll* homozygous and heterozygous null cells derived from the mouse embryo yolk sacs fail to maintain embryonic hematopoietic progenitors (Yu et al., 1995).

Mll is required for proper axioskeletal, cranial, and neuronal development during embryogenesis. Deletion of exon 3b results in the loss of *MLL* expression in mutant mice. Homozygous deletion leads to death by embryonic day 10.5-11.5. The heterozygous mutants show homeotic transformation of the skeleton. Knockdown of the *Hoxa* gene cluster displayed similar developmental defects which lead to the identification of Mll as a regulator of the *Hoxa* gene cluster (Yu et al., 1998; Yu et al., 1995).

Mll maintains the temporal expression of the *Hoxa* gene cluster for segmental development. For instance, Mll is not required for the initial expression of the *Hoxa7* gene, but is required to maintain its expression beyond embryonic day 9 (Yu et al., 1998). *Hox* gene expression is repressed by the Polycomb group of proteins, while Trithorax proteins activate their expression. Simultaneous deletion of the mammalian Trithorax ortholog, *Mll* and the Polycomb gene, *Bmi-1* in mice counterbalance each other. *Bmi* deletion in *Mll* null has been shown to restore the expression of *Hoxc8* and abrogate the axioskeletal defects seen in *Mll* heterozygous null mice (Hanson et al., 1999).

The MLL protein interacts with several different proteins as illustrated in Figure 3. The functions arising from these interactions include cell cycle progression, DNA

damage response, differentiation, gene expression, chromatin regulation, and telomeric integrity.

Studies performed on Mll hypomorphic mice generated by mutating the Taspase-1 cleavage sites shows that Mll regulates the cell cycle via E2F (Takeda et al., 2006). E2Fs are the principal transcription factors that modulate cyclin expression and promote cell cycle progression. MLL, E2Fs, and G1 phase regulatory protein HCF-1 localize to cyclin promoters during G1/S phase, promoting H3K4 methylation and gene expression (Tyagi et al., 2007). MLL also positively regulates expression of the cell cycle inhibitor gene, *CDKN1B* (Milne et al., 2005b; Xia et al., 2005). Additionally, cell-cycle associated ubiquitin ligases, Skp, Cullin, F-box containing complex (SCF) and Anaphase-Promoting Complex (APC), ubiquitinate MLL leading to its degradation (Liu et al., 2007). Temporal degradation of MLL gives rise to peaks of maximal MLL expression during G1/S and G2/M phase, establishing a gradient of MLL concentration through the cell cycle. It is likely that MLL activates the E2Fs at low levels and the Cyclin dependent kinase 1 (CDKI) at high levels, thereby contributing to the regulation of the cell cycle (Liu et al., 2008). Regulation of MLL stability and activity by the cell cycle-associated protease machinery lays emphasis on the importance of the undulating MLL expression levels required for cell cycle progression.

During DNA damage responses (DDR), MLL is phosphorylated on serine 516 by the Ataxia Telangiectasia and Rad-3-related (ATR) protein. This phosphorylation results in MLL stabilization by abrogating its interaction with SCF ubiquitin ligase. The stabilized MLL results in H3K4me3 at the site of DNA damage. The methylated histone

MLL^N

C-myb
Menin
LEDGF
HDAC
BMI
PAFc
Cyp33
ASB2
HCF1

MBD

RD domains   PHD domains

MLL^C

TAD
SET

CBP
MOF

H3
RbBP5
Ash2L
WDR5
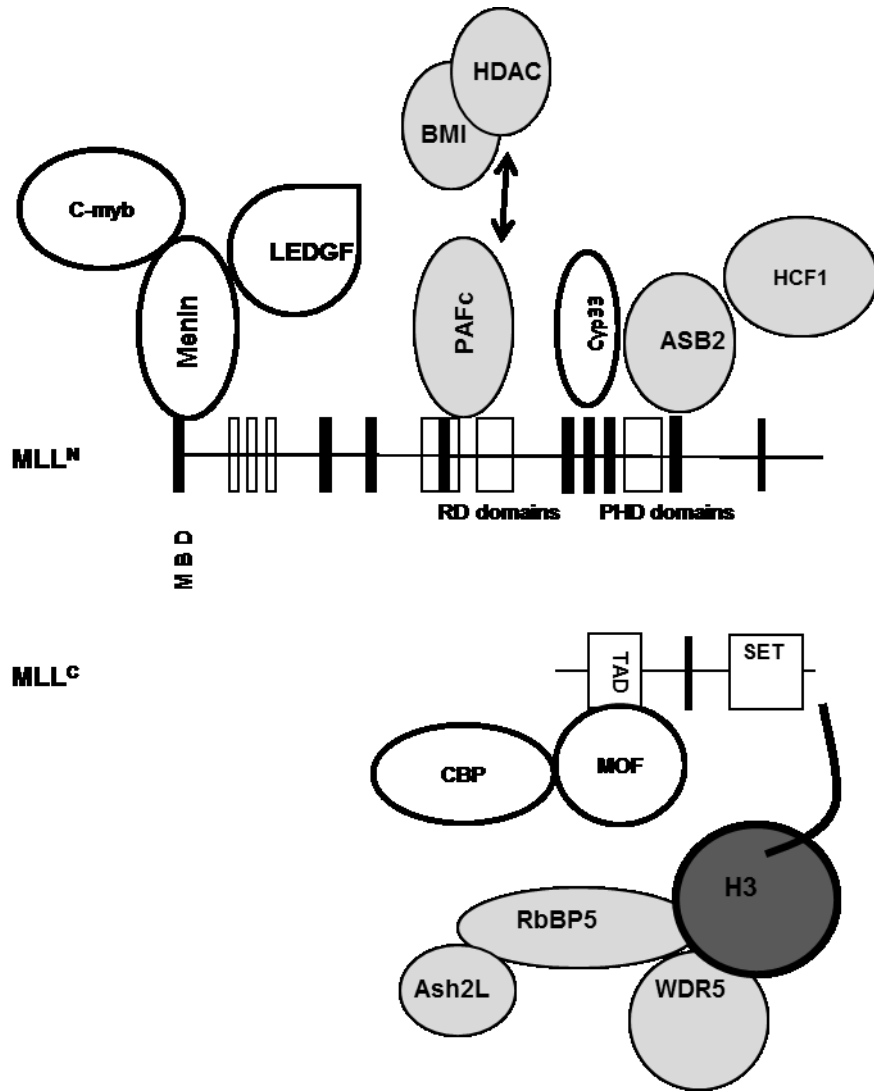
Figure 3   Schematic representation showing protein-protein interactions of MLL

The Menin binding domain (MBD) binds Menin, Lens Epithelium Derived Growth Factor (LEDGF) and C-myb. Transcription associated Polymerase Associated Factor c (PAFc) or Histone deacetylases (HDAC) and BMI interacts with the Repression Domain (RD) of MLL. Cyclophilin, (Cyp33), E3 ubiquitin ligase ASB2, and Host cell factor one (HCF1) bind to the PHD domains. The SET domain interacts with histone H3, WD-40 repeat containing protein-5 (WDR5) which complexes with Retinoblastoma Binding Protein-5 (RbBP5) and Absent small homeotic disc-2 Like (Ash2L). The transcriptional activation domain of MLL^{C} terminus binds CREB Binding Protein (CBP) and histone acetyltransferase MOF.

reduces the binding affinity of CDC45, a protein essential for DNA fork assembly. Hence, it delays the replication of damaged DNA loci, allowing time for DNA repair (Liu et al., 2010). Cells that abrogate the ATR dependent DDR fail to reduce the rate of DNA replication after exposure to ionizing radiation. This replication is known as Radio Resistant DNA synthesis (RDS). *Mll*-null fibroblasts exhibit RDS which can be rescued by *Mll* re-expression.

MLL is required to maintain the hematopoietic progenitor population; however, its role in hematopoietic differentiation is not characterized. More recently, Ankyrin repeat and SOCS box protein 2 (ASB2), an E3 ubiquitin ligase, was found to interact with MLL via the PHD fingers and the bromo domain. ASB2 is upregulated during All Trans Retinoic Acid (ATRA) induced differentiation therapy, and its increased levels correlate with myeloid differentiation and a decrease in MLL protein levels. Conversely, knockdown of ASB2 in murine leukemic cell lines leads to delayed differentiation after ATRA treatment (Wang et al., 2012a). Interestingly, PHD2 itself exhibits E3 ubiquitin ligase activity in the presence of CDC34, a cell cycle associated E2 ubiquitin ligase. The *in vivo* bonafide substrates for this enzymatic activity are not yet identified (Wang et al., 2012b).

MLL-associated chromatin regulation involves methylation and acetylation of histone three. The SET domain of MLL is known to specifically di- and tri-methylate H3K4. These methylation marks are associated with an open chromatin state permitting active transcription (Milne et al., 2002). In addition, the MLL^C terminus also recruits histone acetylases such as Males absent on the first (MOF) and CREB binding protein

complex (p300/CBP). H3K16 acetylation by MOF is required for active transcription of a subset of MLL target genes like *HOXA9* (Dou et al., 2005).

RNA polymerase II, H3K4me3, and MLL co-occupy promoters of more than 5000 genes in cultured lymphoblast and leukemic cells, suggesting a genome-wide regulatory role (Guenther et al., 2005). However, the *Hoxa* cluster of genes is a known target of MLL. This cluster has MLL distributed across extensive regions of the transcribed genes, unlike the 5' proximal binding profile at other genes. This finding suggests that the mechanism of gene regulation by MLL at the *Hoxa* cluster genes differs from other genes (Guenther et al., 2005). *Mll*-null fibroblasts have RNA polymerase II paused at the promoter sites of *Hoxa9*. Re-expression of Mll in these cells leads to a redistribution of RNA polymerase II across the transcribed unit. This suggests that Mll is associated with the process of transcriptional elongation at the *Hoxa* cluster of genes (Milne et al., 2005a). The mechanism of MLL regulation of genes by only 5' proximal binding is not known.

MLL is also known to bind with transcription factors such as MAX, E2F, and p53 and promotes gene expression (Dou et al., 2005). For example, a subset of p53 target genes recruits a complex of MLL, p53 and histone acetyl tranferase MOF-MSL1v1 for gene activation (Li et al., 2009).

In human fibroblasts, MLL directly binds p53 and complexes with Shelterins, a group of proteins that maintain telomeric stability. The MLL-p53 complex at the telomeres promotes H3K4 methylation and RNA polymerase II-dependent transcription of the telomeres, thus promoting telomeric integrity. Conversely, MLL knockdown in

fibroblasts is known to result in loss of telomeric integrity and induction of senescence (Caslini et al., 2009).

Mechanisms of oncogenic transformation by MLL fusions
Loss of function mechanisms

As previously described, MLL is phosphorylated by ATR in response to DDR and causes delay of replication fork assembly. However, the MLL fusions can function in a dominant negative manner, inhibiting the localization of WT MLL at DNA damage sites and thus abrogating phosphorylation of wild type MLL. The fusion protein itself is phosphorylated but it does not prevent the assembly of a replication fork at the damaged loci, leading to abrogation of the MLL dependent DDR (Liu et al., 2010). Studies performed on an inducible mouse model of *MLL-ENL* suggest that induction of the fusion causes a myeloproliferative disorder, in which DDR is activated. Positive selection of clones that can override the DDR lead to the establishment of leukemia (Takacova et al., 2012). Hence, abrogation of the DDR pathway by MLL fusions promotes leukemogenesis.

Cyclophilin 33 (Cyp33) is a peptidyl-prolyl cis-trans isomerase that isomerizes a proline in the PHD3-bromodomain linker region of MLL. The isomerization reaction increases the binding affinity of the MLL for Cyp33 (Wang et al., 2010). As mentioned earlier, Cyp33 further recruits repressors such as histone deacetylases promoting repression. *Cyp33* overexpression is known to repress MLL target genes such as *HOXC8, HOXA9 and C-MYC* (Park et al., 2010). These genes play a role in sustaining

leukemogenesis. Furthermore, it has been demonstrated that an inclusion of the PHD3 domain in the MLL-ENL fusion inhibits its immortalization capacity (Chen et al., 2008a). Similar to MLL-ENL, inclusion of PHD2 and PHD3 in MLL-AF9 diminishes its transformation capacity (Muntean et al., 2008). Hence, loss of PHD3 domain is necessary for leukemic transformation by MLL fusions.

As mentioned earlier, during ATRA-mediated differentiation of the myeloid cells, there is an upregulation of ASB2, an ubiquitin ligase that degrades MLL. This ligase binds MLL via the PHD-bromo-domain which is lost in the MLL fusions (Wang et al., 2012a). Therefore, MLL fusion proteins are less likely to degrade during differentiation. Moreover, unlike WT MLL, MLL fusion proteins do not show a biphasic rise and fall of protein levels during cell cycle progression (Liu et al., 2008). The increased stability of the MLL fusion proteins may contribute to leukemogenesis by cell cycle deregulation.

Gain of function mechanisms

Both nuclear proteins with transactivation capacity and cytoplasmic proteins with coil-coil domains that impart dimerization properties are found as MLL fusion partners. A singular model that explains the disease-causing potential of multiple types of MLL fusion proteins has been difficult to construct because the N-terminus of MLL, which is common to all fusions, has been shown to be insufficient for transformation (Dobson et al., 2000; Slany et al., 1998).

For the cytoplasmic fusion partners and MLL-PTD, a dimerization domain is considered crucial. In order to determine the potential of the dimerization domain, an artificial Mll fusion construct was generated by fusing the first eight exons of *Mll* to *lacZ*. LacZ was chosen as it has dimerization domains and is likely to permit the dimerization of MLL-LacZ fusion protein. The fusion was able to generate leukemia in mice, although it occurred at a lower frequency and with a longer latency (Dobson et al., 2000). In another study, it was shown that an artificial construct of MLL that can be induced to dimerize pharmacologically inhibits myeloid differentiation and upregulates MLL leukemia signature genes. Moreover, the dimerized MLL fusion binds with higher affinity to the *Hoxa9* promoter compared to wild type MLL (Martin et al., 2003). Studies show that dimerization contributes to MLL fusion-mediated leukemias in the case of cytoplasmic fusion genes such as the *AF6, GEPHYRIN, AF1p and GAS7* (So et al., 2003).

Leukemias which express nuclear proteins such as ENL, AF9, AF4, and ELL, as MLL fusion partners, account for 80-90% of all MLL leukemias (Meyer et al., 2009). Most of these proteins participate in the process of transcriptional elongation. Certain developmentally regulated genes carry both H3K4me2 and H3K27me3 marks. On these bivalent marked genes, the RNA polymerase II is known to stall after the transcription of the first 50-100 nucleotides. Further processing requires the recruitment of super elongation complex (SEC) proteins, which include positive transcriptional elongation factor b kinase (PTEFb), AF9, ENL, AF4 or AF5, and ELL (Biswas et al., 2011; Lin et al., 2010b). The recruited PTEFb kinase phosphorylates the largest subunit of RNA

polymerase II on serine 2 and permits further transcription of these genes (Peterlin and Price, 2006). A frequent fusion of MLL to the components of the SEC suggests that this step is deregulated in MLL leukemias. Consequently, a generally accepted model of MLL leukemogenesis states that the MLL fusion protein permits aberrant transcriptional elongation of MLL target genes like *HOXA9* and *MEIS1* that are required to sustain leukemogenesis. This makes the SEC an attractive target for MLL therapy. In this dissertation we inhibit the interaction between the two proteins AF4 and AF9, found within this complex and determine its effect on leukemogenesis. This model is further explained in Figure 4 and 5.
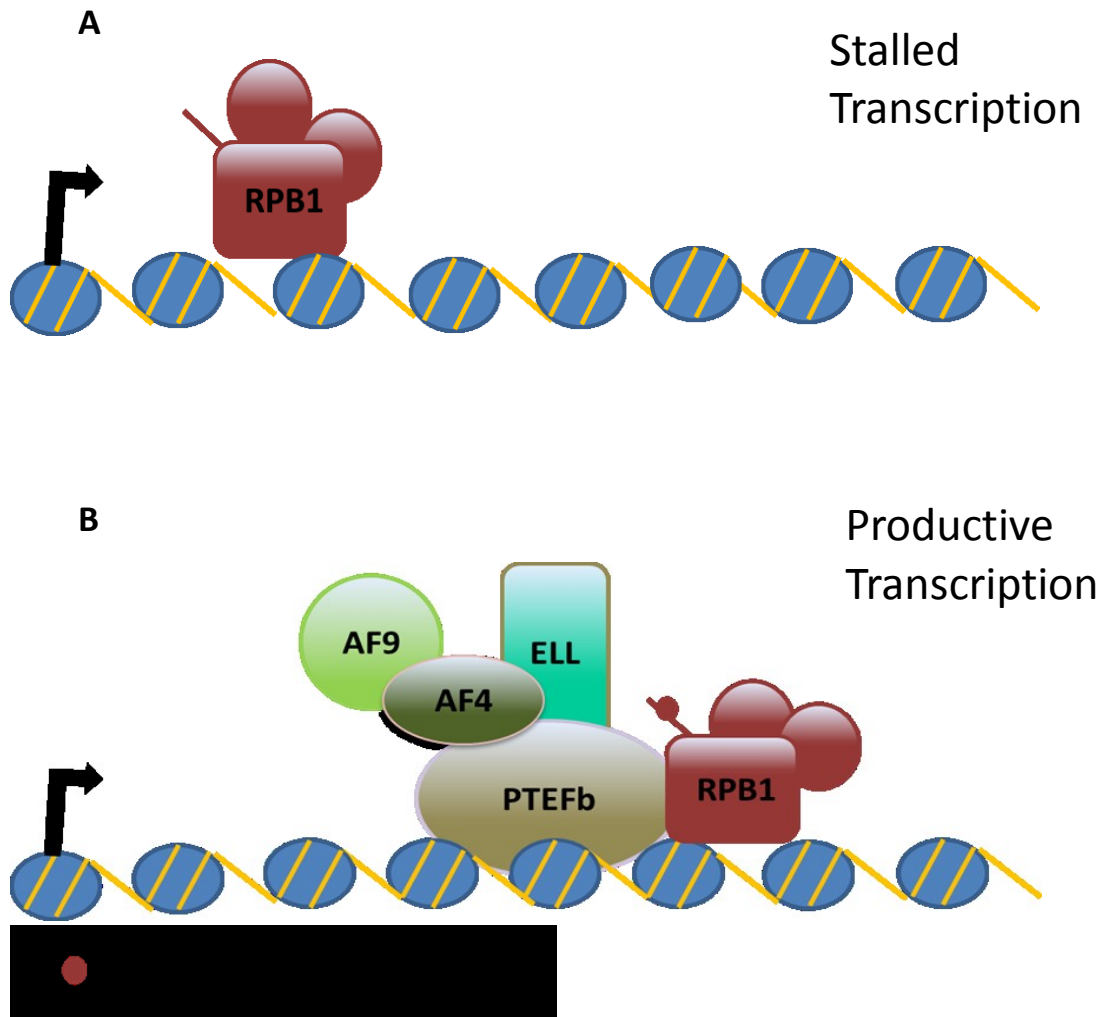
Figure 4 An illustration of transcriptional elongation

A) RNA polymerase II represented by its largest subunit RPB1 is stalled a few base pairs downstream from its transcriptional start site.

B) AF4, AF9, ELL, and PTEFb are components of the super elongation complex, which is recruited to the stalled RNA polymerase II. This recruitment leads to phosphorylation of RPB1 on serine 2 and permits productive elongation.
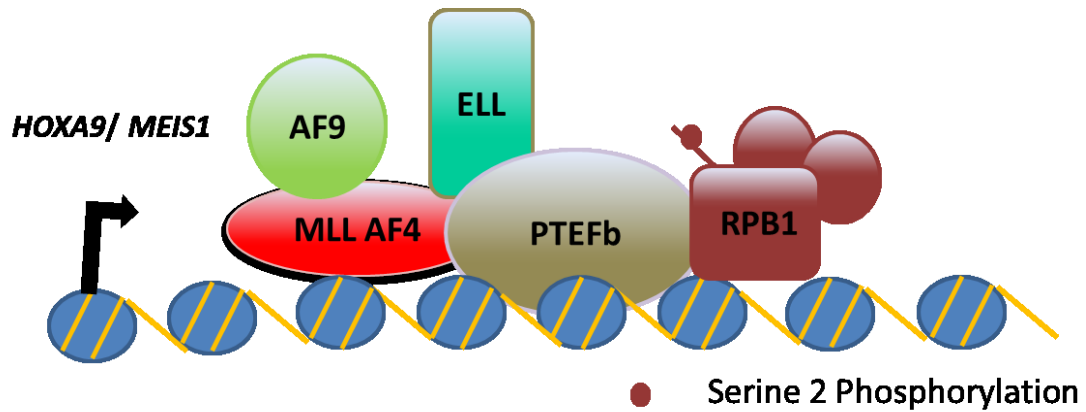
Figure 5 Model for leukemogenesis by MLL fusion proteins

MLL fusion proteins aberrantly recruit the SEC by protein-protein interactions. The recruited complex permits the productive transcription of genes required to sustain leukemogenesis.

Gene deregulation in Mixed Lineage Leukemia

Differential expression of the *HOX* cluster of genes plays a central role in segmental specification during embryonic development and in hematopoiesis. Particularly, genes of the *HOXA* cluster and some genes of *HOXB* cluster are highly transcribed in hematopoietic precursors and their expression gradually decreases with increased differentiation. Hence, deregulated expression of these clusters may contribute to the development of leukemia (Argiropoulos and Humphries, 2007).

Much evidence exists that demonstrates increased expression of *HOXA9* and *HOXA7* in MLL rearranged leukemias. However, conflicting experimental data exists on the necessity of *HOXA9* expression for MLL leukemogenesis. Knockdown of *HOXA9* inhibits the growth of human MLL leukemia cell lines, whereas *MLL-AF9* knock-in animals develop leukemia in a *Hoxa9*-null background (Ayton and Cleary, 2003; Faber et al., 2009; Kumar et al., 2004). Again, loss of either *Hoxa9* or *Hoxa7* in murine hematopoietic stem cells was shown to significantly reduce transformation by *MLL-ENL*, and later it was demonstrated by the same laboratory that *Hoxa9* and *Hoxa7* are dispensable for transformation by *MLL-GAS7* (Ayton and Cleary, 2003; So et al., 2004*).* Furthermore, overexpression of *Hoxa9* was shown to transform mouse-derived primary bone marrow cells in combination with the protein Meis1. The transformed cells induce myeloid leukemia *in vivo*, which recapitulates several features of MLL fusion leukemias (Kroon et al., 1998)*.* Nevertheless, *HoxA9* is an established target of MLL fusions with increased expression in MLL leukemias (Faber et al., 2009).

HOX proteins require additional cofactors for efficient binding to their target genes. *PBX* and *MEIS1* are known cofactors of the HOX proteins (Sitwala et al., 2008). MEIS1 is the best studied cofactor of HOXA9. Expression analysis shows an upregulation of both *MEIS1* and *HOXA9* expression in MLL leukemias (Armstrong et al., 2002; Rozovskaia et al., 2001). Coexpression of these genes is also found in hematopoietic stem cells and early lineage progenitor cells (Hisa et al., 2004; Kawagoe et al., 1999; Lawrence et al., 1997). *Meis1* levels correlate inversely with the latency of the disease (Wong et al., 2007). As stated earlier, *in vitro* retroviral transduction of *Hox9* can transform primary bone marrow derived cells similar to an MLL fusion oncogene, however, these transformed cells exhibit a long latency for *in vivo* disease development. Coexpression of *Hoxa9* with *Meis1* dramatically reduces this latency and increases the penetrance of the disease (Kroon et al., 1998). Further, co-transduction of cells with *MLL* fusion genes and *Meis1* results in an increase in colony forming potential and decreases its differentiation potential. This suggests that Meis1 protein levels have a rate limiting role in MLL fusion-mediated leukemic progression (Wong et al., 2007).

Meis1 deletion mutations in mice showed that the Pbx interaction domain is required for transformation by MLL fusion genes (Wong et al., 2007). Hoxa9 has also been shown to require Pbx interaction for its immortalization potential (Schnabel et al., 2000). Moreover, *Pbx3* expression is upregulated in cells transformed by MLL fusion genes, and decreased expression of *Pbx2* or *Pbx3* substantially reduces transformation capacity of MLL fusion genes (Wong et al., 2007; Zeisig et al., 2004a). A more recent report suggests that coexpression of *Pbx3* and *Hoxa9* has a synergistic effect on leukemic

transformation of lineage-negative progenitor cells derived from mouse bone marrow (Li et al., 2013).

HOXA9, HOXA7, HOXA10 and *MEIS1* upregulation is consistently detected in *MLL*-rearranged leukemias (Armstrong et al., 2002; Rozovskaia et al., 2003; Yeoh et al., 2002). Further, profiling data of AML and ALL patient samples determined a common signature expression profile for MLL leukemias irrespective of the lineage. (Ross et al., 2004). Hence, MLL leukemias can be distinguished based on gene expression profiles compared to leukemias lacking *MLL* translocations.

In another study, a myeloid cell line that is dependent on MLL-ENL expression was established using a Tet inducible system. Induced loss of MLL-ENL led to a decrease in expression of a subset of the *Hoxa* cluster genes. This expression pattern was established as the "Hox code" consisting of genes from *Hoxa4* to *Hoxa11* that are expressed in transformed hematopoietic cells (Horton et al., 2005).

The transcription profile of MLL leukemias resembles embryonic stem cells (ESC) rather than hematopoietic stem cells (HSC). Similar to MLL fusion genes ectopic expression of just three ES signature genes *Myb, Hmgb3*, and *Cbx5* is sufficient for immortalization of HSC (Somervaille et al., 2009). Eya1 and Six1 heterodimeric transcription factors that are important embryonic development were determined to be upregulated in MLL leukemias by expression profiling. Eya1 can immortalize hematopoietic progenitors and can augment Six1-mediated transformation (Wang et al., 2011).

Role of epigenetic enzymes in MLL leukemogenesis and targeted leukemic therapy

Epigenetic changes represent post-translational modifications of histones and chemical modifications of the DNA. They result in heritable states of gene expression without any changes to the DNA code. The epigenetic machinery consists of "writer" enzymes that add the modifications and "eraser" enzymes that remove the modifications. They also include "reader" proteins that can recognize these modifications, bind to them, and regulate transcription. Deregulated epigenetic control is a well-recognized feature of MLL leukemias. Additional epigenetic regulators that act in concert with MLL fusions provide avenues for therapeutic targeting and are discussed below.

Targeting DNA methylation in MLL leukemias

Hypermethylation of a cluster of CpG-rich sequences (also known as CpG islands) within the promoters of tumor supressor genes leads to repression and may promote oncogenesis (Klose and Bird, 2006). Differential methylation hybridization experiments have identified unique DNA methylation patterns in MLL-rearranged ALL. For instance, infant ALL derived samples carrying t(4;11) and t(11;19) showed extensive hypermethylation, and a high degree of promoter methylation in these samples positively correlated with a high relapse rate (Stumpel et al., 2009). Loss of DNA Methyl Transferase 1 (DNMT1), an enzyme that maintains the methylation of CpG islands leads to higher latency for MLL-AF9 mediated AML development in mice (Broske et al., 2009). This suggests that a drug that inhibits DNA methylation can be used for therapy. Indeed, a study shows that treatment of MLL-rearranged ALL cell lines with the

demethylating agent decitabine activates tumor suppressor genes and induces apoptosis (Stam et al., 2006).

Targeting histone acetylation

MLL fusion proteins abrogate the recruitment of CYP33 and histone deacetylase due to loss of PHD-bromo domains (Chen et al., 2008a; Wang et al., 2010). Lack of de-acetylase recruitment promotes leukemogenesis; hence blocking the activity of acetylated histones may prevent leukemogenesis. Indeed, targeting BRD4, a bromodomain containing protein that binds acetylated histone has proven to be efficacious on MLL leukemias in *in vitro* and *in vivo* studies. MLL is known to interact with Polymerase-Associated Factor Complex (PAFc). BRD4 is recruited to MLL target genes due to its interaction with Polymerase-Associated Factor Complex (PAFc). Additionally, this interaction is maintained by the MLL fusions. Moreover, Brd4 is known to recruits PTEFb (Jang et al., 2005; Yang et al., 2005). Hence, inhibiting the recognition of acetylated histones by BRD4 is likely to uncouple BRD4 dependent PTEFb recruitment. Further, Dawson et al. showed that I-BET151, a small molecule inhibitor of BRD4, inhibited MLL leukemic cell lines and prolonged survival in murine xenograft models (Dawson et al., 2011). Similar to these studies, another group using RNA interference screening identified Brd4 as a principle epigenetic regulator required for cell cycle progression and leukemogenesis in MLL fusion-mediated leukemias (Zuber et al., 2011). JQ1, another bromo domain inhibitor, caused monocytic differentiation of MLL fusion leukemic cells and exhibited anti-proliferative activity *in vivo*. An analysis of the

expression profile on JQ1 treatment indicated a down regulation of a C-Myc-mediated transcription program (Delmore et al., 2011).

Targeting histone methylation

Specific histone methylation marks serve as markers of transcriptional status. The methylation on H3K4, H3K36, and H3K79 correlates with active gene transcription, especially transcription of HOX genes that is required for normal hematopoiesis (Kouzarides, 2002; Peterson and Laniel, 2004). MLL leukemias were found to be dependent on the enzymatic activity of Dot1l, an H3K79 methyl transferase (Chang et al., 2010a; Jo et al., 2011). Genome-wide H3K79 methylation profiling and gene expression data correlates H3K79 methylation marks with MLL leukemia signature gene expression (Nguyen et al., 2011). Methylation catalyzed by DOT1L is dependent on the co-factor S-adenosine methionine (SAM). A small molecule named EPZ004777, which is a SAM analog, was shown to inhibit DOT1L enzymatic activity. It inhibits the growth of MLL leukemic cell lines, leads to Go/G1 growth arrest and induces apoptosis. The same study also showed a co-relationship between reduction of H3K79 methylation and MLL fusion target gene expression (Daigle et al., 2011). However, Dot1l is a global H3K79 methyl transferase, and its inactivation in adult mice leads to pancytopenia raising the possibility of hematologic toxicity in patients treated with DOT1L inhibitors (Jo et al., 2011).

The H3K4 methylation mark is added by MLL, and LSD1 is known to demethylate this mark (Shi et al., 2004). The loss of Lysine-specific histone demethylase (LSD1) leads to increases in H3K4 methylation at MLL targeted loci and correlates with

increased differentiation. Treatment with LSD1 small molecule inhibitors was shown to differentiate MLL leukemic cells *in vitro* (Harris et al., 2012).

***Role of Polycomb repressor complex proteins in MLL* leukemia**

The Polycomb group of proteins assembles to form two complexes: Polycomb repressor complex 1, PRC1 and Polycomb repressor complex 2, PRC2. The PRC2 complexes add H3K27 trimethylation marks associated with transcriptional repression. PRC2 consists of three principal protein components: EED, SUZ12, and the enzymatic EHZ1 or EZH2 proteins (Morey and Helin, 2010) . The Polycomb groups of proteins are known to antagonize the function of MLL. In contrast to this, recent studies performed by three different laboratories suggest that PRC2 promotes MLL fusion-mediated leukemogenesis. Knocking down of *Ezh1* or *Ezh2* components of the PRC2 complex separately reduces the colony forming capacity of MLL fusions, but knockdown of both abrogates colony formation, suggesting redundancy between the two proteins. Alternately, knockdown of *Eed*, another component of the PRC2 complex is more effective at inhibiting transformation by the MLL fusion genes. This suggests that the activity of PRC2 group proteins could be targeted for treatment of MLL leukemia (Neff et al., 2012; Shi et al., 2013; Tanaka et al., 2012). Among the PRC1 proteins, Chromobox protein homolog 8 (Cbx8) has been shown to be required for MLL-AF9 fusion mediated leukemogenesis. However, the leukemia promoting capacity of Cbx8 is suggested to be independent of its interaction with other PRC1 component proteins (Tan et al., 2011).

Thus inhibiting the activity of PRC2 components and the recruitment of CBX8 may have therapeutic potential.

Non Coding RNA in MLL leukemogenesis

Micro RNAs provide another potential avenue for MLL leukemic therapy. These small noncoding RNAs hybridize to target messenger RNA, resulting in its decreased translation or its increased degradation. Endogenous levels of beneficial miRs that target oncogenic products can be enhanced by using synthetic mimics. In contrast, miRs that suppress the activity of tumor suppressor genes can be downregulated using antisense oligomers called antagomirs. For instance, miR-196b is highly expressed in AML and translated from a region between *HOXA9* and *HOXA10* in an MLL fusion-dependent fashion. Its expression is shown to be required for immortalization and its inhibition *in vitro* diminishes the replating potential of transformed bone-marrow progenitors (Popovic et al., 2009).

A distinct pattern of miRNA expression is found in AML patient samples carrying MLL translocations versus non-MLL rearranged AML (Stumpel et al., 2011). Both upregulation and downregulation of miRNA plays a role in MLL leukemogenesis. The t(2;11)(p21;q23) translocation is associated with a strong up-regulation of miR-125b. An ectopic expression of miR-125b in mouse bone marrow-derived cells leads to an aggressive transplantable leukemia, and correlates with decreased differentiation capacity of hematopoietic progenitors (Chaudhuri et al., 2012). Conversely, miR495 expression decreases during leukemogenesis and its over expression suppresses MLL fusion induced

leukemogenesis by repression of *MEIS1* and *PBX3* (Jiang et al., 2012). Several other miRNA targets that can serve as therapeutic targets have been identified but we limit our review to a few examples.

AF9

AF9 was identified as the translocation partner gene in MLL leukemias with t(9;11)(p22;q23) translocations. It is the second most frequently occurring fusion partner of MLL in spontaneously occurring acute leukemias. It shares a high degree of sequence homology with another MLL fusion protein known as Eleven Nineteen Leukemia (ENL) (Iida et al., 1993; Nakamura et al., 1993; Rubnitz et al., 1994). Both proteins contain a YEATS domain at the amino terminus. The name YEATS is an acronym derived from the human and yeast proteins in which it was first identified (Yaf9, ENL, AF9, Taf15 and Sas5). The precise function of the YEATS domain is not known; however, it has been shown to interact with histone 1 and histone 3. It is a structural feature found in proteins involved in chromatin remodeling and transcriptional regulation (Schulze et al., 2009b).

A serine, proline rich region follows the YEATS domain and includes a nuclear localization signal. The most striking feature of this region is the presence of long uninterrupted stretches of serine residues that are present in AF9 but absent in ENL. The functional attributes of the polyserine stretch have not yet been identified. The C-termini of AF9 and ENL exhibit transactivation properties in reporter assays. The fusion of *MLL* with the 3' end of *AF9*, gives rise to a potent oncogene that can transform hematopoietic

progenitors. (Lavau et al., 1997; Rubnitz et al., 1994). The AF9 c-terminus is unstructured, permitting a wide variety of interaction-induced structural changes. (Leach et al., 2013).

Large scale phospho-proteomic studies of the human proteome suggest that AF9 has multiple phosphorylation sites (Daub et al., 2008; Dephoure et al., 2008; Olsen et al., 2010; Oppermann et al., 2009). However, so far only phosphorylation of AF9 on serine-435 by serum glucocorticoid kinase 1 (Sgk1) has been verified (Zhang et al., 2007). This phosphorylation event prevents the interaction between Af9 and the protein Dot1a. As indicated earlier Dot1 is a H3K79 methyl transferase shown to be essential for MLL leukemias. Af9 is found in a complex with Dot1a at the promoter of the epithelial sodium channel subunit alpha (*ENaCα*) gene expressed in the renal collecting duct (Zhang et al., 2013). The presence of this complex leads to H3K79 tri-methylation, which results in the negative regulation of the ENaCα gene (Zhang et al., 2006). Aldosterone leads to S435 phosphorylation of AF9 and derepression of *ENaCα* due to a loss of interaction between Af9 and Dot1a at the promoter (Reisenauer et al., 2009; Wu et al., 2011; Zhang et al., 2006) .

An *Af9* knockout mouse shows defects in vertebral patterning similar to those seen in *Mll* heterozygous mice, suggesting that Af9 may also be involved in the regulation of *Hox* genes (Collins et al., 2002). AF9 has also been shown to enhance the expression of GATA-1, a transcription factor associated with megakaryocyte/erythrocyte differentiation. Lentivirus mediated expression of AF9 in cord blood-derived HSC leads

to expansion of erythroid precursor cells, at the expense of colony forming cells-granulocyte monocyte progenitors (CFC-GM). While shRNA-mediated AF9 knock-down in the same HSC leads to loss of erythroid precursors. Gene expression analysis of cord blood-derived cells show a decreasing gradient of AF9 expression as HSC progress to common myeloid progenitor followed by further differentiation to myeloid-erythroid progenitor and granulocyte-myeloid progenitors. AF9 can be detected in myeloid-erythroid progenitor, while its levels dramatically drop in granulocyte-myeloid progenitors (Pina et al., 2008). Hence, it has been suggested AF9 plays a role in specification of hematopoietic lineage.

AF9 mutations have been found in children with neurological disorders like epilepsy and ataxia (Pramparo et al., 2005). An investigation of the role of AF9 in murine neuronal biology shows that Af9 plays a role in the development of intermediate precursor neurons found in the cortex by regulating the (*T brain 1*) *Tbr1* gene. Tbr1 is a transcription factor required for the development and differentiation of neurons. Af9 in a complex with Dot1 localizes to the promoter of the *Tbr1* gene and mediates H3K79 dimethylation which represses its expression. This suppression of *Tbr1* is required for proper development of the cortex (Buttner et al., 2010).

AF9 also plays a role in the planar cell polarity pathway that inhibits canonical WNT signaling. AF9 interacts with a protein named Diversin and promotes JNK-dependent gene transcription, which aids cells in orienting themselves with respect to the body axis (Haribaskar et al., 2009).

The yeast homolog of AF9 generates direction- specific mating projections and maintains sensitivity to osmolarity (Welch and Drubin, 1994). Mutants of the yeast homolog of AF9 enhance the 'hypersensitivity to osmolarity' phenotype of actin mutants. Thus AF9 was identified as an actin-non-complementing gene 1 (*ANC1*) in yeast (Welch et al., 1993).

The MLL-AF9 fusion is most commonly associated with myeloid leukemia in adults (Schoch et al., 2003). However, the same fusion in infants gives rise to both lymphoid and myeloid leukemias. These observed differences occur due to intrinsic properties of the cell that carries an MLL-fusion and are termed the 'cell of origin' effects. The neonatal HSC have a more stem-like gene signature, allowing progression to different cell fates, while adult HSC are biased toward myeloid origin (Horton et al., 2012).

A mouse model that expresses physiological levels of *Mll-Af9* from the *Mll* locus shows variable latency before development of leukemias based on the type of cell transformed. MLL fusions transform HSC with a shorter latency than committed progenitors. This difference in latency is because the *Mll-Af9* has a higher expression level in hematopoietic cells compared to the progenitors (Chen et al., 2008b; Dobson et al., 1999).

AF9 interacting proteins

Yeast two hybrid assays and protein purification studies have identified several AF9 interacting proteins that includes the AF4 family members, Dot1, CBX8, BCoR,

ELL, HSP90 and actin (Bitoun et al., 2007b; Lin and Hemenway, 2010; Mohan et al., 2010a; Monroe et al., 2011; Sobhian et al., 2010; Yokoyama et al., 2010). AF4, DOT1, CBX8, and BCoR bind directly to AF9 through its disordered carboxyl-terminus. AF4 and AF9, the two most common fusion partners of MLL directly interact with each other and co-localize at distinct nuclear foci. This interaction is maintained by MLL-AF9 fusions, forming a common network or complex of fusion partners (Erfurth et al., 2004).

Dot1 and AF9 form a complex of proteins that does not include AF4, CBX8, or BCoR (Biswas *et al*., 2011). Mohan *et al.,* first identified all the components of this complex and named it the Dotcom complex. This complex includes the proteins Dot1, AF9, AF10, AF17, Skp1, TRAPP, and beta-catenin. Its known function is to methylate H3K79 (Mohan et al., 2010a). This methylation activity is required to maintain MLL fusion induced leukemogenesis, *ENaCα* activation in renal epithelia, development of Tbr1 positive neurons in the cerebral cortex, fetal erythropoiesis, postnatal hematopoiesis, cardiac development, and cell cycle regulation (Buttner et al., 2010; Jo et al., 2011; Okada et al., 2005; Schulze et al., 2009a; Zhang et al., 2006).

AF9 has also been identified in the "Tatcom" complex that is recruited by the HIV protein Tat to its long terminal repeats for efficient transcription. Tatcom has the same components as the SEC complex, suggesting that the virus hijacks the endogenous transcriptional machinery to aid in its propagation (Sobhian et al., 2010).

ENL and subsequently AF9 were found to interact with the Polycomb group protein CBX8 (Hemenway et al., 2001). CBX8, also known as Polycomb 3, is a part of the PRC1 complex of proteins that antagonize the effects of trithorax/MLL and generally

repress genes. However, CBX8 has been proposed to play an activating role in MLL-AF9 leukemias independent of the PRC1 complex. A point mutant of MLL-AF9 that abrogates CBX8 binding as well as Cbx8 knockout HSC transformed with *MLL-AF9* fusion genes suggest that this interaction is required to both maintain and initiate leukemias (Tan et al., 2011).

The BCL-6 interacting co-repressor (BCoR) is ubiquitously expressed in several human tissues and has several isoforms. Only one of these isoforms interacts with AF9. The only identified function of BCoR is to promote repression of genes in association with the transcription factor BCL-6. It shows a repressive effect on AF9 reporter constructs in *in vitro* assays (Srinivasan et al., 2003).

The Heat Shock protein 90 (HSP90) has also been identified to interact with AF9. Knock down of Hsp90 by siRNA or its pharmacological inhibition by novobiocin results in cytoplasmic localization of Af9, implicating the role of this interaction in nuclear transport of Af9 (Lin and Hemenway, 2010).

AF4

AF4 is the most common MLL fusion partner in spontaneously occurring acute lymphoblastic leukemias (Daser and Rabbitts, 2004). It is a member of the AF4/LAF4/FMR2 (ALF) family of proteins. Several members of this family localize to nuclear nascent RNA storage sites, bind RNA, and are suggested to play a role in RNA splicing (Melko et al., 2011). A role in pathogenesis has also been identified. AF4, LAF4,
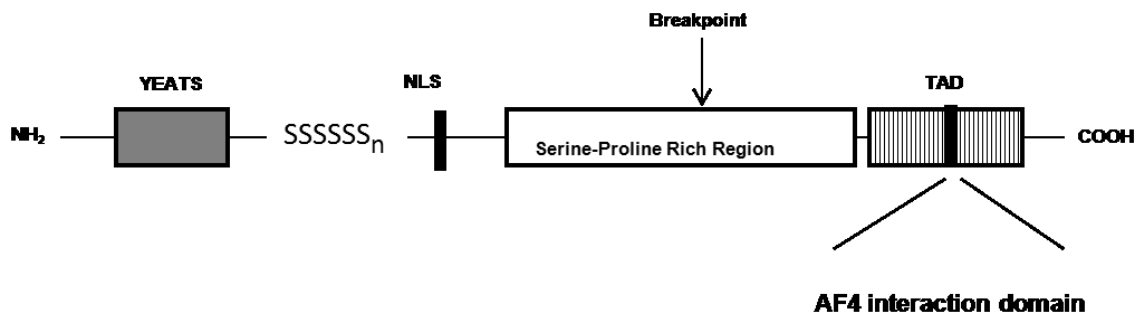
Figure 6 The domain structure of AF9

In order, from the N-terminus are the YEATS domain, SSSn represents a polyserine stretch, Nuclear Localization Signal (NLS), Serine-Proline rich region that includes the MLL fusion break points, and the transcriptional activation domain (TAD) which includes the AF4 interaction region.

and AF5q31 are found as fusion partners of MLL in acute leukemias. Additionally, mutations in *FMR2* and *AF4* affect neuronal function (Gu et al., 1992; Gu et al., 1996; Taki et al., 1999; von Bergh et al., 2002).

The structural features of AF4 (as shown in Figure 7) include the ALF domain, N terminal homology domain (NHD), C terminal homology domain (CHD) and a serine-proline rich transactivation domain which is common to all ALF family members (Ma and Staudt, 1996; Prasad et al., 1995). The CHD can homo-dimerize or hetero-dimerize with other ALF family members (Yokoyama et al., 2010). In addition, our lab identified a 13 amino acid long region of AF4 required for interaction with AF9. This region is conserved among all ALF family members (Srinivasan et al., 2004a). Charged amino acid and the hydrophobic amino acids in this region form an extensive interaction with AF9 (Leach et al., 2013). This interaction will be discussed further in Chapter 2.

 Af4 is highly expressed in brain and germinal centers of mouse embryo. *Af4* knockout mice show impaired maturation of pre-B cells and double negative thymocytes (Isnard et al., 2000). Hence, Af4 plays a role in B cell maturation at the germinal centers (Gu and Nelson, 2003). Lilliputian, the drosophila homolog of AF4, has been shown to participate in growth and cell fate determination by regulating the Ras/MAPK and the PI3K/PKB pathways (Wittwer et al., 2001).

Phosphorylation and ubiquitination of AF4 plays an important role in regulating the protein. Siah1 and Siah2 ubiquitin ligases ubiquitinate AF4, leading to its degradation by the proteasome. A point mutation in this Siah ubiquitin binding motif abrogates ubiquitination, leading to AF4 accumulation in neurons. This accumulation causes the

repression of the *Igf-1* gene in the cerebellum and the thymus. Cerebral Purkinje neurons are sensitive to AF4 protein accumulation and the subsequent decrease in Igf-1 activity. Loss of purkinje neurons leads to decreased motor coordination observed as a robotic gait in the affected mice. However, the abundance of AF4 positively correlates with positive Igf-1 activity in bone marrow and the lens, suggesting a context-dependent role in activation or repression (Bitoun and Davies, 2005; Bitoun et al., 2009; Oliver et al., 2004).

Relevant to this dissertation is the interaction of AF4 and PTEFb (Biswas et al., 2011). PTEFb is a complex of CyclinT1 or CyclinT2 and Cyclin-dependent kinase 9 (CDK9). It phosphorylates the heptameric repeats in the C-terminal domain of RNA polymerase II at serine 2, promoting the transition from initiation to the elongation phase of transcription. AF4 functions as a scaffold to help assemble the transcriptional elongation machinery. Its NHD interacts with CDK9, and maintains an association with other proteins required for transcriptional elongation. As transcription progresses, PTEFb phosphorylates AF4 at serine 212 and 220 (Esposito et al., 2011). This PTEFb-mediated phosphorylation leads to AF4 downregulation (Bitoun et al., 2007b). Also important to this transcriptional elongation function of AF4 is its interaction with AF9. AF4 and AF9 co-localize in the nucleus. As described earlier, the AF4-interacting sequence of AF9 is downstream of the ALF domain and is retained in MLL-AF4 fusion proteins (Erfurth et al., 2004).

In infants, the t(4;11)(q21;q23) translocation predicts a poor prognosis. This translocation may arise *in utero* and result in leukemia that develops with a very short

latency (Heerema et al., 1999). LAF4 and AF5q31, AF4 family members have been identified from patient samples more recently as MLL fusion partners (von Bergh et al., 2002). It has been difficult to model MLL-AF4 *in vivo* compared to MLL-AF9/ENL, since fusion constructs fail to reliably transform hematopoietic progenitors. Enforced expression of *MLL-AF4* in cord blood-derived HSC increased their colony forming capacity but was unable to induce leukemia upon xenograft (Montes et al., 2011).

This raises at least two possibilities: either secondary mutations are essential in the case of MLL-AF4-induced leukemia or MLL fusions are not arising in HSC found in cord blood. Knockin mouse models of *MLL-AF4* with secondary *K-Ras* mutations have been established and support the idea of requirement of additional mutations (Tamai et al., 2011). Enforced expression of *MLL-AF4* in embryo derived HSC leads to transformation and leukemic growth, suggesting that *MLL-AF4* may target pre-hematopoietic mesoderm or hemangioblasts. Hemagioblastic precursors have the potency to give rise to hematopoietic lineage and endothelial lineage (Bueno et al., 2012). Moreover, *MLL-AF4* translocations have been found in bone marrow derived mesenchymal stem cells of patients (Menendez et al., 2009) supporting the possibility that *MLL-AF4* fusion transforms pre-hematopoietic cells.

Some *in vitro* studies suggest that both the chimeric proteins that arise from the translocation cooperate with each other. For instance, when *MLL-AF4* and its reciprocal chimera *AF4MLL* are co-transfected they exhibit greater resistant to apoptosis and higher growth rate compared to an individual chimera (Gaussmann et al., 2007).
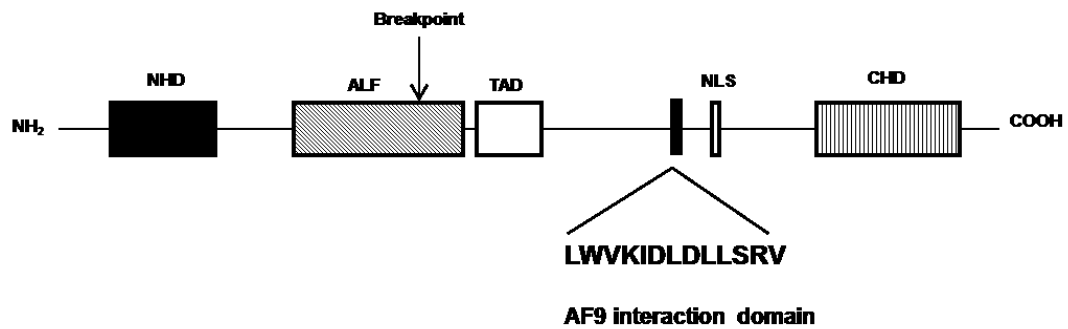
Figure 7   The domain structure of AF4 protein

In order from the N-terminus are the N-terminal Homology Domain (NHD), AF4/LAF5/FMR2 family domain (ALF) that includes the MLL fusion breakpoints, the transcriptional activation domain (TAD), a 13 amino acid AF9 interaction domain, Nuclear Localization Signal (NLS), and the C-terminal Homology Domain (CHD).

AF4 and AF9 directly interact with each other and are constituent components of the SEC. The aberrant recruitment of SEC permits expression of genes required to sustain leukemogenesis. In order to target the SEC, we use an AF4 mimetic peptide that inhibits the interaction between AF4 and AF9. The aim of this study is to determine if the AF4 mimetic peptide has a therapeutic potential for the treatment of MLL leukemias.

Chapter 2 describes the *in vivo* studies performed to determine the therapeutic potential of the AF4 mimetic peptide, SPK111. Its effects on normal hematopoiesis were also assessed. Further, the chapter also documents the ELISA assay that was devised to determine the *in vivo* concentration of the drug. Finally, the potential use of the peptide as a purging agent for *ex vivo* treatment of leukemia initiating cells is also explored.

In Chapter 3, we determine the effect of SPK111 on the AF4-AF9 interaction and the transcription elongation activity.

Treatment with the AF4 mimetic peptide induces rapid membrane permeability and cytoskeletal changes. Hence, the experiments in chapter 4 attempt to determine how the peptide destabilizes the cytoskeleton and if this destabilization is the primary cause of cell death.

Finally, Chapter 5 contains the concluding discussion and potential future experiments for newly arising research questions.

CHAPTER 2

AN *IN VIVO* ASSESSMENT OF THE THERAPEUTIC POTENTIAL OF SPK111

Abstract

Misregulation of transcription elongation is proposed to cause MLL leukemias (Bitoun et al., 2007b; Yokoyama et al., 2010). In this chapter, we discuss the previously identified direct interaction between AF4 and AF9, protein components of the super elongation complex (SEC) that promotes transcriptional elongation. Further, two AF4 mimetic peptides designed to inhibit the AF4-AF9 interaction are described. Treatment with the AF4 mimetic peptide, Peptide FMR2 Wild Type (PFWT) has been shown to decreases the viability of MLL leukemia cells (Palermo et al., 2008; Srinivasan et al., 2004a). Based on these results, we hypothesized that treatment with a modified AF4 mimetic peptide SPK111 would improve the survival of mice, xenografted with MLL leukemia cell lines. *In vitro* treatment of MLL leukemia cell lines with SPK111 showed that it effectively inhibits its growth. However, this efficacy could not be replicated in mice xenografted with MLL leukemias. The absence of the peptide in the circulating serum a few hours after subcutaneous injection was determined using ELISA suggesting decreased serum availability to be the cause of its *in vivo* ineffectiveness. Further, SPK111 does not significantly affect normal hematopoiesis in C57BL/6 mice, and pre-incubation of MLL leukemic cells with SPK111 inhibits the establishment of leukemic xenografts.

Introduction

The AF4 mimetic peptide

AF4 and AF9 proteins are the most common fusion partners of MLL. Our laboratory first identified a direct physical interaction between the AF4 homolog FMR2 and AF9 using yeast two hybrid assays (Erfurth et al., 2004). The minimal AF9 binding domain of FMR2 was mapped to 13 amino acids (residue number 759 -771). This sequence is conserved among ALF family members (AF4, LAF4, and FMR2). A peptide was synthesized to mimic the conserved AF9 interaction domain of FMR2. Its amino terminus was linked with Penetratin, a protein transduction domain, to allow for its transport across the cell membrane. This synthetic peptide was named Penetratin FMR2 Wild Type (PFWT) and its amino acid sequence is shown in Figure 8. Mutational analysis showed that the amino acids sequence of valine, lysine and isoleucine at position 763-765 of FMR2 are important to maintain interaction with AF9. In order to serve as negative control, a mutant version of the peptide was synthesized with V763E and I765S amino acid substitutions and was named PFmut. *In vitro* experiments showed that PFWT inhibited AF4-AF9 interaction while PFmut did not (Srinivasan et al., 2004a).

Leukemic cell lines carrying a MLL translocation had decreased viability when treated with PFWT (Srinivasan et al., 2004a). Analysis of caspase cleavage, tunel staining and several other assays of apoptosis showed no evidence of this process in PFWT-treated MV4-11 cells (leukemic cell lines carrying a MLL-AF4 translocation). Instead, necrotic cell death was determined by electron microscopy after treatment with PFWT. Pretreatment with serine protease inhibitors were shown to render protection against

PFWT induced necrosis (Palermo et al., 2008). Furthermore, PFWT treatment inhibited the colony forming capacity of MV4-11 cells and led to cell cycle arrest in G_o/G_1 phase (Palermo et al., 2008).

PFWT also exhibited a synergistic interaction with chemotherapeutic drugs, etoposide and cytarabine. Synergy was found to be dependent on the order of drug treatment. Etoposide and cytarabine had to be applied to the cells 24 hours prior to addition of PFWT to obtain synergy (Bennett et al., 2009). Thus, it has been demonstrated that PFWT, which targets the AF4-AF9 interaction, decreases the viability of MLL leukemia cell lines *in vitro* and also synergizes with conventional cytotoxic therapies.

Further, an *in vitro* biochemical assay based on protein-protein interaction was designed in our laboratory to monitor PFWT's ability to inhibit the AF4-AF9 interaction (unpublished data). Several substitutions were made in PFWT to increase its *in vivo* stability. L-stereoisomeric forms of amino acids found *in vivo* were substituted with the D-stereoisomers in order to make the peptide resistant to peptidases. These substitutions were tested using the assay to confirm that the peptide retained its ability to inhibit the AF4-AF9 interaction. D-stereoisomeric substitutions made at residues 1, 8 and 10 of the peptide retain the ability to bind AF9. Tryptophan is susceptible to oxidation and was replaced with nor-leucine at position 2 to make the peptide stable for long term storage. Lysine at position 4 forms a charged salt bridge interaction with AF9 (Leach et al., 2013). Substitution of this lysine with ornithine at position 4 forms a more stable salt bridge as it has a higher pKa. Finally, the N-terminus of the modified peptide is attached

to 10 amino acids sequence derived from the HIV Tat protein, whose function is to transduce the peptide across the plasma membrane. It has been shown that mode of entry and distribution of the Tat fusion depends on the size of the fused molecule. Short peptides fused to Tat diffuse directly into the cell without the expenditure of any energy and tend to distribute through the cytoplasm and accumulate in the nucleus (Ho et al., 2001; Tunnemann et al., 2006). The efficiency of cargo delivery for Tat protein transduction sequence was found to be higher than that of penetratin (Hallbrink et al., 2001; Mi et al., 2000). The newly synthesized AF4/FMR2 mimetic peptide with all the above mentioned substitution was named SPK111.

A mutant version of this peptide named SPK110 was also synthesized. It has a glutamic acid substitution at position 4 in place of ornithine. The negative charge on glutamic acid cannot form a salt bridge interaction with AF9; hence SPK110 cannot inhibit the AF4-AF9 interaction. In this chapter, we describe the results of experiments performed to determine the efficacy of SPK111.

MATERIALS AND METHODS

Cell Culture

Leukemia cell lines MV4-11 (MLL-AF4), MOLM13 (MLL-AF9), K562 (BCR-ABL), REH (ETV6-RUNX1) and MOLT4 (T lymphoblast) were obtained from the American Type Culture Collection (ATCC) and KOPN 8 (MLL-ENL) cells were obtained from the Leibniz Institute DSMZ. These cells were cultured in RPMI 1640

hFMR2:   LWVKIDLDLLSRV

hAF4:   LMVKITLDLLSRI

PFWT   (Penetratin)-LWVKIDLDLLSRV

PFmut   (Penetratin)-LW**EKS**DLDLLSRV

Penetratin   RQIKIWFQNRRMKWKK

SPK111- modified Tat(dL)(Nle)V**Orn**IDL(dD)L(dL)-CONH$_2$

SPK110 –modified Tat(dL)(Nle)V**D**IDL(dD)L(dL)-CONH$_2$

Modified Tat   - (dR)(dK)(dK)(dR)(dR)Orn(dR)(dR)(dR)(βA)

Figure 8 Schematic of peptide design based on AF9 interacting domain of AF4

The amino acid sequence of AF9 binding domain of human AF4 and FMR2 is shown in figure. The peptide FMR wild type (PFWT) sequence is based on FMR2 amino acids. The mutant version of the AF4 mimetic peptide PFmut has mutated amino acids which are in red. The amino acid sequence of the protein transduction domain Penetratin has also been shown. The peptide SPK111 and SPK110 generated by stereomeric and isomeric substitution of amino acids is also shown. Substituted dextro stereoisomers of amino acids are represented by (d), and the beta isomers of an amino acid are represented by (β). Some of the lysine residues are substituted with ornithine represented by Orn and tryptophan is replaced with Norleucine represented by (Nle). Ornithine residue (**Orn**) in SPK111 forms a salt bridge interaction with AF9. In SPK110, **Orn** is substituted with negatively charged aspartic acid **D**.

medium (ATCC, Manassas, VA) supplemented with 10% fetal bovine serum (FBS) (Atlanta Biologicals, Lawrenceville, GA), 1.1 % penicillin/streptomycin (Pen/Strep) (Invitrogen), and 2.2% glutamine (Cell Grow, Mediatech, Manassas, VA).

HEK293T cells (Clontech) and HeLa (ATCC) cells were maintained in Dulbecco's modified Eagle's medium (DMEM) (Cellgrow, Mediatech, Manassas, VA), supplemented with 10% FBS, and 1.1% Pen/Strep. All cells were incubated at 37°C with 5% carbon dioxide.

Peptide Stock

The AF4 mimetic peptide, SPK111 (modified Tat- (dL)(Nle)VOrnIDL(dD)L(dL) or its mutant control SPK110 (modified Tat-(dL)(Nle)VDIDL(dD)L(dL) were synthesized and purified by HPLC to > 85% purity by New England Peptide (Gardner, MA). The modified Tat protein transduction sequence is ((dR)(dK)(dK)(dR)(dR)-O(dR)(dR)(dR)(bA)). A stock of 37.5mg/ml of SPK111 or SPK110 was dissolved in cell culture grade 99% pure Dimethyl sulfoxide (DMSO) (Edward lifesciences, CA) to obtain a 1000x stock. Aliquots of the stock were stored at -80^{0}C.

Cell Viability Assay

The Promega Cell Titer-Glo luminescent cell viability assay measures the total cellular ATP and can be used to quantify metabolically viable cells. This assay was used to measure the cell viability. MV4-11, MOLM13, KOPN8, K562, REH and MOLT4 were seeded at a density of 1 million cells per ml. They were exposed to SPK111 or SPK110 at concentrations of 12.5µg/ml, 25µg/ml, and 37.5µg/ml. As an additional

control, cells were exposed to the same final volume of DMSO as used in peptide treatments. Cells (100µl) were dispensed in 96 well plates in quadruplicates for each given concentration. The plates were incubated at $37^{o}C$ for 24 hours. After equilibration, 100 µL of Cell Titer Glow Reagent (Promega) was added to each well and placed on a rotating platform for 2 minutes to aid cell lysis. Cells were incubated for additional 10 minutes at room temperature to stabilize the luminescent signal. Luminescence was recorded using POLAR Star Omega plate reader (BMG Labtech).

Viability of the peptide treated cells was calculated as percentage of DMSO treated cells.

Generating mouse xenografts

Six week old female NOD/SCID mice were sublethally irradiated with 250 cGy of total body irradiation. On the same day, post irradiation $2x10^{6}$ MOLM13, KOPN8, MV4-11, or K562 leukemia cells were injected into the tail vein. The number of mice used in each experiment is indicated in the results section.

A post mortem analysis was performed to confirm the presence of xenografted leukemic cells at the end of each experiment. Bone marrow samples were obtained by flushing femurs with PBS. The samples were lysed in 1X RBC lysis buffer (8.3g/l ammonium chloride in 0.01M Tris-HCl pH 7.5) for 2-3 minutes. The lysed sample was centrifuged. The cell pellets were blocked with 2% FBS in PBS and stained with anti-human $CD45^{+}$ FITC (BD Pharmingen # 55482) and analyzed by flow BD canto II flow cytometer and Flow Jo 2.0 software.

In vivo treatment with SPK111

In order to calculate the dose for animals we assumed that the density of mouse tissue is equivalent to that of water. Hence the *in vivo* equivalent of 25µg/ml will be 25mg/kg.

Treatment was started one week after the injection of leukemia cells unless otherwise indicated. Mice were injected subcutaneously with the specified dose of SPK111 or with vehicle alone (2% DMSO in PBS). Survival was measured as the time from leukemia cell injection until a moribund state developed. Extreme lethargy or paralyses were considered end points. Survival benefit was assessed by Kaplan–Meyer analysis using Prism Graph Pad software. In order to detect a significant change ($p < 0.05$) in mean survival from 21+/-4 days to 28+/-4 days with a power of 0.80, seven animals were needed per group (2 sample t-test, calculations performed by Dr. Rong Guo, institutional biostatistician).

Effect of SPK111 on leukemia-initiating cells/ex vivo purging of leukemic cells

2×10^6 MOLM 13 cells were incubated *ex vivo* with 37.5 µg/ml SPK111 or 2% DMSO in PBS for 24 hours. The cells were then collected by centrifugation at 1200 rpm for 4 mins, re-suspended in PBS and injected into sub lethally irradiated NOD/SCID mice via tail vein. Mice were monitored for 2 months after cells were injected.

Bioluminescent monitoring of leukemic growth in vivo

Leukemic progression was monitored in mice xenografted with MV4-11 cells expressing luciferase. MV4-11 cells expressing luciferase were provided to us by Dr. Scott Armstrong's Laboratory (Dana-Farber Cancer Institute, Boston, MA). Images were acquired using the xenogen imager 10 minutes following intra peritoneal injection of 125 mg/kg of D-luciferin. Luminescent images were analyzed using the caliper life science live image software.

Hematologic Toxicity

SPK111 (50 mg/kg) or 2% DMSO in PBS was administered subcutaneously to 6-week old female C57BL/6 mice daily for 5 days. Three mice were used per group. Seven days after the administration of the last dose, mice were euthanized and whole blood was collected by heart puncture. Whole blood analysis was performed with a Hemavet 950F instrument (Drew Scientific) in order to determine any short term hematological toxicity.

To determine the effect on myeloid cells, bone marrows were flushed from the femur and red blood cells were lysed in buffered ammonium chloride. Cells were then collected by centrifugation. The cells were incubated in 2% FBS in PBS for 30 minutes, followed by labeling with the following eBioscience antibodies: anti-mouse CD41 (#12-0411-81), anti-mouse Ter119 (#17-5921-81), anti-mouse CD11b (#48-0112-80) and anti-mouse LyGr-1 (#85-5831-81). After incubation, the cells were washed twice with 2% FBS in PBS and suspended in the same buffer. Cells were analyzed using a BD Canto II flow cytometer and Flow Jo 2.0 software.

Enzyme Linked Immunosorbent assay (ELISA)

ELISA was used to measure the peptide concentration in the serum following subcutaneous injections. The anti-SPK111 antibody used in this assay is a polyclonal antibody purified from the serum of a rabbit immunized with SPK111 peptide plus an adjuvant (New England Peptides, Gardner, MA). In order to establish a standard curve for the ELISA, dilutions of SPK111 stock were prepared in FBS containing 0.05% tween-20. Standards and blank (100µl) were added to wells in triplicate. To assess the concentration of peptide in the serum, 6 week old female C57BL/6 mice were subcutaneously injected with 50mg/kg of SPK111 and were sacrificed 1 h or 3 h after treatment. Whole blood was collected by heart puncture. The whole blood was allowed to clot at room temperature and then centrifuged at 10, 000 x g at 4°C for 15 minutes. The serum was collected and 100µl loaded into the wells of a protein binding 96-well plate. (About 100-150µl of serum is obtained from a single heart puncture sample, hence it is not possible to monitor the peptide levels in the same mouse). Hence each sample well represents a single animal. Plates were covered with thin plastic film and incubated in the refrigerator at 4°C overnight. The next day the wells were washed 3 times with PBS and then incubated with 100µl of anti-SPK111 antibody diluted 1:1000 in PBST (PBS+ 0.05% Tween) for 1 hour at room temperature (RT). Wells were then washed 5 times with PBST. Horse radish peroxidase conjugated anti-rabbit IgG antibody (Invitrogen) was diluted 1:7500 in PBST and added to the wells, and incubated at room temperature for 30 minutes followed by 5 washes with PBST. The HRP activity was detected using tetramethylbenzidine (TMB)/peroxide (100µL) for 10-15 mins. The reaction was stopped

by addition of 50µl of HCl to the wells (R&D Systems, Cat. #DY999). Absorbance was measured at 450nm using a POLAR Star Omega plate reader (BMG Labtech).

Results

SPK111 is toxic to leukemia cells

Incubation of leukemic cells with the AF4 mimetic peptide, PFWT, results in decreased viability. The same decrease is not observed on incubation of the peptide with peripheral blood derived mononuclear cells (Palermo et al., 2008; Srinivasan et al., 2004a). In order to confirm that the modified AF4 mimetic peptide, SPK111, has the same effect, viability assays were performed. The human leukemia cell lines MV4-11, MOLM13, and KOPN8 carrying MLL-AF4, MLL-AF9 and MLL-ENL translocations, respectively, were treated with 12.5µg/ml, 25µg/ml and 37.5µg/ml of the active peptide SPK111 and the mutant peptide SPK110 for 24 h. Viability after treatment was determined by quantification of cellular ATP using the Promega Cell Titer-Glow luminescent cell viability assay. Treatment with the vehicle, DMSO, served as negative control. As shown in Figure 9, the viability of MLL leukemia cell line decreases with increasing concentrations of SPK111. However, treatment with the mutant peptide, SPK110, which has a single amino acid mutation in the AF9 binding region, does not affect the viability at the same concentrations. This suggests that inhibition of the AF4-AF9 interaction results in decreased viability.

The myeloid leukemia cell line K562 expressing a BCR-ABL fusion gene, a pro-B-leukemia cell line REH expressing the ETV6-RUNX1 fusion gene, and a T-

lymphoblatic cell line MOLT4 carrying a p53 mutation were representative of non-MLL-rearranged leukemias. These leukemia cell lines lack MLL fusion genes and are comparatively less sensitive to SPK111 as shown in Figure 9.

SPK111 is ineffective against xenografted MLL leukemias

In order to determine if SPK111 treatment improves the survival of mice xenografted with human MLL leukemic cell lines, we injected mice with $2x10^6$ MOLM13 and KOPN8 cells. The presence of the xenograft was confirmed at the end of each experiment by detecting the presence of hCD45 antigen from the extracted bone marrow derived whole blood samples (data not shown). In two independent experiments, xenografted mice were subcutaneously injected with 37.5mg/kg SPK111 or DMSO vehicle solution for 5 consecutive days. The first dose was administered 7 days after transplant. Assuming a volume of distribution of one, 37.5 mg/kg corresponds to an *in vitro* dose that results in less than 15% viability of MOLM13 and KOPN8 cells.

The results depicted in Figure 10 show a trend towards improved survival. However, no statistical significance was obtained. In addition, mice in the SPK111 treatment group developed skin irritation and ulceration at the site of injections indicating toxicity to dermal tissue. Two days after tail vein injection of leukemic cells in mice, the leukemic burden is likely to be low. In the next experiment, we sought to determine if dosing when the disease burden is low improves survival. KOPN8 xenografted mice were subcutaneously injected with 37.5 mg/kg SPK111or DMSO two days after transplant. A total of five doses were administered to KOPN8 xenografted mice in
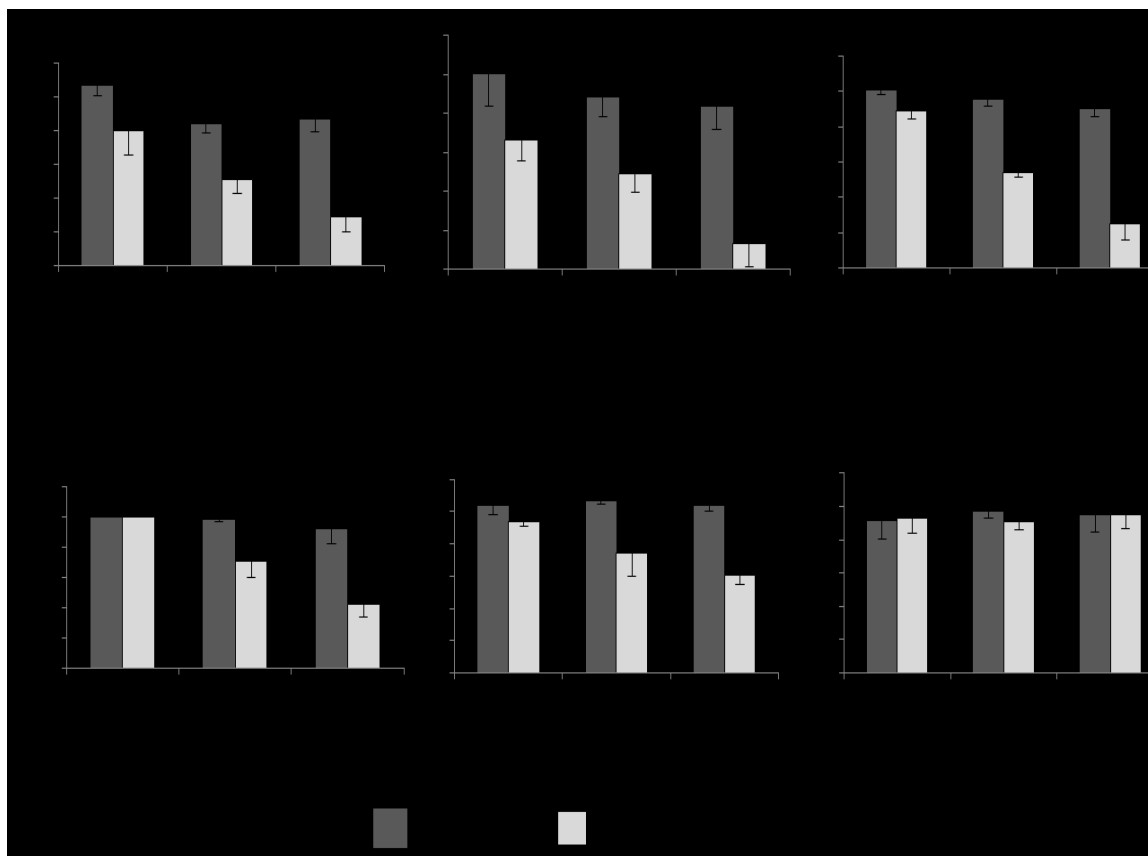
Figure 9 Treatment of leukemic cells with SPK111 results in decreased viability

MV4-11, MOLM13, KOPN8, K562, REH, and MOLT4 leukemic cells were treated with increasing concentrations of SPK111 or the mutant peptide SPK110 for 24 hours. Viability was measured using Promega Cell titer-glow luminescent viability assay. Viability is expressed as a percentage of DMSO treated cells. The error bars represent % standard error. Significance is determined using student's t-test. '*' indicates p<0.01. No significant difference is indicated by n.s. IC_{50} calculated using ED50 plus software.

this experiment. Survival analysis shown in Figure 11 indicates that there was no survival advantage for the treatment group.

The adverse effects of SPK111 on the skin of the mice raised the possibility of secondary events like bleeding and infection. In order to minimize the effect on skin, we tested treatment with a smaller dose of SPK111 (25mg/kg) but with an increased number of doses. Dosing frequency was maintained at one dose given per day. The total amount of drug administered to KOPN8 xenografted mice during therapy was 5 mg of SPK111 over 10 doses which is 30% higher than the 3.75mg administered at a larger dose for 5 days previously. Similarly, the total amount of drug administered to MOLM13 xenografted mice during therapy was 6 mg of SPK111 over 12 doses which is 60% higher than the 3.75mg administered at a larger dose for 5 days. However, this dosing scheme had no effect on the skin lesions or the survival of MOLM 13 or KOPN8 xenografted mice (Figure 12).

Effect of SPK111 on normal hematopoiesis

It is important to determine the effects of an experimental drug on normal hematopoiesis in order to identify any acute toxicity. C57BL/6 mice were treated with a daily subcutaneous dose of 50mg/kg of SPK111, SPK110 or vehicle control for 5 consecutive days. The dose 50mg/kg is the largest amount of dose administered in any survival experiment. An analysis of the whole blood collected by heart puncture a week after dosing shows no significant differences in the total white blood cell count, platelet count or the hemoglobin level (Figure 13).

A   MOLM13

B
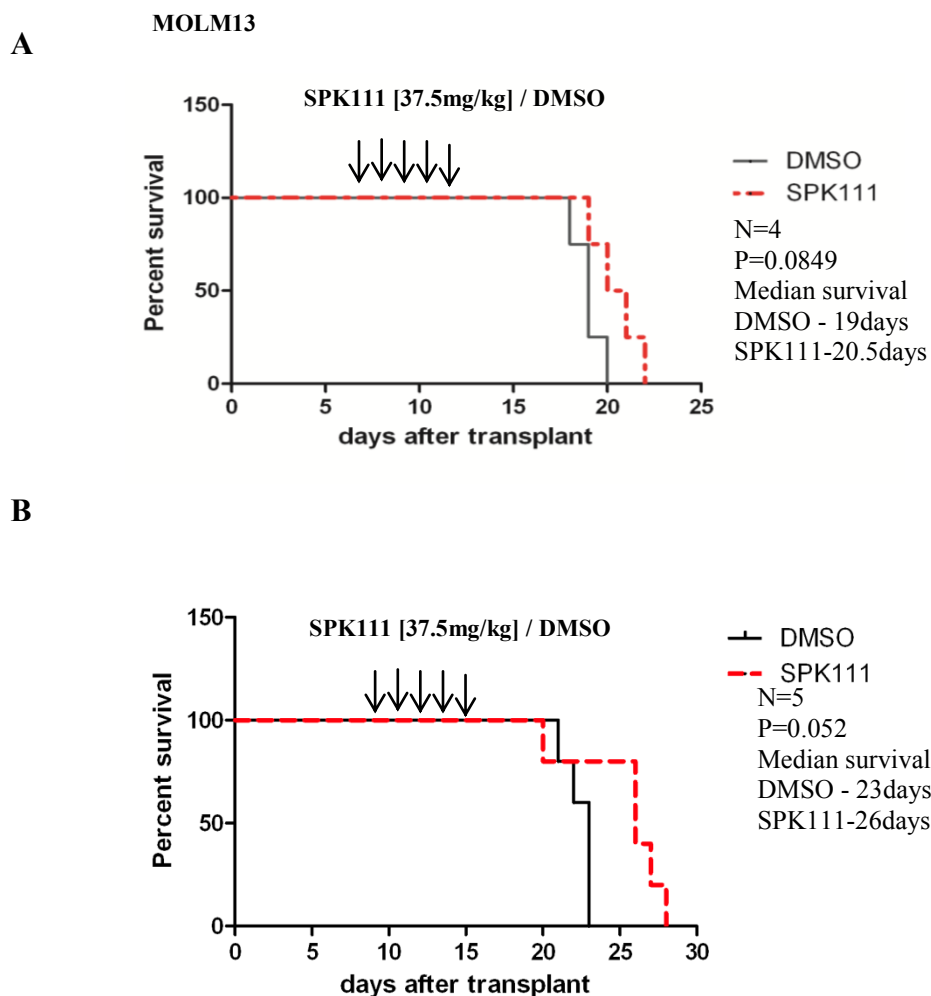
Figure 10 Survival of mice with MLL leukemia xenografts after treatment with 37.5mg/kg of SPK111 for 5 daily doses

MOLM13 (A) and KOPN8 (B) xenografted mice were injected subcutaneously with 37.5mg/kg SPK111 or 2% DMSO in PBS daily for 5 consecutive doses. The first dose was administered on day 7 after transplant. N represents the number of animals in each group and p value was calculated using log rank test (prism graph pad software). Median survival of DMSO and SPK111 treated mice is shown.
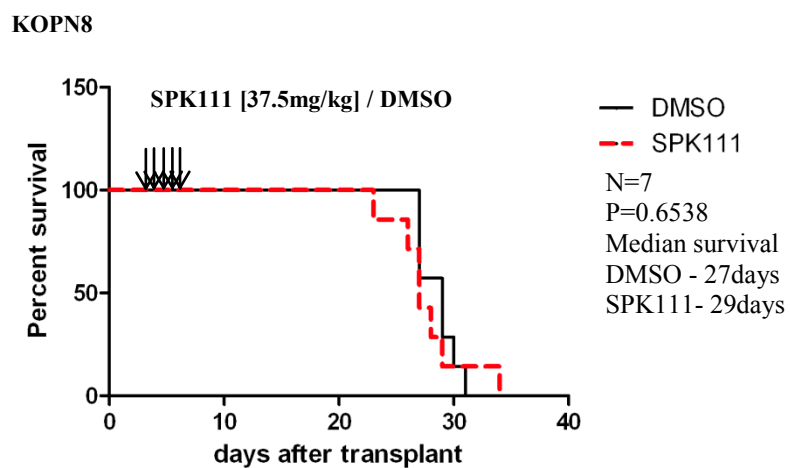
Figure 11 Survival of mice with MLL leukemia xenografts treated 2 days after transplant

KOPN8 xenografted mice were injected subcutaneously with 37.5mg/kg SPK111 or 2% DMSO in PBS daily for 5 consecutive doses. The first dose was administered on day 2 after transplant. N represents the number of animals in each group and p value was calculated using log rank test (prism graph pad software). Median survival of DMSO and SPK111 treated mice is shown.

A   MOLM 13

B

     KOPN8

Figure 12 The effects of frequent treatment with 25mg/kg of SPK111 on mice with MLL leukemia xenografts

MOLM13 (A) and KOPN8 (B) xenografts were injected subcutaneously with 25mg/kg SPK111 or 2% DMSO in PBS for the indicated number of doses. The first dose was administered on day 2 and day 7 after transplant for MOLM13 and KOPN8 respectively. N represents the number of animals in each group and p value was calculated using log rank test (prism graph pad software). Median survival of DMSO and SPK111 treated mice is shown.
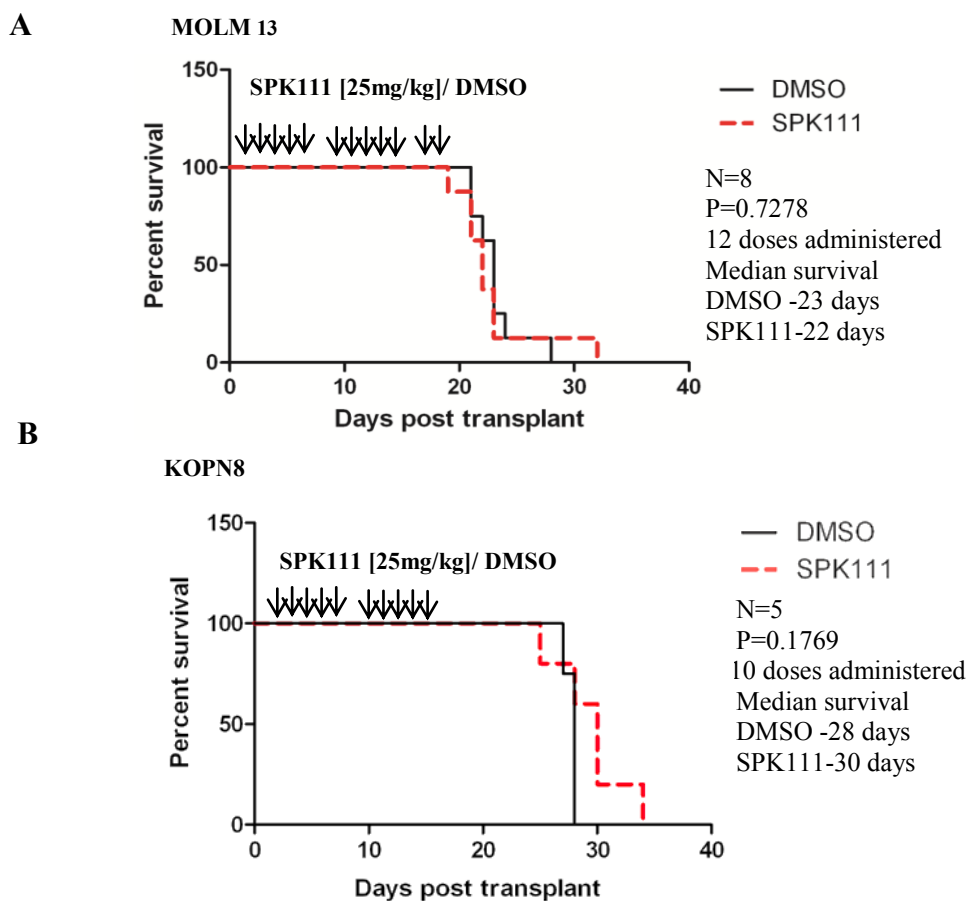
AF9 positively regulates genes that promote erythroid-megakaryoctic lineage precursor development (Pina et al., 2008). Hence, flow cytometry analysis using markers of erythroid-myeloid precursor cells was done on bone marrow samples derived from the same mice as Figure 13. We observed a two fold increase in Gr-1 expressing granulocyte macrophage precursors in samples derived from mice treated with active and mutant peptides compared to mice treated with the vehicle, suggesting that the peptide may affect the myeloid population (Figure14). Ter119 antibody binds erythroid cells from pro-erythroblast through mature erythrocyte stages. Hypotonic lysis buffer is used to lyse the mature erythrocytes in the whole blood collected from the bone marrow of mice. Variation in the number of cells of the erythroid lineage determined using TER-119 antibody could be an effect of increased lysis of the mature erythrocytes (Figure14). CD41 is a marker of megakaryocytes and is also present on certain hematopoietic stem cell populations. CD41 labeling shows variation in the sample derived from mice treated with SPK111, however this variation is not statistically significant (Figure 14).

SPK111 can be used for purging of leukemia initiating cells

Leukemia initiating cells are slow dividing cells that evade conventional chemotherapeutics and play a role in re-establishing leukemia after a period of latency (Clevers, 2011). In order to test the effect of SPK111 on leukemia initiating cells, we treated $2X10^6$ MOLM13 cells with 37.5µg/ml of SPK111 for 24 hrs. The viability of MOLM13 cells at this concentration *in vitro* is 15% or less. In order to determine if the remaining viable cells are resistant leukemic cells, the entire cell suspension was injected
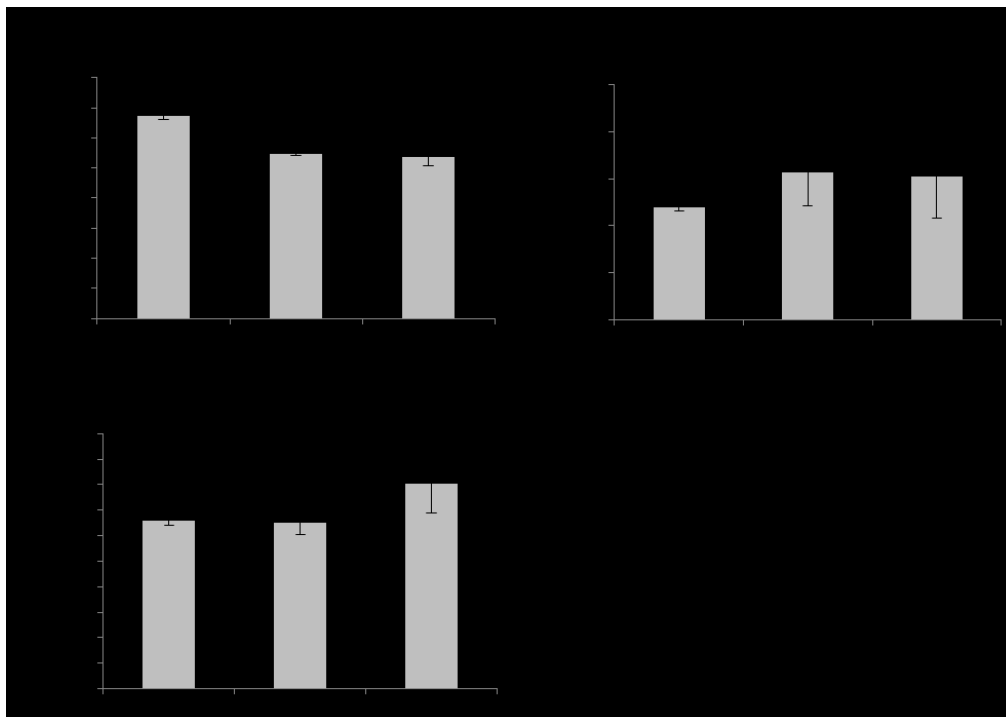
Figure 13   SPK111 does not affect the whole blood composition

50mg/kg of SPK111, 50mg/kg of SPK110 or DMSO was administered to C57BL/6 mice daily for five consecutive days. Seven days after the last injection whole blood collected by heart puncture was analyzed on a hemavet. No significant differences were found in the platelet, hemoglobin and the total white blood cell count between samples derived from mice treated with vehicle, SPK111 or SPK110. Hemoglobin content in grams/deciliter (g/dL) and cell count is thousand cells per micro liter (K/µl). Each group consisted of three mice. Error bars represent standard deviation and significance difference between DMSO treatment derived sample and peptide treatment derived samples was determined using students t-test.
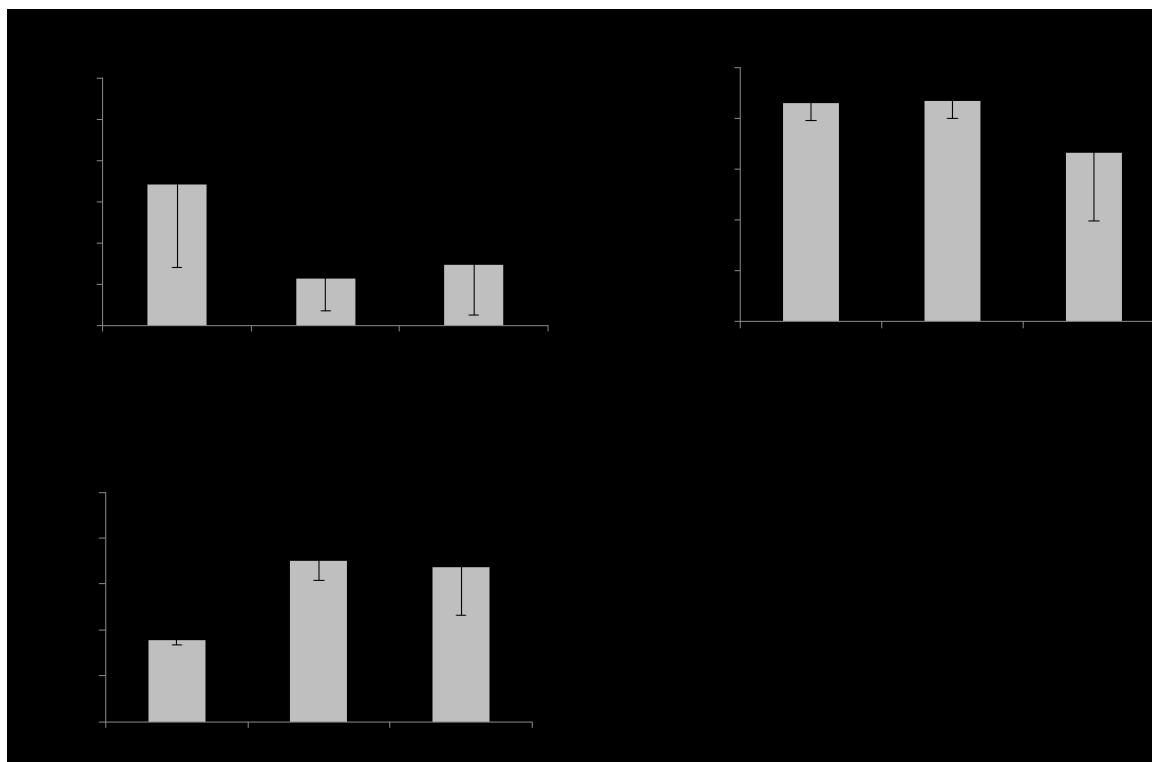
Figure 14 Effect of SPK111 on myeloid differentiation

50mg/kg of SPK111 was administered to C57BL/6 mice daily for five consecutive days. Seven days after the last injection the bone marrow was collected and labeled with fluorescent antibodies to the surface markers Gr1(Granulocyte Myeloid precursor), CD 41(Multipotent hematopoietic precursor and megakaryocyte), and Ter119 (pro-erythroblasts) and analyzed by flow cytometer. Gating was restricted to viable cells. There were three mice in each group. Error bars represent standard deviation and significance was determined using students t-test.

into the tail veins of sub-lethally irradiated NOD/SCID mice. Cells exposed to vehicle control caused fatal leukemia in all mice approximately 21 days following injection. In contrast, cells exposed *ex vivo* to SPK111 did not cause measurable disease in five of six animals during the 60 days of observation (Figure 15).

Similarly, $2X10^6$ MV4-11 cells that express luciferase were cultured for 24 h in the presence of 37.5µg/ml SPK111 or vehicle control. The entire cell suspension was then injected into the tail veins of sub-lethally irradiated NSG mice. Luminescence at various time points is depicted and shows that the treated cells fail to establish leukemia (Figure 16).

Establishment of ELISA to determine serum SPK111 concentration

SPK111 treatment leads to decreased viability of leukemic cells *in vitro* (Figure 9). However, it has little effect on mice engrafted with MLL leukemic cell lines. One possibile reason for *in vivo* ineffectiveness is a low serum concentration. We established a direct ELISA to determine the levels of SPK111 in the serum after subcutaneous injections. Dot blot analysis confirmed that the anti-rabbit polyclonal antibody generated by New England Peptide Incorporated binds to SPK111. Further, several variations of buffer and incubation times were tried in order to establish a standard curve of SPK111 for ELISA estitmation. The concentration range of the established standard curve was 1.87µg/ml to 37.5µg/ml (Figure 17). From cell viability assays (Figure 9), the MLL leukemia cell lines exhibit sensitivity to SPK111 in the concentration range of 12.5µg/ml-37.5µg/ml. Hence, we established a standard curve that included this concentration range.
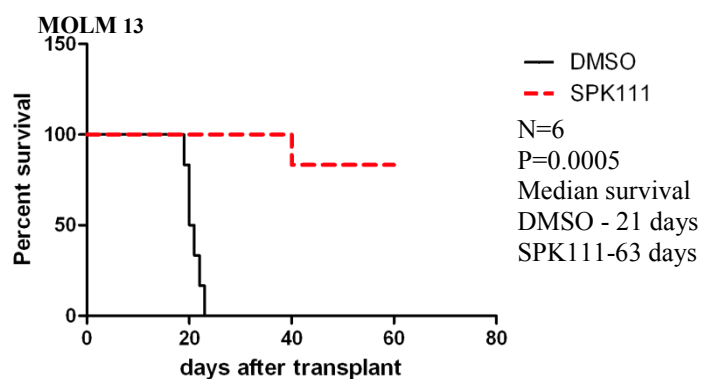
Figure 15   SPK111 treated leukemia cells fail to engraft after incubation with SPK111

$2X10^6$ MOLM13 cells were exposed to 37.5µg/ml SPK111 or 2% DMSO in PBS for 24 hours *in vitro* before they were injected into the tail vein of a NOD/SCID mouse. Survival was measured from the time of tail vein injection until the development of a moribund state. N represents the number of animals in each group and p value was calculated using log rank test (prism graph pad software). Median survival is shown.

.

A

Day 7

Day 14

Day 18

Day 22

Day 28

B

Day 7

Day 14

Day 18

Day 22

Day 28

Day 54
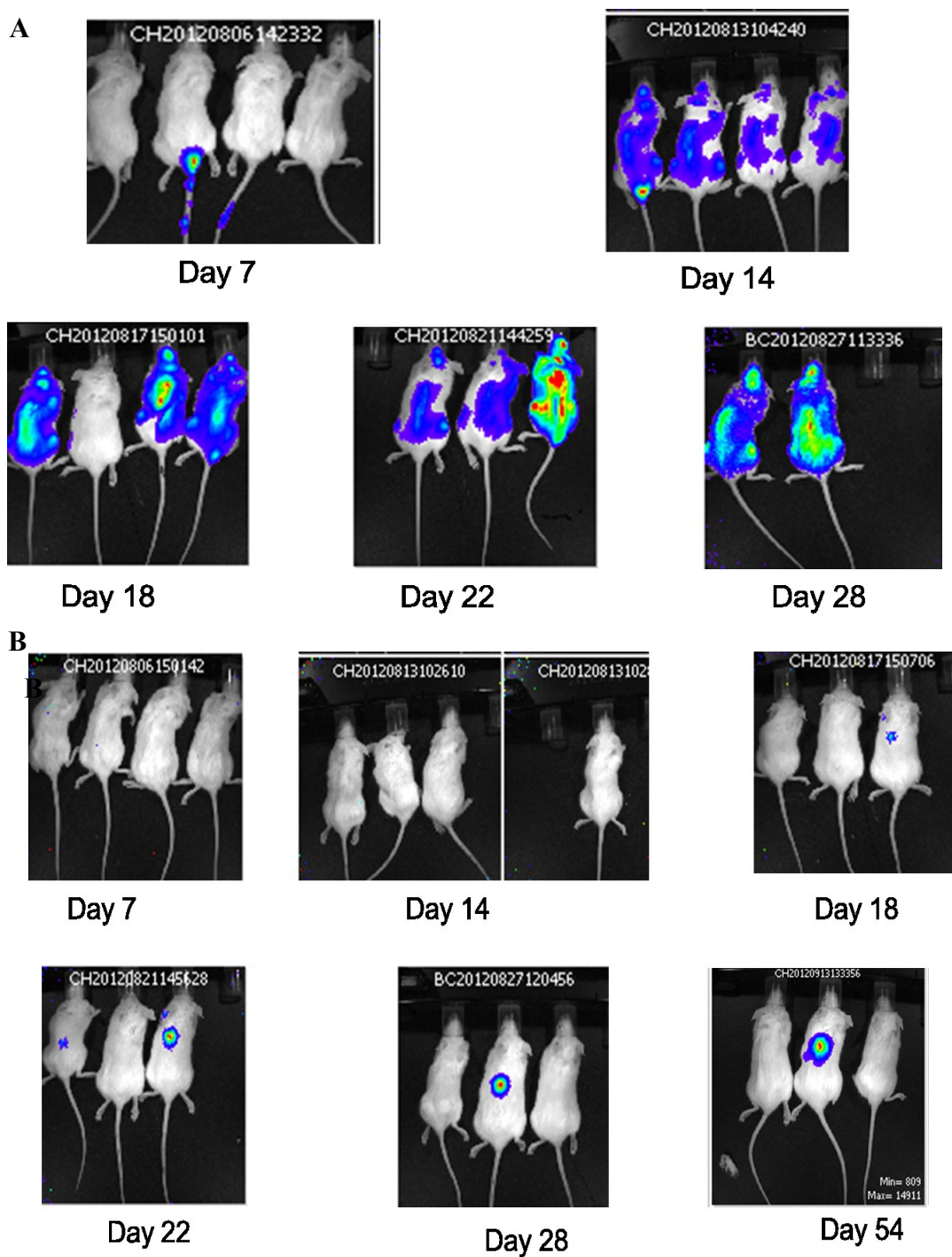
Figure 16 Luciferase expressing MV4-11 cells fail to engraft after incubation with SPK111

2X10^6 MV4-11 cells that express luciferase were treated *ex vivo* with vehicle control (2%

DMSO in PBS)(A) or 37.5µg/ml of SPK111(B) for 24 hours before tail vein injection.

Luminescence is measured following subcutaneous injections of D-luciferin. The day on

which luminsescence was measured post tail vein injection is indicated.

A

ELISA- Working Concentration Range

B

Serum SPK111 concentration 1 hour after 50mg/kg subcutaneous injection
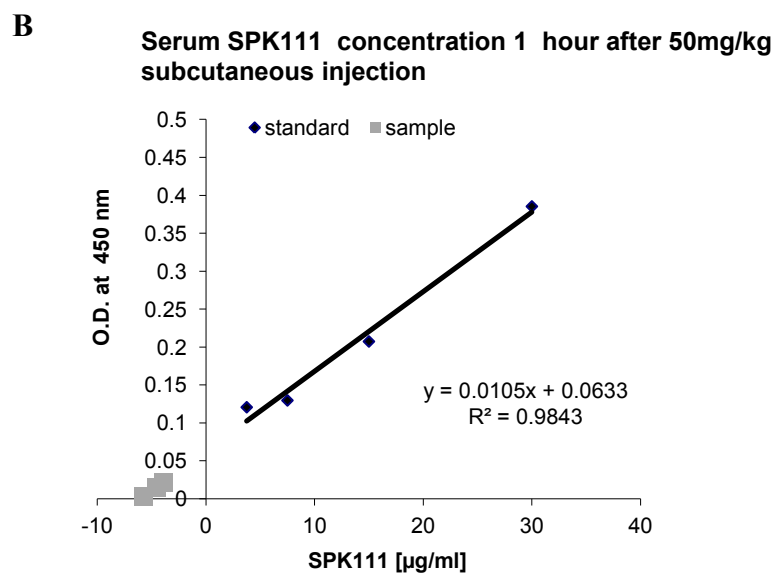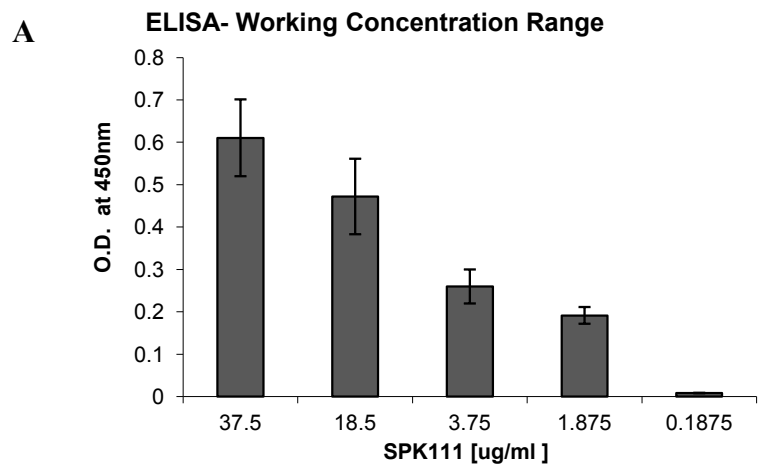
C   **Serum SPK111 concentration 3 hours after 50mg/kg subcutaneous injection**
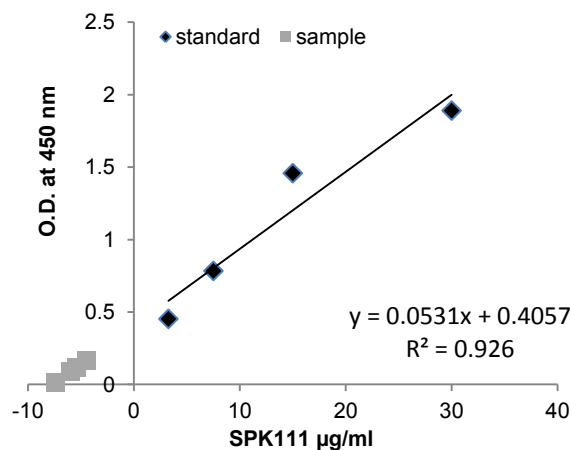
Figure 17 Quantiative detection of SPK111 using a newly synthesized polyclonal anti-SPK111 antibody

(A) A standard curve of SPK111 was established by incubating the peptide in FBS and 0.05% tween and detecting a concentration dependent signal. The signal was detected using anti-SPK111 antibody, HRP conjugated secondary antibody and tetramethylbenzidine (TMB)/peroxide based colorimetry detection. Error bars represent standard deviation of triplicate wells. (B) C57BL/6 mice were subcutaneously injected with 50mg/kg of SPK111. Whole blood was collected by heart puncture at 1 hour and 3 hours (C) after administration of the peptide. 100 µl of serum obtained after clotting whole blood was loaded into the wells of a 96 wells plate along with standards and processed. The measured negative value in the samples suggests the absence of SPK111 in the serum

Using this assay, we performed a set of kinetic experiments. C57BL/6 mice were subcutaneously injected with 50mg/kg of SPK111 and its levels in the serum were determined by ELISA, 1 h and 3 h after subcutaneous injection. As shown in figure 17, we could not detect the presence of SPK111 in the serum of the subcutaneously injected mice at any time point. The implications of these results are further considered in the discussion.

Discussion

Therapy related MLL rearrangements and infants diagnosed with MLL fusion bearing leukemias have a particularly poor prognosis. Hence effective therapies that target the aberrant molecular mechanisms harnessed by the *MLL* rearrangements need to be developed. Our laboratory has previously established that the AF4-AF9 protein-protein interaction is important to sustain the viability of MLL fusion carrying leukemic cell lines. Disruption of this interaction on exposure to PFWT, an AF4 mimetic peptide reduced the viability of the leukemic cell lines *in vitro* (Srinivasan et al., 2004a). We further modified this peptide to possibly increase its *in vivo* stability. Discussed here are the results of the experiments performed to test the efficacy of the modified AF4 mimetic peptide SPK111.

Exposure to increasing concentrations of the SPK111 peptide effectively decreases the viability of MV4-11 (MLL-AF4), MOLM13 (MLL-AF9), and KOPN8 (MLL-ENL) leukemia cells carrying MLL-fusions (Figure 9). SPK110 is a control peptide with a single amino acid ornithine substituted with aspartic acid. Exposure to

SPK110 does not lead to a similar decrease in viability suggesting that the observed effects are specific to SPK111 (Figure9). Moreover, MLL-fusion carrying leukemia cells exhibit greater sensitivity to the peptide compared to the non MLL rearranged leukemia cell lines such as K562 (BCR-ABL), Reh (TEL-ETV6) and MOLT4 (p53 mutant, T lymphoblast) (Figure 9). This therapeutic specificity is attributed to the dependence of MLL fusions on the super elongation complex (SEC).

The most frequently occurring MLL fusion partners ELL,AF4, AF9 and ENL are components of the SEC (Mohan et al., 2010b). The MLL fusions function as oncoproteins by recruiting the SEC due to protein-protein interaction (Bitoun et al., 2007a; Mueller et al., 2009; Yokoyama et al., 2010). The recruited SEC promotes ectopic expression of genes required to sustain leukemia. SPK111 was designed to inhibit the AF4-AF9 interaction, which is a part of the SEC. In chapter 3, we demonstrate that SPK111 effectively decreases the AF4-AF9 interaction and reduces the activity of the SEC. Hence, we attribute the observed specific sensitivity of MLL leukemia cells to the disruption of SEC integrity by SPK111. Leukemic cell lines with wild type MLL do not depend on SEC and hence exhibit less or no sensitivity to the peptide.

The observed sensitivity to the peptide cannot be attributed to a difference in uptake of the peptide between different cell lines. The Tat transduction sequence is known to transport short peptides similar to the AF4 mimetic peptide across the plasma membrane in an energy independent manner (Tunnemann et al., 2006). As this occurs by passive diffusion, it is less likely that SPK111 uptake varies between different leukemic cell lines.

In order to further test the efficacy of SPK111 *in vitro*, we generated xenografted mice. Non obese diabetic severe combined immunodeficiency (NOD/SCID) mice were sub-lethally irradiated with 250cGy of whole body radiation prior to transplant. Sub-lethal irradiation leads to a decrease in bone marrow density permitting an enhanced long-term xenograft (Andrade et al., 2011). Using tail vein injections, we established xenografted mice carrying MOML13 or KOPN8 leukemia (Appendix Figure 30). Similar attempts to transplant K562 in NOD-SCID mice did not result in xenografts. (Appendix Figure 31). Previous studies in literature describe orthotopic xenografts of K562 cells in immunocompromised mice. However, disseminated K562 xenografts are not described (Ren et al., 2010; Yu et al., 2006). It is possible that the grafted K562 human leukemic cell lines do not survive in the hematopoietic environment of the murine system. It is known that human hematopoietic cells are less responsive to murine GM-CSF and IL-3 cytokines. This effect may play a role in failure to form a disseminated graft (Auffray et al., 1994; Drake et al., 2012). Also attempts to xenograft leukemic cells by retro-orbital injection did not yield a robust xenograft due to technical failure (data not shown).

The established MOLM13 and KOPN8 xenografted mice were used in subsequent independent experiments to test the effect of SPK111 administration on survival. Identification of human CD45 antigen using immunolabeling and flow analysis from the whole blood of the grafted mice was used to confirm the presence of the graft at the end of each survival experiment (data not shown). The parameters varied for these experiments include the amount of (drug) SPK111 administered, the number of doses administered, and the time point at which the first dose was administered. Neither

treatment with 25mg/kg for prolonged period of time (10-12 doses) nor treatment with a larger dose of 37.5mg/kg (5 doses) significantly improved the survival of KOPN8 or MOLM13 xenografted mice (Figure 10 and 12).

We observed skin lesions with 25mg/kg SPK111 injections which worsened with increased dose of 37.5mg/kg. These lesions raised the possibility of secondary infections and hence limited the amount of peptide that could be administered in a single dose. In chapter 3, we show that SPK111 induces necrosis of leukemic cells (Figure 18). Hence it is possible that the administered SPK111 induces necrosis at the site of injection. To circumvent the problem of skin toxicity, in one experiment we administered 50 mg/kg of SPK111 by intraperitoneal injections. However, the intraperitoneal injections of the drug were not well tolerated by the mice resulting in death of the mice and termination of the experiment. SPK111 was also administered two days after transplant, when leukemic burden is presumed to be low. However, this strategy did not result in improved survival of xenografted mice (Figure 11).

The lack of activity of peptide administration *in vivo* is in direct contrast to decreased viability of leukemic cells seen *in vitro*. Several parameters such as the serum levels of a drug and its rate of clearance from the system impact its *in vivo* efficacy (Lin, 2009). We designed an enzyme linked immunosorbent assay (ELISA) to test the serum levels of SPK111 at various time points after subcutaneous injections (Figure 17). However, we could not detect its presence in the serum 1 hour and 3 hours after 50mg/kg subcutaneous injection (Figure 17). This suggests that the peptide does not distribute evenly throughout the body or does not enter systemic circulation or is cleared rapidly.

Alternatively, the protein transduction domain tagged to the N-terminus of the peptide could result in higher intracellular accumulation and hence its presence could not be detected in the serum samples or it could be rapidly degraded by proteases. Further testing of whole blood cell lysate and organ homogenates such as skin from the site of injection, kidney and liver after SPK111 administration will help determine how SPK111 is distributed in the murine system. Fluorophore labeled SPK111 can be synthesized to monitor its dynamic distribution in mice (Vasquez et al., 2011). Knowledge of dynamic distribution can help guide better dosing strategies for effective treatment.

AF9 is highly expressed in hematopoietic stem cells. A shRNA mediated knockdown of AF9 in cord blood derived lineage-negative-multipotent-hematopoietic-progenitor cells results in decreased erythrocyte colony formation (Pina et al., 2008). In contrast, overexpression of AF9 in the same cells results in increased erythrocyte and megakaryocyte colonies with a corresponding decrease in granulocyte and monocyte precursors (Pina et al., 2008). As SPK111 is an AF4 mimetic peptide that binds to the AF9-carboxyl terminus and blocks its activity, we tested its effect on normal hematopoiesis in C57BL/6 mice. These mice were subcutaneously injected with 50mg/kg/day of SPK111 for five consecutive days. This dose corresponds to the maximum dose of SPK111 we used in our survival experiments. Seven days after SPK111 treatment; we did not observe much effect on the total white blood count, platelet count and the hemoglobin content in the whole blood samples collected from the treated mice (Figure13). Further, a comparison of cells derived from the bone marrow of SPK111, SPK110 and vehicle treated mice showed no significant changes in the number

of cells expressing CD41, a multipotent hematopoietic precursor and megakaryocyte marker. The increased variability seen in Ter119 expressing cells is a possible effect of an excessive lysis by the RBC lysing buffer (Figure14). A two fold increase in Gr-1, a marker of myeloid precursors, is seen in both SPK110 and SPK111 treated cells. This suggests that the observed increase in myeloid population is based on the entire sequence of the peptide and does not represent the effect of the charged interaction of ornithine on SPK111. A future study using a large number of animals needs to be performed to determine if both the active and the mutant peptide induce changes in the myeloid lineage.

In humans, autologous transplant of hematopoietic stem cells is perfomed after a high dose of radiation. Purging of cancer cell with drugs like 4-hydroperoxycyclophosphamide or using cancer cell specific antibodies prior to autologous transplant is a therapeutic strategy under study (Kasamon et al., 2011; Selvaggi et al., 1994; Yeager et al., 1986). We determined if SPK111 can be used for purging of leukemic cells *ex vivo* prior to autologous transplant. Treatment of MOLM13 and luciferase expressing MV4-11 cells *in vitro* before tail vein injection leads to a failure in establishment of leukemia in the grafted mice (Figure 15 and 16). Hence, there is the possibility of using SPK111 to "purge" bone marrow prior to autologous transplantations. This purging treatment will decrease or preferably eliminate the incidence of minimal residual disease present in the transplant sample, thereby preventing a relapse after transplant. Several studies on leukemic initiating cells have been performed by *ex vivo* exposure of leukemic cells to experimental drugs prior to transplant. The drug is

considered effective if the exposed cells fail to transplant (Diamanti et al., 2013). The failure of   SPK111 exposed MOLM13 and MV4-11 cells to establish xenografts, suggests that the peptide effectively eliminates leukemia initiating cells.

CHAPTER 3

WORKING MECHANISMS OF SPK111

Abstract

SPK111 is an AF4 mimetic peptide, designed to inhibit AF4-AF9 interaction. AF4-AF9 is a part of the super elongation complex whose activity is required to sustain MLL mediated leukemogenesis. Hence, inhibition of this interaction may be of therapeutic value for MLL leukemia. Here, we demonstrate that MLL leukemic cell lines undergo necrotic cell death on treatment with SPK111. Further, we show that SPK111 inhibits the AF4-AF9 interaction using co-immunoprecipitation experiments. Incubation with SPK111 also leads to a decrease in the activity of the super elongation complex dependent luciferase reporter. Further, we observe a decreased stability of RPB1, the largest subunit of RNA polymerase II on incubation with SPK111. This is consistent with the known degradation of RPB1 due to irreversible stalling of RNA polymerase II under conditions of cellular stress. Based on the results described in this chapter, we conclude that SPK111 inhibits AF4-AF9 interaction which leads to decreased SEC activity.

Introduction

The super elongation complex (SEC) promotes productive elongation of genes at which RNA polymerase II pauses thirty to forty base pairs from the transcriptional start site. This type of regulation promotes rapid induction of genes such as heat shock genes,

serum-inducible genes, and also facilitates synchronous induction of developmental genes (Fuda et al., 2009; Gilmour, 2009).

The constituent proteins of the SEC are the ALF family of proteins (AF4/AF5), the ELL family of proteins (ELL1/2), the YEATS domain-containing proteins (AF9/ENL) and the positive transcription elongation factor b (PTEFb)(Lin et al., 2010a). AF4 and AF5 of the ALF family form heterodimers. They functions as a central scaffold for the assembly of the SEC. Deletion mapping of AF5 suggests that it directly binds Cyclin T1, ELL1/2 and AF9/ENL through distinct domains (Chou et al., 2013). ELL and AF9 independently associate with PAFc which mediates the interaction of SEC with RNA polymerase II (Chou et al., 2013; He et al., 2011). PTEFb, another component of SEC, is a dimer of cyclin dependent kinase 9 (CDK9) and cyclinT1. It phosphorylates the Serine 2 residue of the heptamer repeats found within the C-terminal domain of RPB1, the largest subunit of RNA polymerase II, and also phosphorylates two negative transcription elongation factors, DSIF and NELF. These phosphorylation events permit dissociation of the negative transcriptional elongation factors and productive transcription of genes with paused RNA polymerase II (Isel and Karn, 1999; Peterlin and Price, 2006).

Under physiological conditions, specific interactions with transcription factors or transcriptional co-activators lead to the recruitment of the SEC. Retinoic acid receptor complex is a transcription factor that leads to the recruitment of SEC to *Hoxa1*, *Cdx1* and *Cyp26a* genes to promote neuronal differentiation (Lin et al., 2011). Further, ELL which is a part of the SEC is known to interact with the mediator complex. The mediator complex is a transcription co-activator and plays a role in recruitment of

SEC on transcriptionally paused genes. Knock down of MED26, a component of the mediator complex, leads to decreased presence of SEC components on the transcribed regions of *Hsp70* and the *MYC* genes (Dawson et al., 2011; Takahashi et al., 2011).

The SEC also plays are role in HIV pathogenesis. The basal transcription of HIV genome is dependent on SEC. However, this transcription is inefficient due to the liable nature of ELL2, a component of SEC. During productive elongation, the viral Tat protein recruits more ELL2 and PTEFb to its long terminal repeat (LTR). The association of ELL2 with active PTEFb increases its half-life and accelerates the transcription of the provirus (He et al., 2010).

In addition to their role in HIV, the SEC proteins are found as fusion partners of MLL. They aberrantly recruit the SEC through protein-protein interaction, resulting in deregulated transcriptional elongation of genes required to promote leukemogenesis (Yokoyama et al., 2010). Further, the N-terminal MLL domain of the MLL fusions interacts with RNA polymerase associated factor c (PAFc), which in turn interacts with the yeats domain of AF9 or ENL and recruits the SEC (He et al., 2010). It has been shown that the Bromodomain 4 (Brd4) protein that binds acetylated histones can also recruit SEC. Uncoupling of the transcription elongation from acetylated histones by small molecule inhibitors that block the acetyl binding by Brd4 inhibits MLL leukemogenesis (Dawson et al., 2011; He et al., 2010).

Thus the recruitment of the SEC either by Brd4 or MLL-N terminal or by the fusion partner (AF4, AF9, ENL and ELL) is required for leukemia. In this chapter, we explore the possibility of inhibiting the SEC activity by competitively inhibiting the

interaction between AF4 and AF9, two of its constituent proteins using the AF4 mimetic peptide SPK111.

Materials and Methods

Annexin V and Ethidium Bromide staining

BD Pharmigen Annexin staining kit (# 559763) was used for these experiments. One million MOLM13 and MOLT4 cells were treated with 25µg/ml SPK111 or 25µg/ml SPK110 or DMSO for 6 hours. Cells were then washed in ice cold PBS and suspended in 100µl 1X binding buffer (0.1M Hepes pH 7.4, 1.4M NaCl, 25mM $CaCl_2$). 7-AAD (5 µL) and PE annexin V (5 µL) were added to the cell suspension and incubated for 15 minutes in the dark at room temperature, followed by detection of labeled cells within 1 h on a BD Canto II flow cytometer. Analysis of data was done using the Flow Jo 2.0 software.

Electron Microscopy

MOLM13 cells were exposed to 25µg/ml SPK111 or SPK110 or DMSO for 6h and 24 h. After treatment, the cells were collected by centrifugation and suspended in 3 % glutaraldehyde prepared in 0.1 M sodium cacodylate buffer. Cells were then treated with 1% osmium tetroxide, dehydrated, embedded in resin and sectioned. Ultra-thin sections were then stained with aqueous solutions of uranyl acetate (2%) for 10 mins and lead citrate (0.3%) for 5 min, and digitally photographed using a Hitach H600, transmission electron microscope.

Western blot analysis of RNA polymerase II protein level

For western blot analysis, K562 and MOLM13 cells were treated with 25 µg/ml of SPK111 or SPK110 or equal volume of DMSO for 6 h and 24 h. Following incubation, cells were lysed in Tris buffer (30 mM Tris pH 7.4, 150mM NaCl, 0.5 % Triton-X 100 (v/v)) supplemented with 1X protease inhibitor cocktail (Sigma P8340) and 1mM DTT. Lysed cells were sonicated. After sonication, the lysate was centrifuged at 4$^\text{o}$C to separate insoluble debris. The cleared lysate was boiled along with an equal volume of 2X Laemlli buffer for 10 mins. Proteins were separated on 8% Tris-acetate gels (Invitrogen), transferred to PVDF membranes and probed with anti-RNA pol II clone CTD 4H8 antibody (Millipore) diluted to 1:2000 and anti-actin (Sigma-A5441) diluted to 1:10,000 in 5% - milk containing PBS. The signal was detected by chemiluminescence using Amersham ECL Plus reagents.

Co-immunoprecipitation

Co-immunoprecipitation experiments were performed to determine effect of SPK111 on the AF4-AF9 interaction. HEK293T cells were transfected with FLAG-AF9 and GFP-AF4$_{755-777}$. The transfected cells were treated with 37.5µg/ml SPK111, SPK110 or DMSO for 24 h before they were lysed in Tris buffer (30mM Tris pH7.4, 150mM NaCl, 0.5% Triton-X 100 (v/v), 1X protease inhibitor cocktail and 1mM DTT) and sonicated. The sonicated lysate was centrifuged at 11,000rpm at 4^{0}C for 10 mins. 37.5µg/ml SPK111, SPK110 or DMSO was added to the cleared cell lysate. After peptide incubation for 3h at 4^{0}C, the anti-FLAG M2 agarose beads or isotype control antibody

bound agarose was added to immunoprecipitate AF9 associated proteins. The agarose bound proteins were washed three times with lysis buffer, suspended in 2X Laemlli buffer, boiled and separated by electrophoresis (Invitrogen Nupage SDS 4-12% gradient gels). The FLAG-AF9 immunoprecipitate was blotted using anti rabbit polyclonal GFP anti body (life technologies # A11122). The expressed Flag AF9 was detected in cell lysate using M2 antibody (Sigma #F1804).

Luminescent reporter assay

HeLa cells were transfected with expression vectors carrying HIV LTR firefly luciferase, HIV Tat, and Renilla luciferase (a gift of Dr Andrew Rice, Baylor College of Medicine) at a ratio of 15:3:7 weight by weight using Lipofectamine 2000 (Invitrogen). In control experiments, we replaced Tat with empty vector. Media was changed after 6-8 hours to avoid any lipofectamine-related toxicity. Twenty-four hours after transfection, the cells were treated with the indicated concentration of SPK111 or DMSO. After 24 hours of treatment, cells were lysed according to the Promega Dual Luciferase Reporter Assay protocol (E 1960), and the signal was read using a Veritas 96-well luminescent plate reader equipped with a dual auto-injector system. The luminometer was pre-programmed to perform injections and to complete sequential readings of both firefly and Renilla luciferase reporter activity. Renilla luciferase activity was used to normalize for transfection efficiency.

Results

SPK111 induces necrotic cell death

The AF4 mimetic peptide, PFWT, has been shown to induce necrosis in MLL leukemia cell lines (Palermo et al., 2008). The amino acid sequence of SPK111 peptide is the same as PFWT except for the modification of the amino acids to enhance *in vivo* stability (Figure 8). Hence, SPK111 was predicted to induce necrosis of MLL leukemia cell lines. Following exposure to SPK111, the ultra-structural changes observed by electron microscopy in MOLM13 cells expressing MLL-AF4 are consistent with necrotic cell death. The electron micrograph shows that cell have intact plasma membrane after vehicle treatment or treatment with the mutant peptide, SPK110. In contrast, SPK111 treated cells features of cells undergoing necrosis such as disruption of the plasma membrane and release of cellular contents (Figure 18).

Annexin V staining is used to detect phosphatidylserine on the outer cell membrane which is a distinctive feature of apoptotic cells. This is combined with 7AAD staining which stains cells that have lost membrane permeability and hence are no longer viable. A double positive staining with Annexin V and 7AAD with no increase in the staining of annexin V alone would indicate that the cells lose viability due to loss of membrane permeability.

MOLM13 cells that were incubated with 25µg/ml of SPK111 for 6 hours showed a 58% increase in double positive stained cells and a small 7% increase of annexin stained apoptotic population compared to vehicle (DMSO) treated cells. This indicates

that there is loss of membrane permeability following SPK111 treatment (Figure19). A similar exposure of MOLM13 to SPK110, the mutant peptide also leads to a 25 % increase in double positive stained cells suggesting that the mutant does retains some activity. MOLT4, a T-ALL leukemic cell line expressing wild-type MLL was also incubated with SPK111, shows the absence of any staining. This cell line is resistant to SPK111 and is used to demonstrate the specificity of the peptide.

SPK111 inhibits AF4- AF9 interaction

The peptide sequence of SPK111 mimics the AF9 binding region of AF4 (Figure 8). It has been designed to competitively inhibit the AF4-AF9 interaction. Structural studies performed by Leach *et al* suggest that amino acid 761-775 of AF4 interact with AF9. Hence we used the GFP tagged fragment of AF4 expressing the amino acids 755-777 for co-immunoprecipitation experiments. HEK293T cells were transfected with FLAG AF9 and GFPAF4$_{755-777}$ and exposed to 37.5µg/ml SPK111, 37.5µg/ml SK110 or DMSO vehicle control for 24 hours. The GFPAF4$_{755-777}$ fragment immunoprecipitates with FLAGAF9 in the presence of DMSO. The amount of GFPAF4$_{755-777}$ fragment immunoprecipitated by FLAGAF9 decreases on treatment with both the SPK111 and the SPK110 peptide. However, the amount of the immunoprecipitated GFPAF4$_{755-777}$ AF4 in the presence of SPK111 is quantitatively lower than the amount precipitated from cells treated with SPK110 (Figure 20). This suggests that the peptide inhibits AF4-AF9 interaction.
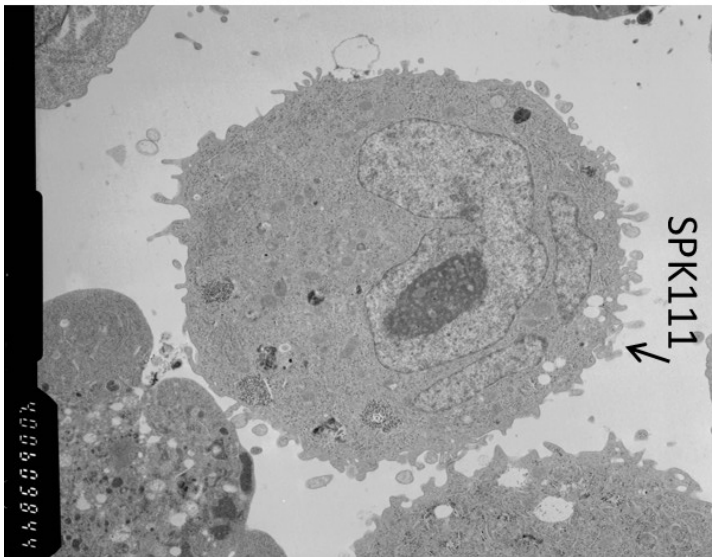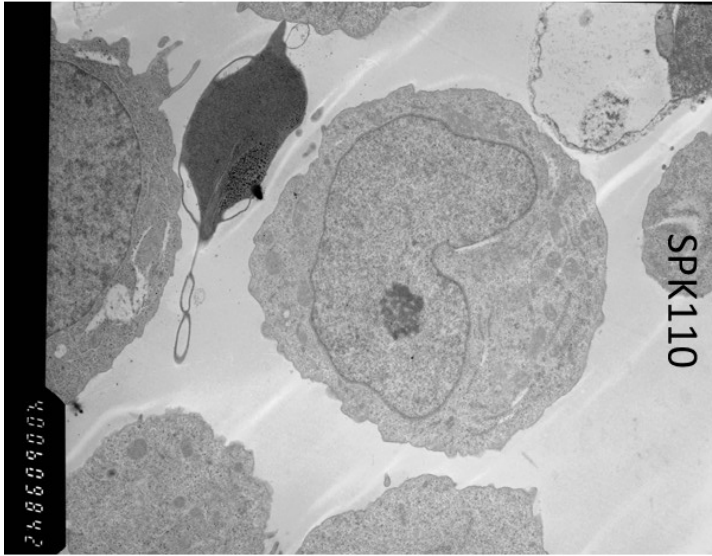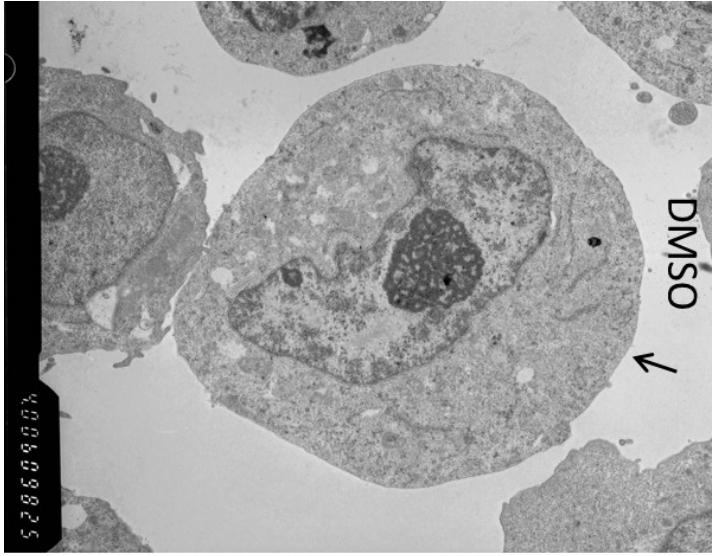
DMSO

SPK110

SPK111

B
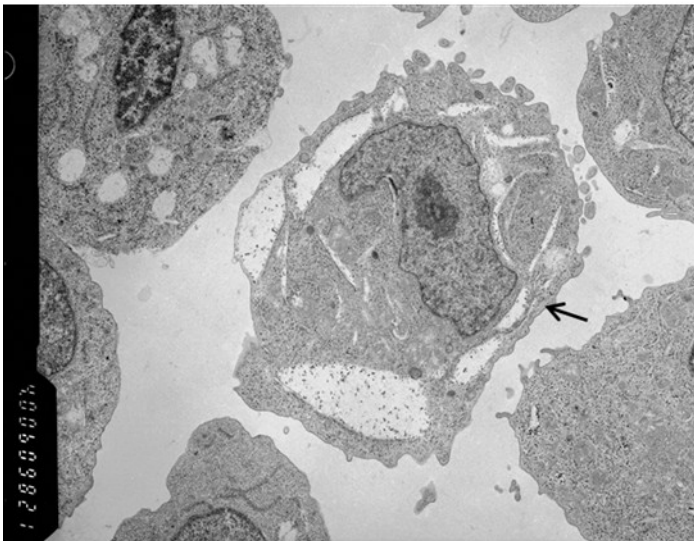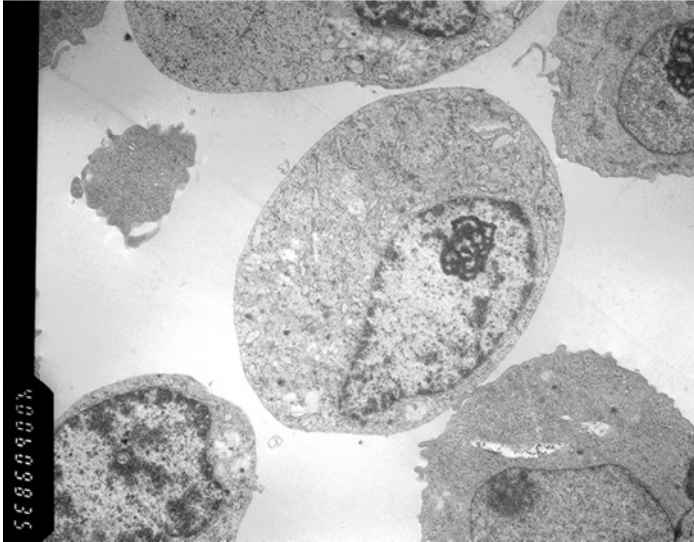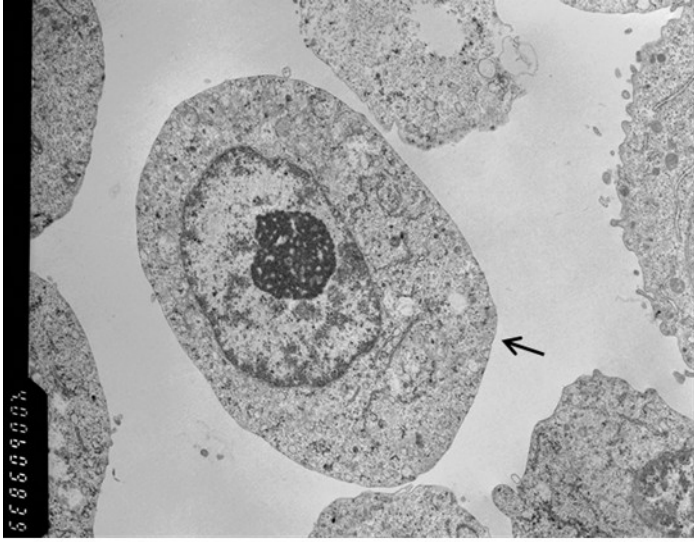
Figure 18 Necrosis induced by SPK111

Electron micrograph of the morphological changes in MOLM13 cells treated with 25µg/ml of SPK111 for 6 hours (A) and 24 hours (B). Vehicle (DMSO) treated and mutant peptide treated cells show intact plasma membranes (arrows). SPK111 treatment induced necrotic changes include plasma membrane (arrows) disintegration.

A
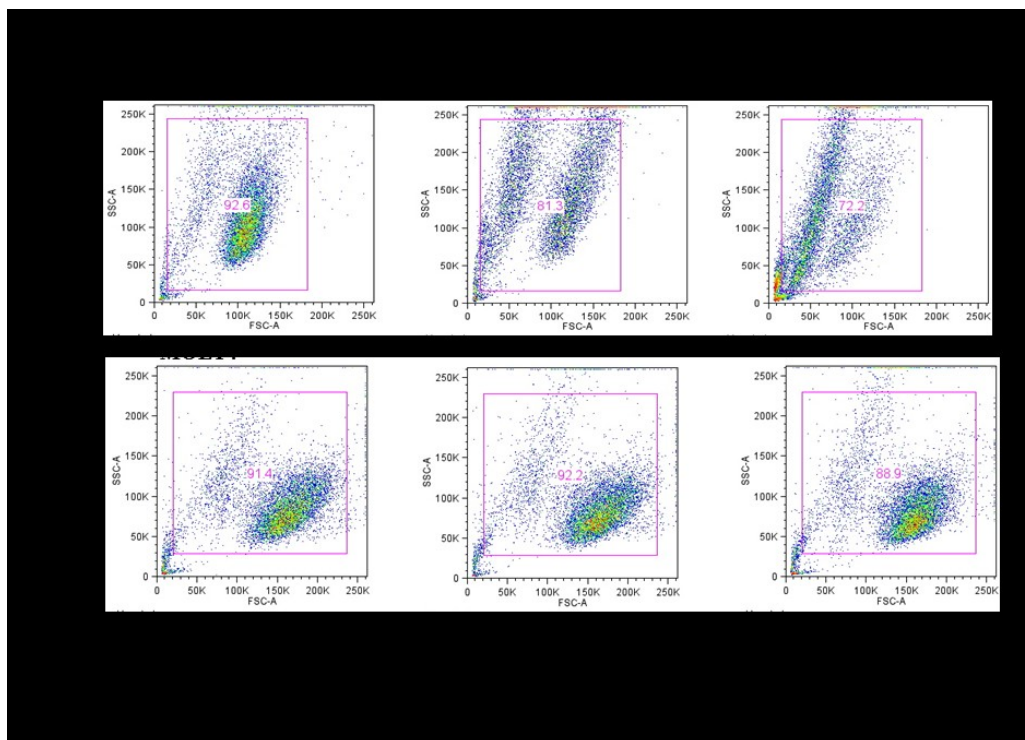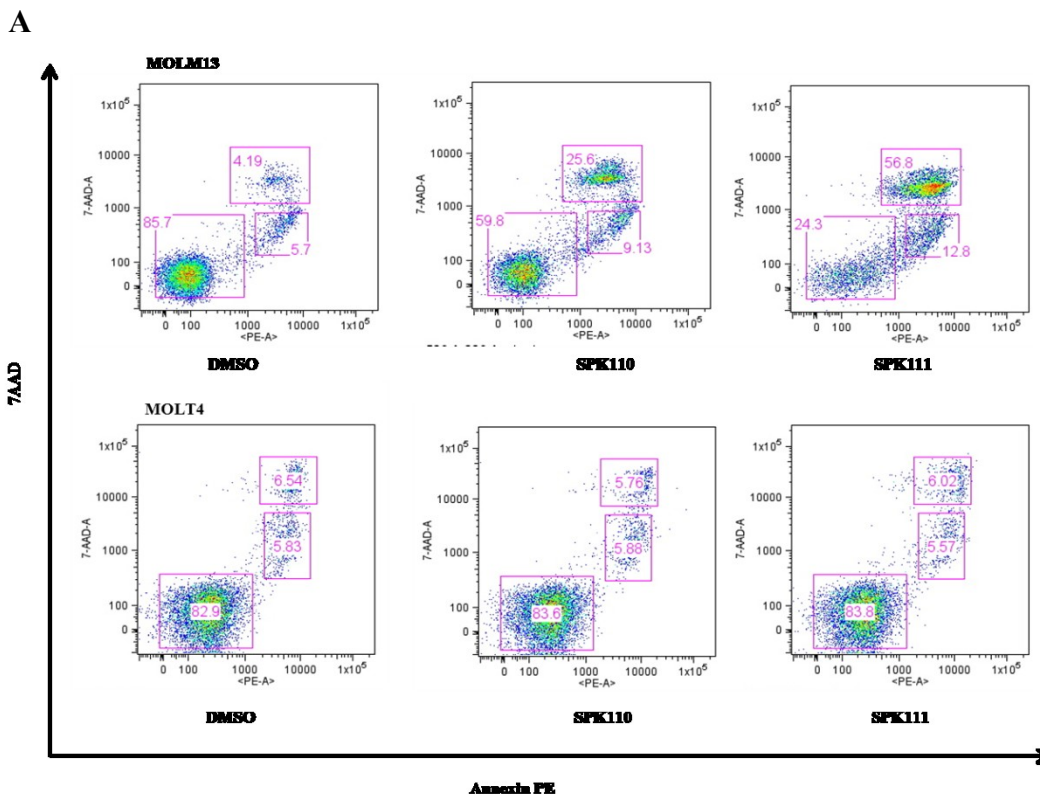
Figure 19 Loss of membrane integrity on incubation with SPK111

(A) Annexin and 7 AAD labeling of MOLM13 (MLL-AF9) and MOLT4 (WT-MLL) cells incubated with DMSO or 25 µg/ml of SPK110 or 25 µg/ml SPK111 for 6 hours. Double positive staining indicates loss of membrane permeability in MOLM13 cells and the absence of staining of SPK111-insensitive MOLT4 cells is used to indicate the specificity of the SPK111 peptide. The data is representative of two independent experiments. (B) Forward scatter and Side scatter plots are used for gating of cells analyzed in A.

Exposure to SPK111 decreases SEC dependent transcription

Productive transcription of the HIV long terminal repeats (LTR) depends on the SEC. The basal transcription of the HIV occurs at a very low rate due to the instability of the ELL2 protein, a component of SEC. The ELL2 is a short lived protein that is further stabilized through its interaction with active PTEFb. During basal transcription, the levels of active PTEFb are low. The viral Trans-activator of transcription protein (Tat) overcomes this limitation by recruiting more ELL2 and active PTEFb, resulting in the stabilization of ELL2 and faster HIV transcription rates (He et al., 2010; Liu et al., 2012). A HIV LTR-driven luciferase reporter was designed to monitor the pro-virus transcriptional activity. This reporter plasmid had previously been used to demonstrate the efficiency of transcription elongation by the Tat-recruited SEC (Lin et al., 2010b). As AF4 and AF9 are the constituent components of the SEC, we hypothesize that inhibition of this interaction by the peptide SPK111 will negatively affect the transcriptional activity of the viral Tat-recruited SEC. HeLa cells are known to express all the protein components of SEC, and hence were used as a model system to test effect of SPK111 on HIV LTR reporter activity. Viability assays (data not shown) were performed to test the sensitivity of Hela cells to SPK111. A concentration of SPK111 below 50µg/ml did not affect its viability. Hence a concentration range of 25µg/ml to 50µg/ml was used to perform assay. HeLa cells were transiently transfected with HIV LTR reporter plasmid and Tat or empty vector. As shown in Figure 21, we observe a concentration dependent decrease in Tat mediated reporter activity following exposure to SPK111. Further,

exposure to SPK111 does not affect the basal transcriptional activity in the absence of Tat. This shows that SPK111 impairs Tat recruited SEC transcriptional activity.

SPK111 exposure decreases the stability of RNA polymerase II

Phosphorylation of serine 2 on the carboxyl terminal domain of RPB1, the largest subunit of RNA polymerase II, is a mark of active transcription catalyzed by PTEFb. As hypothesized, if SPK111 treatment disrupts the interaction between SEC component proteins AF4 and AF9, then we should detect the changes in serine 2 phosphorylation of RPB1. However, we observed an overall decrease in the levels of RPB1 on SPK111 exposure as illustrated in Figure 22. Incubation of the sensitive MOLM13 (MLL-AF9) cell line with 25μg/ml of SPK111 for 24 hours leads to a decrease in levels of RPB1, the largest subunit of RNA polymerase II. This decrease is specific as it is not observed following incubation of MOLM13 with SPK110 and on incubation of K562 (WT MLL) with SPK111. These results are further explained in the discussion.

Discussion

AF4 and AF9 are among the most common MLL fusion partners (Prasad et al., 1995). They directly interact with each other and importantly, both the MLL-AF4 and the MLL-AF9 fusions retain the domain required for this interaction (Erfurth et al., 2004). Further, AF4 and AF9 are a part of the SEC and it is suggested that the misregulated
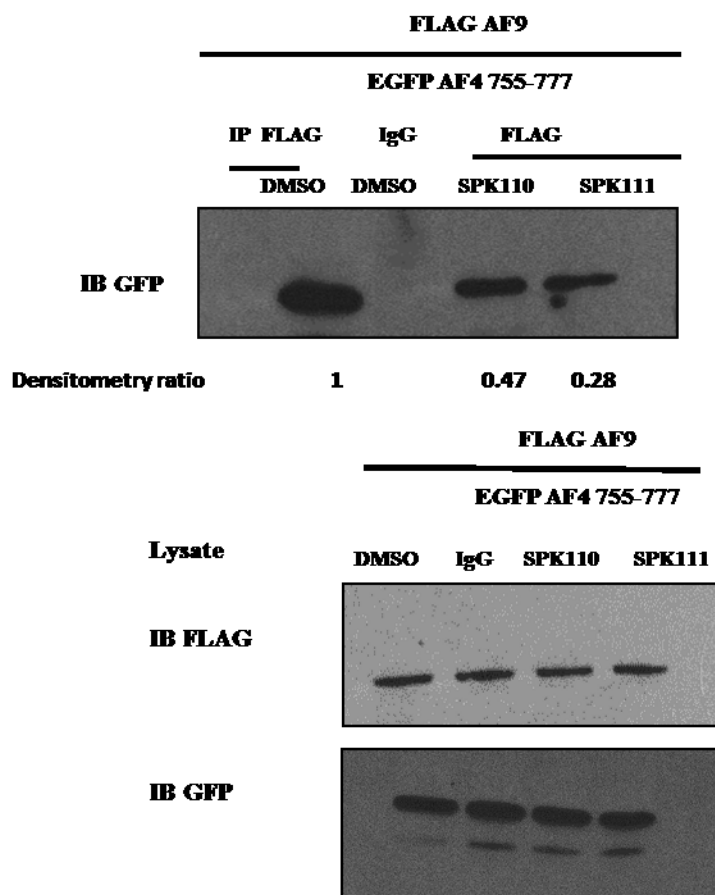
Figure 20 SPK111 inhibits the binding of AF4 and AF9

HEK293T cells were transiently co-transfected with FLAG-AF9 and GFP-AF4 $_{755\text{-}777}$ and incubated with 37.5µg/ml of SPK111 for 24 hours. After treatment, Flag AF9-bound GFP AF4 was immunoprecipitated with anti-FLAG antibody bound to agarose and analyzed by western blot using anti-GFP antibody. The blot is a representative of two independent experiments.
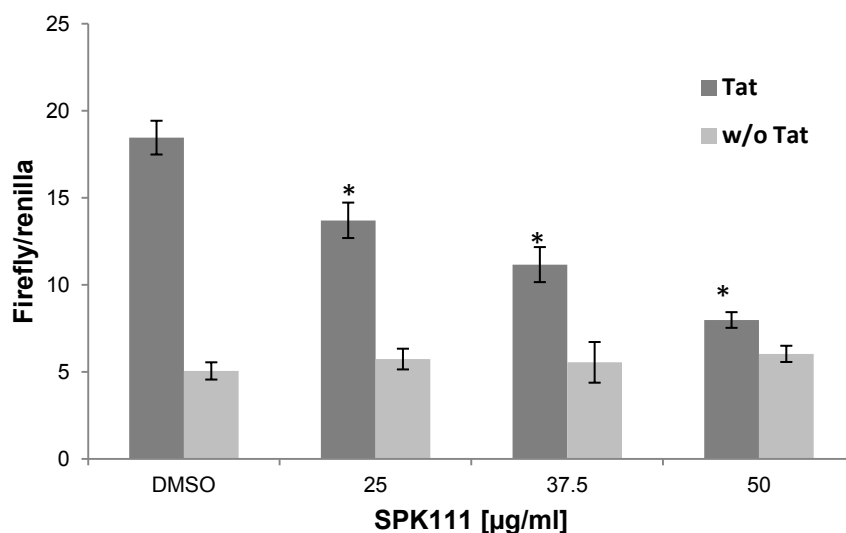
Figure 21 Decrease in HIV LTR assay activity on incubation with SPK111

Hela cells transiently transfected with plasmids expressing the HIV LTR luciferase reporter, Tat/ empty vector, and renilla luciferase are exposed to increasing concentration of SPK111 for 24 hours. After incubation luminescence is measured. The measured luminescence of the reporter is normalized to the luminescence of the co-transfected renilla luciferase. Error bars indicate standard deviation of triplicate wells. * indicates p values <0.05 using a two tailed student t-test. Figure is representative of three independent experiments.
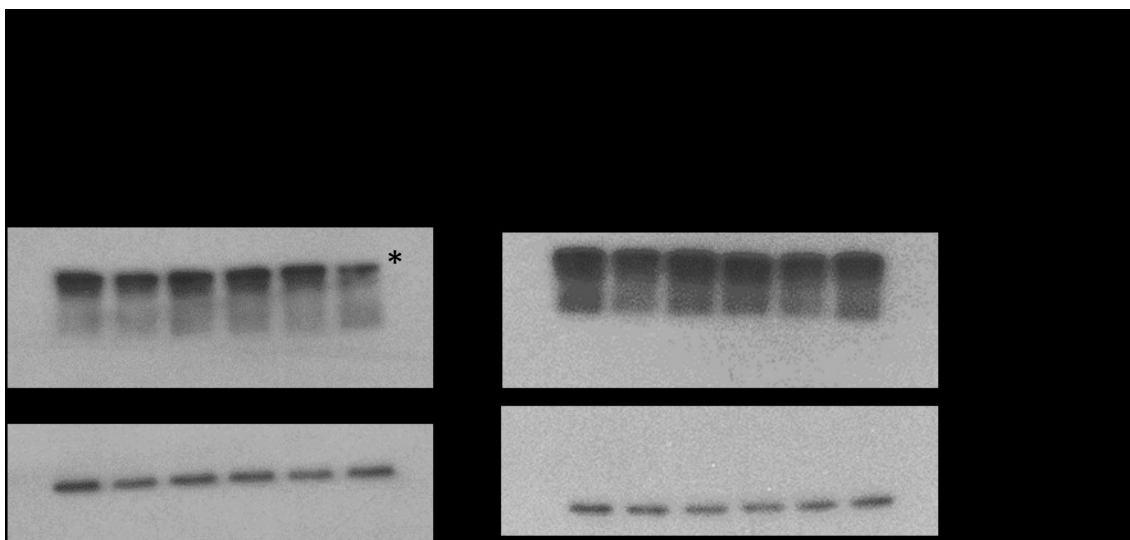
Figure 22 SPK111 exposures leads to decrease in RPB1 stability

MOLM13 and K562 cells are treated with 25ug/ml SPK111 for 6 hours and 24 hours.

After treatment, cells are lysed and RPB1 levels are determined by western blot. Actin is

used as loading control. A decrease in the level of RPB1 is observed after 24 hours in

MOLM13 cells indicated by the *. The figure is representative of two independent

experiments.

activity of the SEC leads to MLL leukemogenesis (Mueller et al., 2009). Hence, targeting of the AF4-AF9 interaction may lead to decreases in the activity of abnormal SEC.

SPK111 mimics the AF9 binding domain of AF4 which spans the amino acids 759 to 771. Hence, the peptide should competitively inhibit the coimmunoprecipitation of the FLAGAF9 and GFPAF4 $_{755-777}$. Results shown in figure 20 confirm that the presence of SPK111 displaces the AF4-AF9 interaction (Figure 20). Structural analysis of the AF4-AF9 interaction performed by Leach *et al* suggests a charged interaction between AF4 lysine 764 and glutamic acid 544 of AF9. The positive charged lysine 764 is replaced by the amino acid ornithine in SPK111 peptide. Ornithine has a higher pK_a than lysine and hence forms a stronger salt bridge interaction with AF9 that competitively inhibits the interaction with endogenous AF4.

The amino acid sequence of the mutant peptide SPK110 is the same as SPK111 except for the substitution of positively charged ornithine with negatively charged glutamic acid. This glutamic acid repels the complementary negative charge in AF9. Thus, it is less likely to interfere with endogenous AF4 and AF9 electrostatic interaction. However, SPK110 exposure also leads to a decrease in AF4 coimmunoprecipitated with AF9. This decrease is quantitatively smaller compared to SPK111 (Figure 20). The structural studies of AF4-AF9 interaction performed by Leach et al., 2012 suggests that the AF4 residues 761-775 are structurally ordered in AF4-AF9 complex. In addition to the described electrostatic interaction, several hydrophobic interactions stabilize AF4-AF9 interactions. These include valine at position 763 and isoleucine at position 765 that are adjacent to charged lysine 764. Hence, it may be possible that SPK110 acts as

competitive inhibitor for hydrophobic interactions due to which it displaces the AF4-AF9 interaction to some extent. Future competitive inhibition studies using charged mutants of AF4 at 763 and 765 and at amino acids 771-775 will help determine the importance of this hydrophobic interaction.

AF4 and AF9 individually have several biological functions. However, their interaction together has only been described as a part of the SEC. Biswas *et al* have shown that AF9 mutations that selectively reduce AF4-PTEFb interaction decrease the *e*xpression of MLL and MLL fusion target gene *HOXA9*. Our data shows a decrease in Tat recruited SEC-driven transcription following SPK111 exposure as measured by HIV LTR reporter assay (Figure 21). This suggests that displacement of the AF4-AF9 interaction reduces the transcriptional activity of SEC.

RPB1 is the largest protein subunit of RNA polymerase II. During transcriptionally coupled DNA repair, RNA polymerase is paused at the site of DNA lesions. If the DNA repair mechanism fails to repair the lesion, then RPB1 is degraded. This degradation is also observed on treatment with α-amanatin which is a specific irreversible inhibitor of RNA polymerase II (Wilson et al., 2013). We found that the levels of RPB1, the largest subunit of RNA polymerase II decrease after 24 hours of exposure to SPK111 in MOLM13 cell line (Figure 22). This degradation is specific as it does not occur in the less sensitive K562 cells. This suggests that targeting the AF4-AF9 with SPK111 may lead to irreversible stalling of the SEC, promoting the instability of the stalled RNA polymerase II.

Our laboratory had previously established that the AF4 mimetic peptide PFWT induces necrotic cell death (Palermo et al., 2008). The SPK111 synthetic peptide is based on the same sequence as PFWT, hence it should also induce necrotic cell death. As shown in Figure 18, SPK111-treated MOLM13 (MLL-AF9) cells show enlargement of cells, loss of membrane integrity and spillage of cytoplasmic content into the extracellular matrix, all distinctive features of necrosis.

The absence of increase in annexin V positive and 7AAD negative staining upon SPK111 treatment of MOLM13 cells excludes apoptosis induction by the peptide (Figure 19). However, double positive staining suggests that the peptide induces loss of membrane permeability. Upon exposure of MOLM13 to SPK110, the mutant peptide also exhibits a 20% increase in double positive stained cells. As discussed earlier, SPK110 may disrupt the hydrophobic interaction between AF4 and AF9 and hence inhibit the AF4-AF9 interaction but to a lesser extent.

Previous studies performed to determine the mechanism of necrotic cell death induced by the AF4 mimetic peptide PFWT have ruled out tumor necrosis factor (TNF) activation, reactive oxygen species (ROS) production, a decrease in ATP production, the necroptotic pathway, and the lysosomal calpain-cathepsin pathway as modes of necrosis. Further, the same studies suggest specific loss of plasma membrane integrity and disruption of filamentous actin in MLL leukemic cell lines to be the cause of AF4 mimetic peptide induced cell death (Amanda Winters, dissertation). The possibility of a decrease in actin cytoskeletal stability following PFWT treatment was investigated and is further discussed in chapter 1V.

CHAPTER 4

THE EFFECT OF THE AF4 MIMETIC PEPTIDE, PFWT ON THE PROTEIN AF9
AND THE STABILITY OF THE ACTIN CYTOSKELETON

Abstract

The AF4 mimetic peptide PFWT was shown to selectively reduce the viability of
MLL leukemia cell lines. Previous studies performed to identify its mode of action show
that it induces an irreversible increase in membrane permeability. The induced
permeability was shown to coincide with an increase in monomeric actin (G-actin) and a
corresponding decrease in filamentous actin (F-actin) by fluorescent microscopy
(Amanda Winters, dissertation). Hence, we performed further studies to determine the
effect of PFWT exposure on the actin cytoskeleton. The ultracentrifugation sedimentation
and flow cytometry analysis presented in this chapter show no significant changes in F-
actin after PFWT treatment. Importantly, pre-treatment with actin stabilizing drugs fail to
protect against PFWT induced cell death. Thus, we conclude that actin destabilization is
not the primary cause of PFWT induced cell death.

Previous studies had also identified a 10 kDa increase in the molecular weight of
AF9 after PFWT treatment. Hence, we explored the possibility that AF9 is
posttranslationally modified by ubiquitination or O-glycosylation. However, our results
failed to detect these modifications. Finally, multiple putative phosphorylation sites and a
possible acetylation site were identified by mass spectrometry analysis.

Introduction

Actin cytoskeleton

Actin exists in two principal forms, globular monomeric actin (G-actin) and filamentous polymeric actin (F-actin). F-actin is a dynamic polymer. It has a fast growing end also known as barbed end where ATP bound actin monomers are rapidly added to elongate the polymer. Opposite the barbed end is the pointed end where the rate of monomer addition is very slow. Due to hydrolysis of ATP, the ADP bound actin dissociates leading to break down of F-actin. Under steady state, the rate of association of ATP-actin and the rate of dissociation of ADP-actin are in equilibrium. This equilibrium is known as actin treadmilling (Wanger et al., 1985). During actin polymerization the equilibrium shifts in favor of ATP-actin association and during de-polymerization it shifts in favor of ADP-actin dissociation.

Actin binding proteins promote either polymerization or the depolymerization of F-actin. The protein profilin preferentially binds to ATP-actin, stabilizes it and accelerates polymerization (Carlsson et al., 1977). In contrast, the protein cofilin binds both forms of actin and functions to sever filaments into short fragments and promotes subunit loss from the pointed ends. Some proteins like thymosin sequester the ATP bound monomeric actin and then release it on an appropriate signal for actin polymerization (Irobi et al., 2004). Several naturally occurring small molecules also bind to actin and alter its dynamics. These include Phalloidin and Latrunculin A. Phalloidin is a heptapeptide toxin derived from mushrooms. It inhibits F-actin depolymerization by binding adjacent actin subunits, locking them together and preventing dissociation.

Latrunculin A is a toxin derived from sponge that promotes actin depolymerization. It irreversibly binds ADP actin monomers and inhibits adenine nucleotide exchange leading to a decrease in the concentration of ATP bound actin monomers that can be polymerized. This shifts the actin dynamics in favor of depolymerization (Morton et al., 2000; Yarmola et al., 2000).

Functionally, actin plays a role in cytoplasmic process such as cell motility, endosome trafficking, scaffolding and in nuclear processes like chromatin remodeling, transcription and RNA splicing. Nuclear actin is required for efficient transcription by RNA polymerase I, II and III (Hofmann et al., 2004; Hu et al., 2004; Philimonenko et al., 2004). Actin associates with RNA polymerase II C-terminus domain via actin binding protein N-WASP which polymerizes actin to establish a scaffold to organize protein-protein interactions (Wu et al., 2006).

The actin cytoskeleton also participates in programmed cell death. A drop in cellular ATP levels during ischemia or mitochondrial damage results in depletion of the ATP bound actin monomers preventing actin polymerization. This eventually results in cell death due to diminished cytoskeletal rearrangement capacity (Atkinson et al., 2004). Further, actin plays a modulatory role in JNK and NF-κB signaling which participates in cell death programs (Papakonstanti and Stournaras, 2008). Genetic studies have also identified a role for actin in necrosis. Disruption of the *β-actin* gene by retroviral insertion, decreases β-actin protein levels, and prevents perinuclear aggregation of mitochondria and reactive oxygen species production in TNF-treated fibrosarcoma cells preventing necrosis (Kim et al., 2003; Li et al., 2004). In summary, the actin cytoskeleton

can lead to cell death either by compromise of cytoskeleton dynamics or by modulation of signaling pathways. Previous studies of PFWT treated cells showed an absence of apoptotic and necrotic markers. In this chapter we examine the effect of the PFWT peptide on F-actin dynamics.

Post translational modifications of nuclear factors.

We observed an approximately 10 kDa addition to the molecular weight of AF9 following PFWT treatment. Cellular fractionation determined that the modified AF9 localized to the nuclear compartment. O-glycosylation and ubiquitination are known to increase the apparent molecular weight of a protein in the range of 7-10 kDa and occur on nuclear transcription factors; hence we tested for these modifications. They are briefly reviewed here.

A sugar molecule named N-acetylglucosamine, when added to serine or threonine residues of the target protein, results in O-glycosylation. This sugar residue is added by the enzyme **O-GlcNAc** transferase (OGT) and it can be easily reversed by the activity of hexosaminidase called OGlcNAcase (Wells and Hart, 2003). Generally, transmembrane proteins are glycosylated on their extracellular domain or secreted proteins are glycosylated to increase their solubility. However the transmembrane and extracellular proteins carry a different form of glycosylation called N-glycosylation and typically have multiple sugar residues attached as a modification. O-glycosylation on the other hand is attachment of a single N-acetylglucosamine residue. It is found on cytosolic proteins and nuclear transcription factors including Oct-1, c-Myc, and p53. The transcription factors

Stat5 and Pax6 are O-glycosylated in the nucleus, and this modification restricts them to the nuclear compartment (Guinez et al., 2005).

Another modification found on transcription factors is monoubiquitin. It mediates nuclear transport, transcriptional activity, and protein-protein interaction. The well-known tumor suppressor, Phosphatase and tensin homolog on chromosome ten (PTEN) requires monoubiquitination for nuclear import (Trotman et al., 2007). In contrast, monoubiquitination of p53 signals its nuclear export (Nie et al., 2007).

In many transcription factors such as Myc, Jun and Fos, the transcriptional activation domain overlaps with sequences that promote rapid proteasomal degradation (degrons). Deletion of the transcription specific ubiquitin ligase (E3) blocks transcriptional activation. But, fusion of a single ubiquitin moiety to the transcription factor restores the normal transactivation without degradation (Muratani and Tansey, 2003; Salghetti et al., 2000). However, there are also examples of transcription factors such as Tax, where monoubiquitination reduces transcriptional activity without proteolytic degradation (Peloponese et al., 2004). Hence both monoubiquitination and O-glycosylation are important modifications found on transcription factors that play a role in localizing the transcription factor to the nucleus and regulating its transcriptional activity.

Materials and Methods

Flow cytometry analysis of filamentous actin content

MV4-11 cells (1 X 10^6 per ml) were suspended and treated with 25µg/ ml of PFWT, 25µg/ ml PFmut and vehicle control (DMSO) for 1hour. Following incubation, cells were rinsed with PBS and fixed with 3.4% paraformaldehyde in PBS for 15 minutes at room temperature. The fixed cells were rinsed in PBS and permeablized with 0.1% triton-x 100 in PBS for 10 minutes, then blocked with 2% BSA in PBS and stained with 1:40 diluted Phalloidin alexa488 for 15 minutes in the dark to stain filamentous actin. After incubation with Phalloidin the cells were washed twice with 2% FCS in PBS, re-suspended in the same, and analyzed on the BD Canto II flow cytometer to determine the filamentous actin content.

Ultracentrifugation assay

MV4-11 cells were treated with 25µg/ml of PFWT, 25µg/ml PFmut, and vehicle control (DMSO) for 1hour. As a positive control for actin depolymerization, MV4-11 cells were treated with 0.2µg/ml Latrunculin A (0.5µM) for 20minutes. Following this, cells were lysed in lysis and actin stabilization buffer, LAS buffer (# LAS01. Cytoskeleton, Denver, CO). The lysate was centrifuged at 2000 rpm to pellet any unlysed cells. The supernatant was spun in an ultracentrifuge at 100,000g at 4^0C. After ultracentrifugation, the supernatant containing G-actin was stored on ice. The F-actin in the collected pellet was depolymerized for an hour on ice by addition of 10 nm

Cytochalasin D in milli-Q water. The volume of depolymerization solution in which F-actin is dissolved was equal to the volume of the supernatant containing G-actin. 20µl of F and G actin containing solution was added to 2X sample buffer and run on 8-12% NuPAGE gel (Invitrogen). The gel was transferred to a nitrocellulose blot. The blot was developed using antibody to actin (Sigma # A5441). Quantification of actin was performed using image J.

Phalloidin protection assay

MV4-11 cells were treated with 2.5 µM phalloidin oleate 1 hour prior to being exposed to 25µg/ ml of PFWT, 25µg/ ml PFmut, and vehicle control (DMSO) for 1hour. Viability was assessed using cell titer glow assay as described in chapter 2.

Production of lentivirus

The lentivirus expression vectors CSIEmMLLT3, LLXshMLLT3 and CSIEm encoding for AF9, shRNA to AF9 and empty vector respectively have previously been described in Pina et al., 2008. In addition to expression of AF9, these lentivirus vectors also encode Green Flourscent Protein (GFP) which can be used for selection of the transduced cells. The lentivirus stocks of these three expression vectors were produced using Virapower lentivirus packaging mix and the 293FT cell line according to the manufacturer's protocol (Invitrogen, Carlsbad, CA). The stocks were stored at –80°C.

The titer of the lentivirus for each batch of stock was determined by Lenti-X GoStix (Clontech) using manufacturer's protocol.

Lentivirus transduction of cell line and selection by flow cytometry

For lentiviral transduction, 100,000 MV4–11 or K562 leukemia cells were mixed with 8μg/ml polybrene, lentivirus particles (Multiplicity of infection 50) in RPM1640 medium without FBS. This mix was centrifuged at 2000 RPM for 2 hours at 32° C. After centrifugation, the spinoculated mix was incubated for an additional 4 hours at 37° C. Following incubation, the cells were plated in 100 μl of RPMI 1640 media supplemented with 10% FBS and 5 ng/ml of recombinant GM-CSF (peprotech). These transduced cells were sorted for EGFP expression 7 days post transduction using fluorescent activated cell sorter (BD FACS ARIA).

SDS PAGE and western blot

Cells were lysed in lysis buffer (50 mM Tris, 150 mM NaCl, 0.25% SDS and protease inhibitor). The lysate was mixed with Laemmli buffer and boiled for 5 minutes before loading onto 4-12% Bis-Tris gradient gels (Invitrogen) for separation of proteins by electrophoresis. The separated proteins were transferred to nitrocellulose membranes, blocked in 5% milk in PBS, and incubated overnight with primary antibodies for AF9 (Novus biologicals NB-1566) at 1:1000 dilution, and actin (Sigma A5441) at 1:4000 dilution. Incubations with HRP-conjugated secondary antibodies were done at room

temperature for 1hour. The chemiluminescence signal was developed using ECL Plus detection kit (Amersham) or Dura Supersignal (Fisher).

Cellular fractionation

K562 ($1X10^6$) transduced with AF9 (modified K562) were washed in PBS, and lysed in 100 µL hypotonic lysis buffer (10 mM HEPES, 10 mM KCl, 1.5 mM $MgCl_2$, pH 7.9) at 4°C supplemented with 1 mM DTT, protease inhibitor (Sigma P8340), and phosphatase inhibitor (Sigma P0044). After incubation for 15 minutes on ice, NP-40 was added to a final concentration of 0.6% and samples were vortexed. Following vortexing, the cells were centrifuged at 11,000 rpm for 10 minutes at 4°C to pellet the nuclei. The supernatants containing cytoplasmic fraction were transferred to separate tubes, and nuclei were washed with excess hypotonic lysis buffer (11,000 rpm x 5 minutes at 4°C). Laemmli buffer was added to both nuclear and cytoplasmic fractions (100 µL each).

Sample preparation for mass spectroscopy

For initial mass spectroscopy samples, endogenous AF9 was immunoprecipitated (3 immunoprecipitation reactions were combined, each reaction used 2 ug of novus 1566 antibody for immunoprecipitation from a cell lysate of 10^7 MV4-11 cells) and separated on 4-12 % Bis-Tris gradient gel (Invitrogen). The gel was fixed using coomassie fix solution (45% methanol and 1% acetic acid) for 1 hour and then stained with colloidal coomassie reagent (170 grams ammonium sulfate, 1g coomassie G250, 5 mL acetic acid and 450 mL methanol per liter) for 2-4 hours. This was followed by 3 washes of ultra-

pure water. Using a clean scalpel, bands corresponding to 62 kDa AF9 and 58 kDa AF9 were cut out and placed in a clean eppendorf tube and shipped on ice to the mass spectroscopy facility (Louisiana State University).

For a second mass spectroscopy analysis, 20µl of αFLAG-M2 agarose was used to immunoprecipitate FLAGAF9 from cell lysate transfected HEK293T cells. The lysis and immunoprecipitation was performed in Tris buffer (50mM Tris, 150mM Nacl, 0.25% SDS and protease inhibitor). Three immunoprecipitates were combined and separated on 8-12 % Bis-Tris gradient gel, stained with coomassie, band corresponding to AF9 were cut and shipped to University of Illinois Chicago mass spectroscopy facility on ice.

Glycosylation analysis

Alkali treatment

Modified K562 ($2x10^8$) were lysed in 1ml lysis buffer (50 mM Tris, 150 mM NaCl, 0.25% SDS and protease inhibitor), sonicated for a pulse of 10 seconds then centrifuged at 11,000 rpm at 4^oC. 10 µl of 1N NaOH was added to 90 µl of cell lysate to obtain a final concentration of 0.1N NaOH. The solution was incubated at room temperature for 30 minutes. As a control, 10 µl of distilled water was added to 90 µl of cell lysate and incubated at room temperature for 30 mins simultaneously. After incubation, the samples were boiled in Laemmli for 5 minutes followed by western blot analysis.

Enzymatic deglycosylation

Enzymatic deglycosylation of modified K562 cells was performed using a deglycosylation kit purchased from QA Bioscience using the manufacturer's protocol (QA bioscience kit E-G001). For a negative control, the enzyme mix was substituted with water. For protease inhibiton IX protease inhibitor (sigma P8340) was added along with the enzyme mixture prior to incubation.

Wheat germ agglutinin (WGA) affinity assay

Modified K562 ($5x10^6$) were lysed in 100 µL buffer (40 mM Tris with 1%SDS and 2.5% mercaptoethanol buffer). The cell lysate was diluted 1:10 into immunoprecipitation buffer (500mM HEPES, 150mM NaCl, and protease inhibitors) then incubated with WGA conjugated agarose. To test for specificity of binding, WGA agarose that had previously been incubated with 1 M N-acetyl glucoseamine was also incubated with the diluted lysate. The WGA was incubated with the diluted cell lysate for one hour on a rotating platform at 4°C. The agarose was washed several times in immune precipitation buffer. The precipitated glycoproteins were mixed with Laemmli buffer and boiled for 5 minutes followed by Western blot analysis to detect AF9 (Novus 1566).

Co-immunoprecipitation

HEK293T cells were transfected with FLAGAF9 and HA tagged Ubiquitin (HA-UB) or FLAG AF9 alone or HA-UB alone. The transfected cells were lysed in Tris buffer

(30mM Tris pH7.4, 150mM NaCl, 0.5% Triton-X 100 (v/v), 1X protease inhibitor cocktail, 1mM DTT and NEM [a deubiquitin enzyme inhibitor] and sonicated. The sonicated lysate was centrifuged at 11,000rpm at 4^0 C for 10 minutes. The Anti-FLAG antibody bound beads (M2 agarose beads) were added to immunoprecipitate AF9 associated proteins. The agarose bound proteins were washed three times with lysis buffer, suspended in 2X Laemlli buffer, boiled and separated by electrophoresis (Invitrogen Nupage SDS 4-12% gels). The immunoprecipitate was blotted using anti HA antibody (Roche #1167475). The expressed FLAG AF9 was detected in cell lysate using monoclonal anti-FLAG antibody (Sigma #F1804).

Generation of AF9 point mutants

K297A and K297Q point mutations were generated in FLAG tagged full length AF9 and EGFP tagged AF9 expression vectors using Invitrogen's gene tailor site directed mutagenesis kit and the manufacture's protocol. Primers (F: GAAGAACTCTCAGCCA AAGCTAGGAAAAAGAGT, R: TTTGGCTGAGAGTTCTTCAGAATCTGAAAT) were used to generate the alanine point mutant and primers (F: GAAGAAACTCTCA GCCAAACAGAGGAAAAAGAGT, R: ATAGTTCCTAAGATGGCCCTTCAAGGAA CCT) were used to generate the glutamine point mutants.

Fluorescence microscopy

HeLa cells plated on four chamber slides (duplicates for each construct) were transfected with EGFP-AF9 and EGFPAF9K297A expression vectors using

Lipofectamine 2000 (Invitrogen) and the manufactures' protocol. 48 hours after transfection the chamber slides were washed with PBS and the cells were fixed in 3.7% formalin. DAP1 containing antifade reagent and a cover slip were then placed on the slide. Fluorescent images were taken using a Zeiss LSM-510 microscope.

Results

PFWT exposure does not significantly alter the actin cytoskeleton dynamics.

Previous microscopic examination of PFWT exposed MV4-11 cells suggest a decrease in F-actin content (Amanda Winters, unpublished data). Monomeric actin has a mass of 33 kDa and filamentous actin is a polymer, hence they can be separated based on size. Ultracentrifugation is a technique used to separate molecules based on size and has previously been used to separate F-actin and G-actin to study actin cytoskeleton remodeling (Kim et al., 2008). Hence, ultracentrifugation was used to determine changes in actin cytoskeleton following PFWT incubation. For these experiments, MV4-11 cells were exposed to 25µg/ml of PFWT, vehicle control DMSO, and latrunculin A (0.2 µg/ml). As described in the introduction, the toxin latrunculin A promotes actin depolymerization, and hence it was used as a positive control. Treatment with this toxin shows a decrease in filamentous actin indicating that the centrifugation separation works efficiently. However, there is no significant decrease in F-actin content recovered from cells incubated with PFWT compared to that recovered from DMSO incubated cells (Figure 23A). This shows that PFWT exposure did not lead to actin depolymerization in MV4-11 leukemic cells. The results of ultracentrifugation experiments were contrary to

the previous findings; hence we performed additional flow cytometry analysis of F-actin labeled MV4-11 cells after treatment with the peptide. Phalloidin binds specifically to filamentous actin and is often used for F-actin detection (Wulf et al., 1979). We performed phalloidin-FITC staining of MV4-11 cells incubated with 25µg/ml of PFWT, 25µg/ml PFmut, or vehicle control DMSO. The cells were fixed with formaldehyde after treatment and prior to labeling to ensure that the phalloidin reagent itself does not induce any dynamic cytoskeletal changes. As shown in Figure 23B, there is no shift in the F-actin (phalloidin-FITC) label intensity of the cells incubated with PFWT. Thus there is no progressive depolymerization in these cells.

Phalloidin-oleate is a semi-synthetic derivative of phalloidin with increased cell membrane permeability. This compound was used to study the role of F-actin in various cellular functions (Laudadio et al., 2005). We used phalloidin-oleate to determine if pre-incubation with an F-actin stabilizing compound could inhibit PFWT induced cell death. We first tested the sensitivity of MV4-11 cells to phalloidin-oleate and determined that a concentration range from 1µM to 5µM is nontoxic. We then incubated the MV4-11 cells with 5µM phalloidin-oleate an hour prior to incubation with vehicle control DMSO, 25µg/ml PFWT or 25µg/ml PFmut. The results of the viability assay shown in Figure 24 identified that pre-incubation with phalloidin does not protect against PFWT induced cell death.
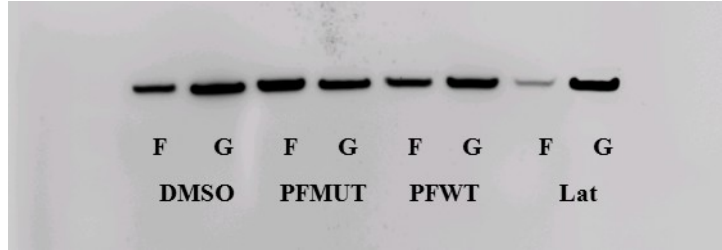
A

B
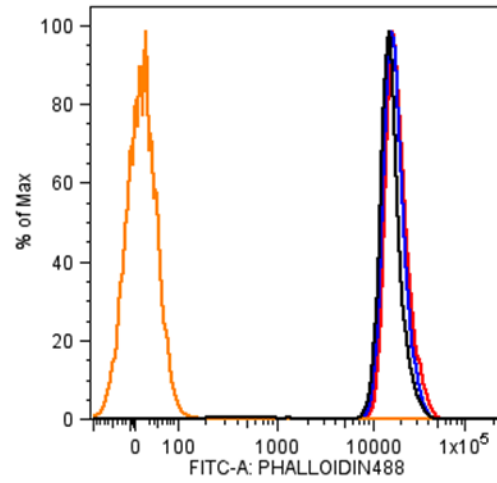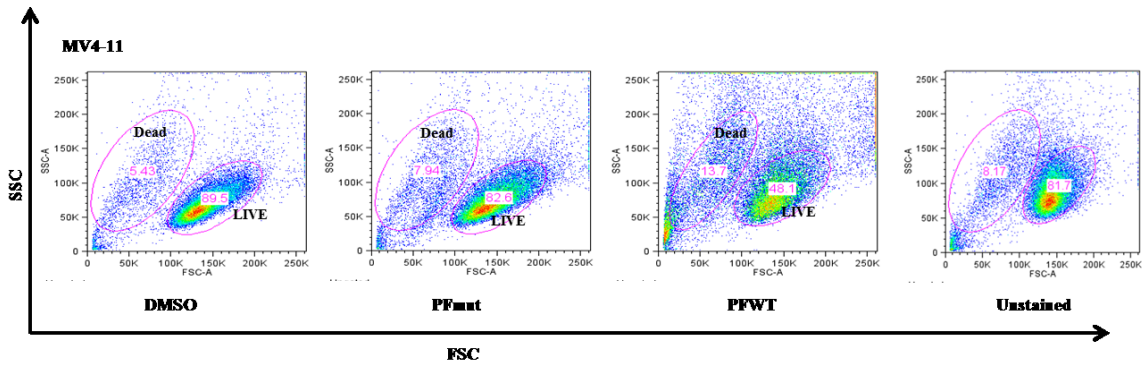
Figure 23 MV4-11 cells incubated with PFWT show no significant decrease in F-actin content

 (A) MV4-11 cells were treated with 25µg/ml of PFWT, 25µg/ml PFmut, vehicle control (DMSO), and 0.2µg/ml Latrunculin A. The F-actin and G-actin content of treated cells is separated by ultracentrifugation and blotted as described in materials and methods. The blot is a representative of two different experiments. **(**B) MV4-11 cells were treated with 25µg/ml of PFWT, 25µg/ml PFmut and vehicle control (DMSO) and labeled with FITC phalloidin. Forward scatter and Side scatter plots were used for gating live cells. The plot of phalloidin-FITC intensity shows consistent F-actin staining intensity on treatment. Results are representative of three independent experiments. (C) Orange-unstained cells, Red-DMSO treated cells, blue- PFMUT treated cells and Black- PFWT treated cells.
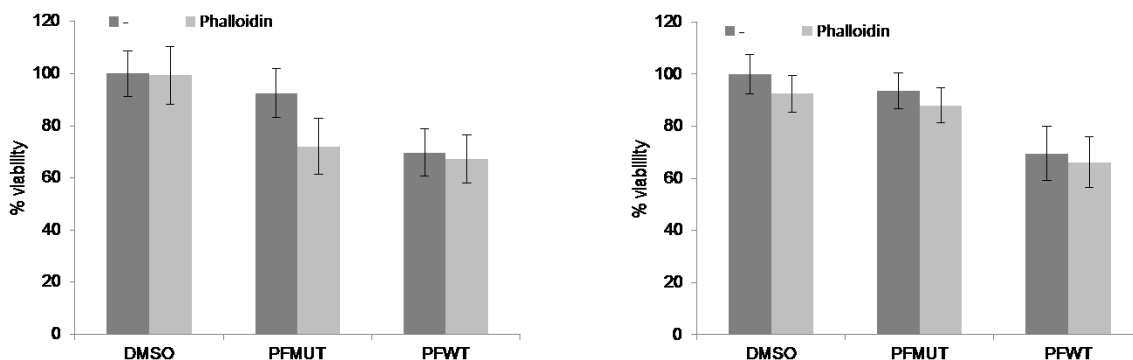
Figure 24 Phalloidin-oleate does not affect PFWT induced cell death

MV4-11 cells were pre-incubated with 5µM phalloidin-oleate for 1 h followed by an additional 1 h treatment with either DMSO, 25µg/ml PFWT, or 25µg/ml PFmut. Cell viability was measured using Promega Cell Titer-Glo luminescent viability assay. Viability is expressed as a percentage of DMSO treated cells. The error bars represent standard deviation. n.s. indicates no significant difference. The two graphs represent two independent experiments. Dark bars represent viability in the absence of phalloidin pre-treatment and light bars represent viability after treatment with phalloidin. The experiment was performed in quadruplicate.

Establishment of a permanent cell line expressing post translationally modified AF9

In order to study the effects of wild type AF9 on the actin cytoskeleton of MLL leukemic cells, we used lentivirus to knock down or overexpress AF9 in MV4-11 and K562 cells. These lentivirus constructs have previously been described and express GFP which can be used for selection (Pina et al., 2008). Due to technical challenges we were not able to efficiently transduce MV4-11 cells. Hence, we could not address the primary aim of determining the cytoplasmic effects of AF9 in MLL leukemia cell line. However, the leukemic cell line, K562 (BCR-ABL) was transduced efficiently. A GFP marker was used to sort the transduced population. A western blot showing AF9 expression in each of the sorted populations of cells is shown in Figure 25A. In the cell lysates of K562 cells that were transduced with lentivirus expressing AF9, we detected both a 58 kDa AF9 and a slow mobility 68 kDa AF9 molecule by western blot. The shRNA mediated-knockdown of AF9 was not efficient as AF9 was still detected in the shRNA transduced cell lysate.

A post translationally modified 68 kDa AF9 moiety had previously been identified from the lysate of MV4-11 cells incubated with the peptide PFWT and it was shown to localize to the nucleus (Amanda Winters, dissertation). Hence, we further characterized the 68 kDa AF9 observed in the transduced K562 cells using cell fractionation. As seen in figure 25B, the 68 kDa AF9 exhibits the same nuclear localization as observed on PFWT exposure. Lamin B and cytochrome oxidase IV (COX IV) were used as markers to determine the purity of the separated nuclear and cellular fractions respectively (Figure 25B). The K562 cells that express both species of AF9 have been stably transduced and served as a source of protein to attempt to analyze the

nature of 68 kDa AF9 protein. Henceforth, I will refer to these cells as modified K562 for simplicity.

Absence of O-glycosylation on 68 kDa AF9 protein

In order to determine if O-glycosylation contributes to the increase in molecular weight of AF9 observed in modified K562, we used wheat germ agglutanin affinity pull down and enzyme and alkali based degylcosylation assays (Laudadio et al., 2005).

Carbohydrate binding proteins known as lectins are often used to immunoprecipitate glycosylated proteins as they bind to specific sugar moieties. Wheat germ agglutanin (WGA) is known to specifically bind O-glycosylated proteins. Preincubation with sugars like N-acetylglucosamine saturates the sugar binding sites on WGA and hence should exclude or compete away glycosylated proteins. This exclusion by the sugar was used to measure the specificity of binding. As shown in the Figure 26A, AF9 binding to WGA appears to be non-specific as preincubation with 1M N-acetyl glucosamine does not block its ability to precipitate the 68 kDa AF9.

Incubation with deglycosylating enzymes followed by a shift in electrophorectic mobility is another way of detecting glycosylated proteins. We used a commerically avaliable O- deglycosylation kit to determine if it would diminish the amount of 68 kDa AF9 while increasing the amount of the 58 kDa AF9 protein. However, deglycosylation does not have an effect the 68 kDa AF9 protein (Figure 26). As a control, the enzyme was substituted with deionized water. The O-glycan linkage is easily hydrolyzed using dilute alkaline solution such as 0.1N sodium hydroxide.
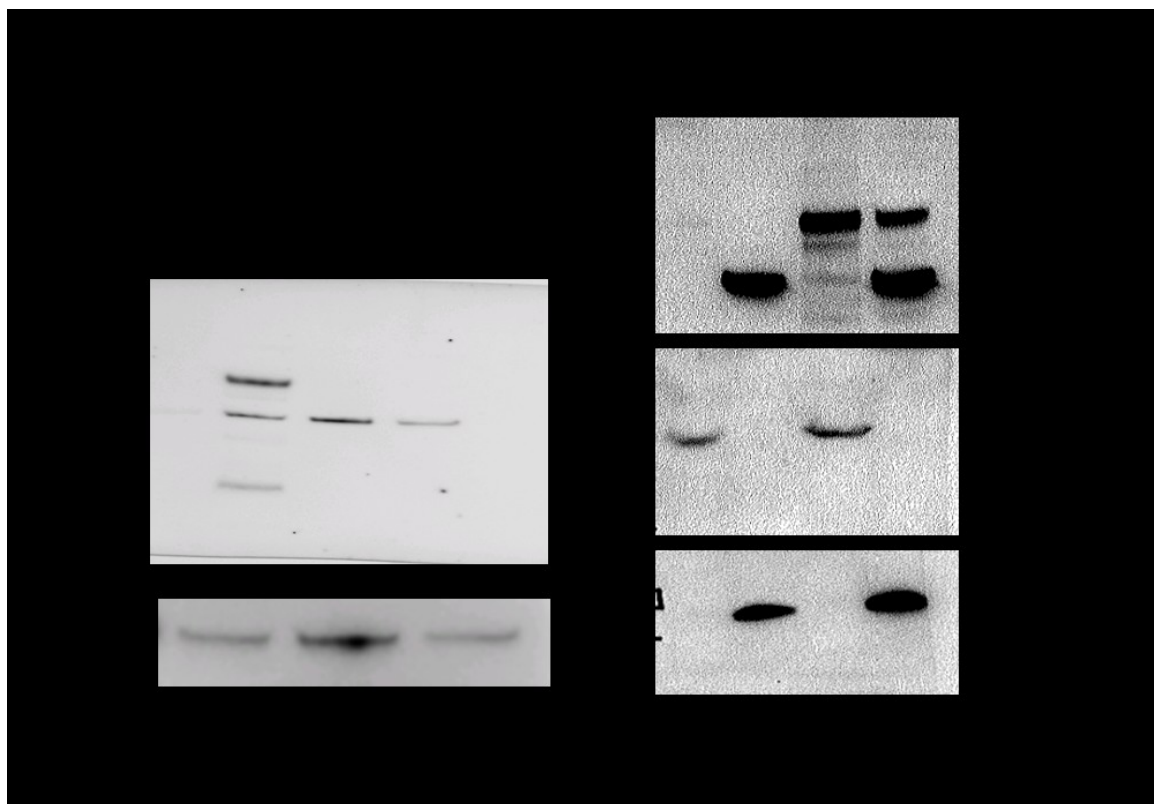
Figure 25 Modified K562 cells expressing 68 kDa AF9 band

(A) AF9 expression in GFP sorted cell population after transduction of lentivirus encoding AF9, shRNA targeting AF9 and empty vector (control). (B) Cytoplasmic (C) and Nuclear (N) fractionation of modified K562 cells showing nuclear localization of the 68 kDa AF9 band. This figure is representative of three independent experiments.

This chemical reaction is known as beta elimination and is used for chemical digestion of O-glycosylated proteins prior to mass spectroscopy analysis. Following incubation with mild alkali, we observed an increase in protein mobility suggesting that an alkali-labile

post translational modification occurs on the AF9 protein. However, the shift in mobility is greater than expected, revealing a 55kD AF9 band (Figure 26 B).

Absence of monoubiquitination on 68 kDa AF9 protein

We performed experiments to determine if AF9 is monoubiquitinated. HA-ubiquitin (HA-UB) was co-transfected with FLAGAF9 in HEK293T cells. Anti-FLAG antibody was used to immunoprecipitate AF9. A western blot analysis with anti HA antibody was done to determine if the immunoprecipitated AF9 is ubiquitinated. Results in Figure 27 show that the HA antibody failed to detect a 68 kDa band. Hence, we concluded that AF9 is not modified by ubiquitination.

Post Translational modification of AF9

We immunoprecipitate AF9 from MV4-11 cell lysate using anti-AF9 antibody and sent it to Louisiana State University (LSU) for mass spectroscopic identification of post translational modifications. Their analysis identified K297 to be a possible acetylation site. In order to study this site, we generated the following point mutants: $K_{297}A$, which cannot be acetylated and $K_{297}Q$, which constitutively mimics acetylation. These mutations were generated in both FLAG and EGFP expression vectors to aid in immunoprecipitation and immunofluorescence experiments. The expression of the FLAG tagged AF9 $_{K297A}$ and AF9 $_{K297Q}$ mutants in HEK293T cells were detected by western blots (Figure 28). The expressed EGFP AF9 $_{K297A}$ was detected in the nucleus and in the

A   B
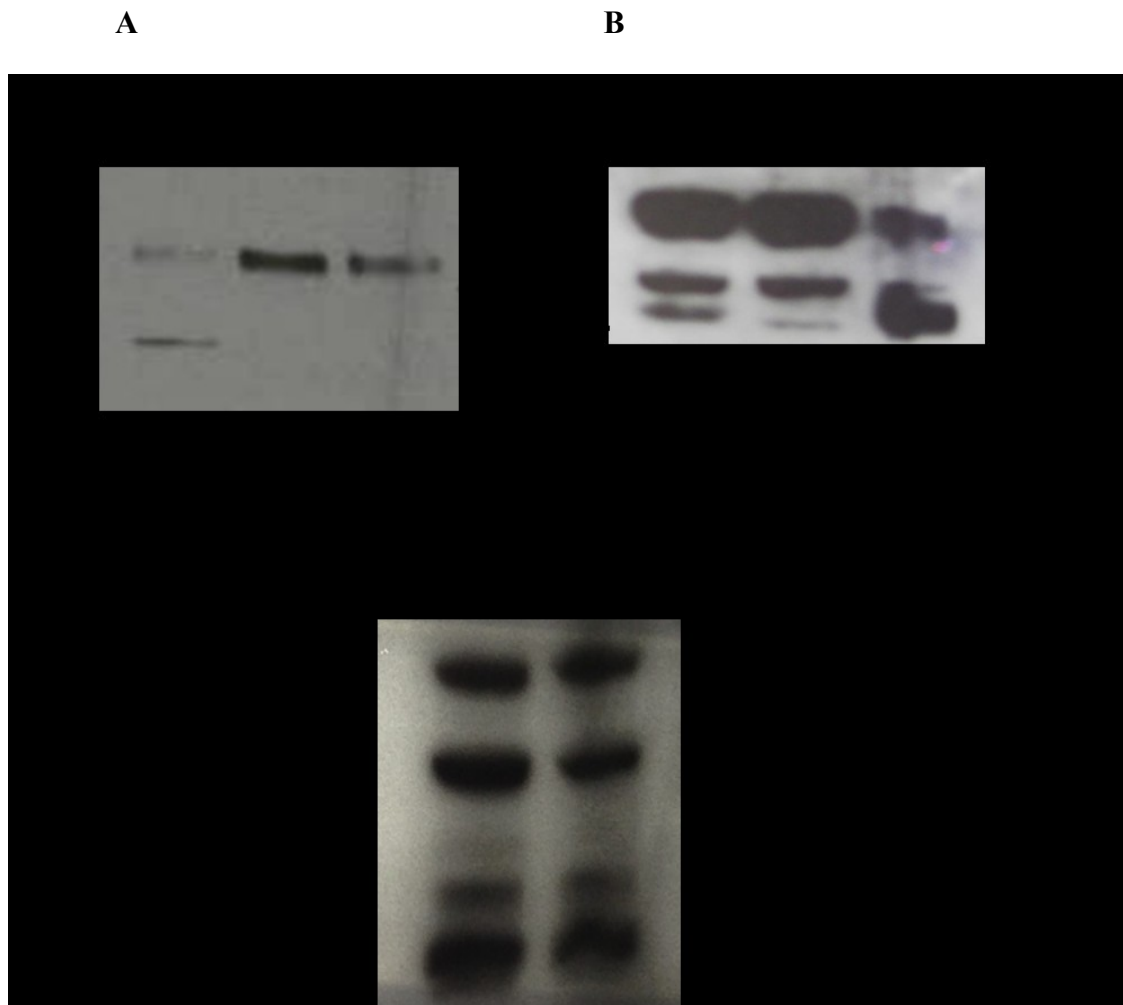
Figure 26 Absence of O-glycosylation of 68 kDa AF9

(A) Wheat Germ Agglutinin (WGA) affinity pull down shows non-specific binding of the 68 kDa AF9. Cell lysates from modified K562 cells were incubated with WGA agarose or with WGA agarose previously saturated with 1 M N-acetyl glucoseamine (NAcGlc). WGA precipitated proteins were analyzed using anti-AF9 antibody. (B) Alkali incubation results in the appearance of a 55 kDa AF9 protein. Cell lysates from modified K562 cells were incubated with water or 0.1N NaOH for 0.5 hour at room temperature and then

analyzed by western blots. (C) Enzymatic deglycosylation has no effect on AF9. Cell lysate from modified K562 cells were incubated with water (control) or with a O-glycosidase enzyme mix (Enzyme). All the blots in this figure are representative of three separate experiments.
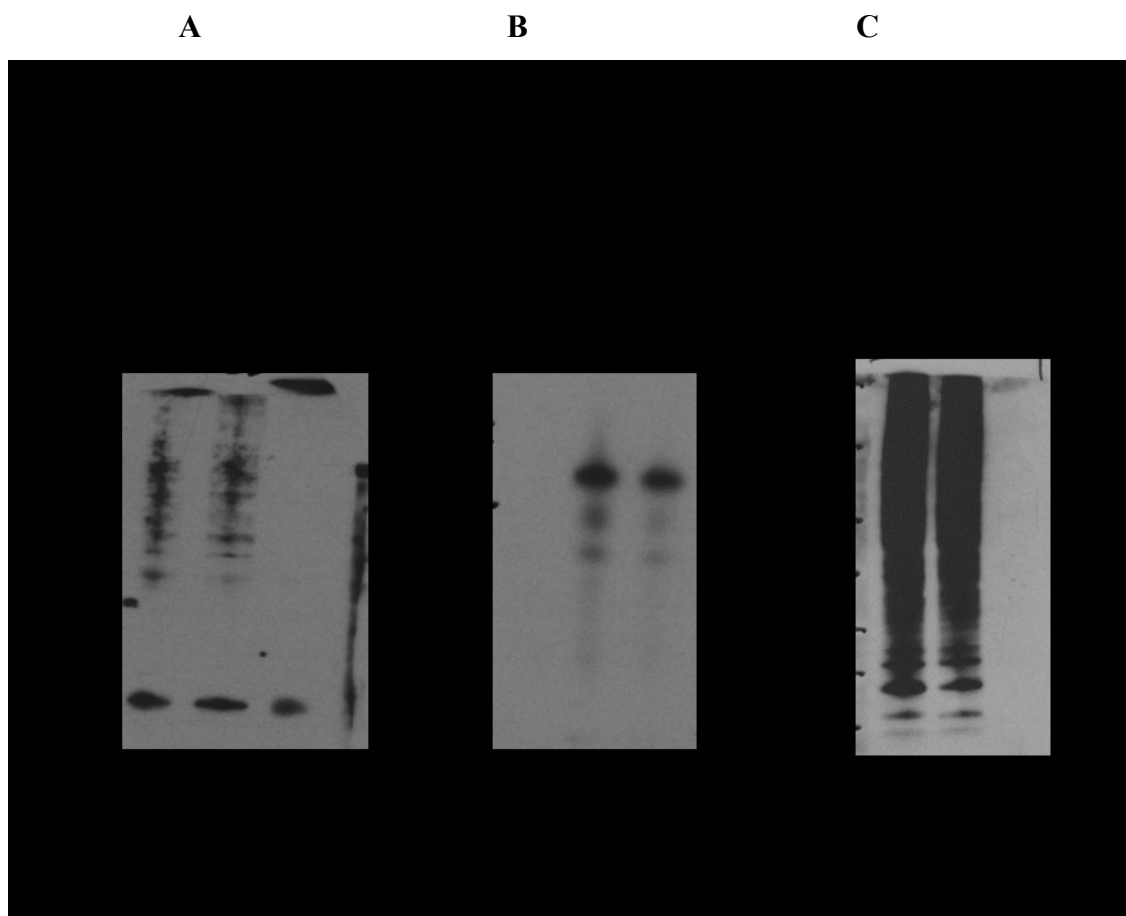
Figure 27 Absence of Monoubiquitination on 68 kDa AF9

(A) HEK293T cells were transiently transfected with Flag AF9 and HA-UB or with HA-UB or Flag AF9 only. Cell lysate was immunoprecipitated with an anti-Flag antibody. The precipitate was then analyzed by western blot to detect ubiquitin using an anti-HA antibody. (B) The western blot of the immunoprecipiate shows the presence of FlagAF9. (C) Western blot of whole cell lysates showing the expression of HA-UB.

cytoplasm of HeLa cells. This pattern of localization is different from the EGFP AF9 which localized to the nucleus (Figure 28).Immuo-labeling of wild type AF9 in leukemic cells MV4-11 shows that it is has a cytoplasmic localization. Immuno-labeling also shows that AF9 is compartmentalized to the nucleus on treatment with the PFWT peptide (Amanda Winters, thesis). This change in localization is accompanied by a 10 kDa increase in the molecular weight of AF9. A single acetylation on K297 is less likely to induce this increase in weight. Hence, we did not perform further experiments with these mutants.

Meanwhile, we transiently transfected FlagAF9 in HEK293T cells, purified the expressed AF9 using anti-Flag (M2) conjugated agarose and sent the precipitated proteins to University of Illinois, Chicago (UIC) mass spectroscopy facility. Mass spectroscopic analysis of the immunoprecipitated AF9 suggests probable lysine 364, 405, 412, 448, and 452 phosphorylation (multiple lysine phosphorylations).

Discussion

PFWT exposure specifically decreases the viability of MLL leukemic cell lines. Previous studies showed the absence of known apoptotic and necrotic markers after PFWT treatment (Amanda Winters, dissertation). These studies also demonstrated a decrease in F-actin content of MV4-11 by fluorescence microscopy on exposure to the peptide. Hence, in the current chapter we tested the hypothesis that PFWT treatment induces cell death by F-actin depolymerization. If the peptide PFWT actively induced

A

FLAGAF9 K297Q   FLAGAF9 K297A   FLAGAF9 WT

WB : FLAG

WB : GAPDH

62

49

B
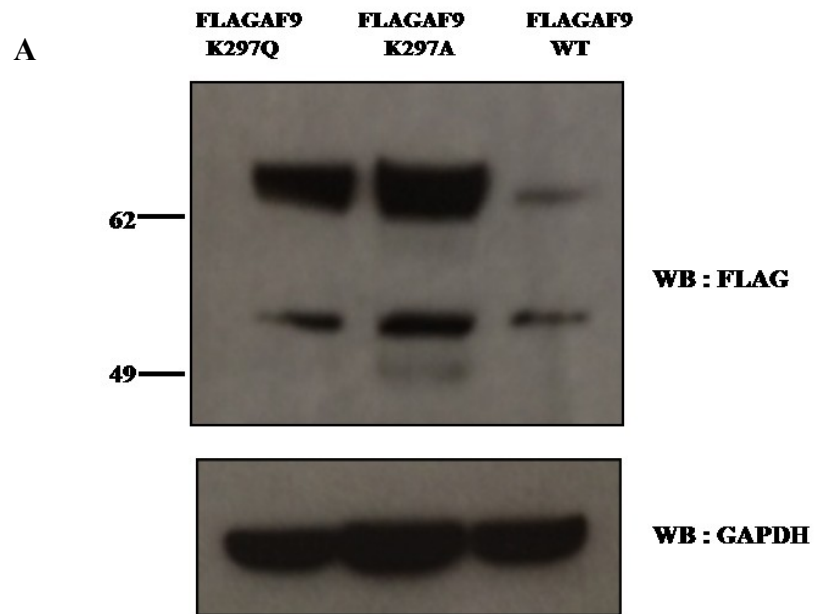
EGFP AF9

C   EGFP AF9$_{K297A}$
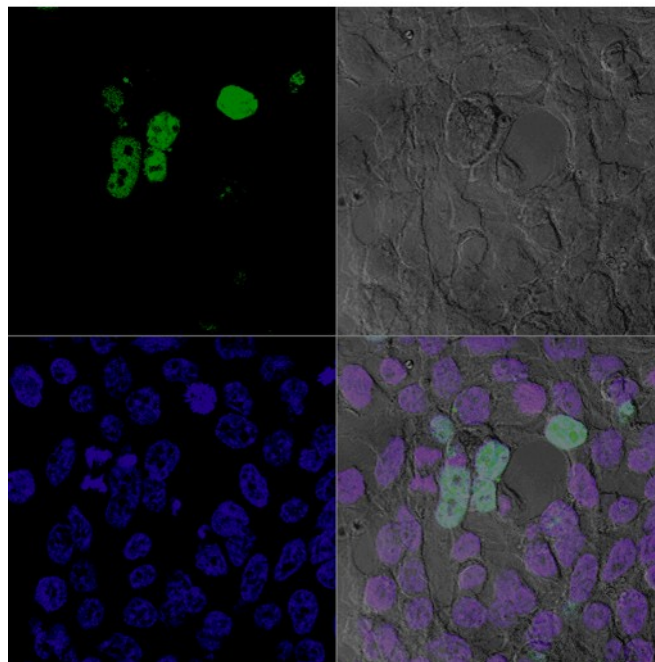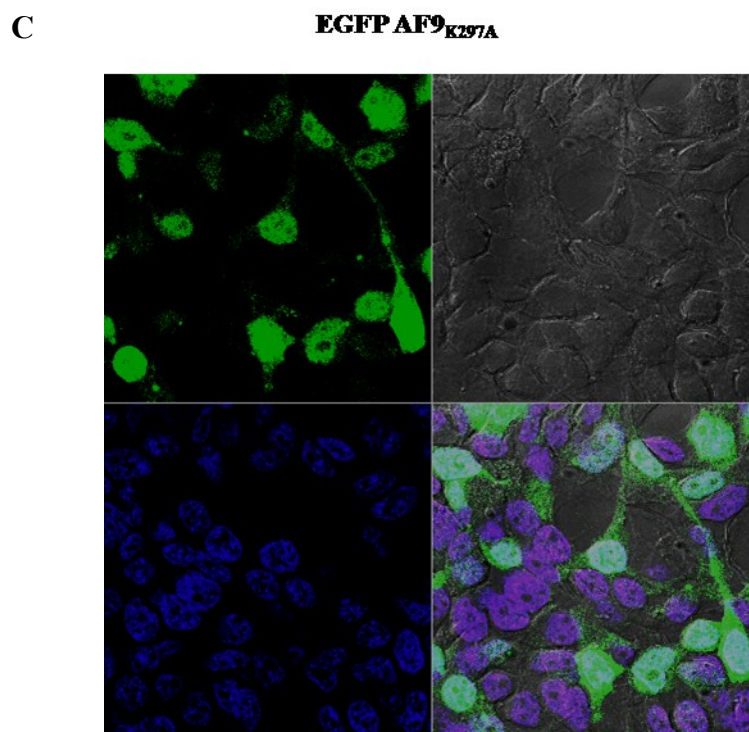
Figure 28 Expression of lysine K297 mutants of AF9

(A) Western blot analysis of transiently transfected HEK293T cells shows the expression of FLAGAF9, FLAGAF9$_{K297A}$ and FLAG AF9$_{K297Q.}$ The blot is representative of one experiment among three separate experiments performed. (B) Fluorescent microscopy detects the presence of transiently transfected EGFPAF9, (C) EGFPA9$_{K297A.}$ EGFP expression is shown top left, differential interface contrast microscopy (DIC) picture is shown top right, DAPI stained nuclei in blue, right bottom is the overlay. Images are representative of two separate experiments.

depolymerization then we would observe a decrease in F-actin content and a corresponding increase in G-actin content after exposure to PFWT.

However, the ultracentrifugal separation of F-actin and G-actin does not show a decrease in F-actin content (Figure 23 A). Again, if PFWT leads to progressive depolymerization then affinity labeling after PFWT exposure would show a decrease in intensity of FITC-phalloidin labeling. However, we do not observe such shift, further confirming the absence of progressive depolymerization (Figure 23B). More importantly, pretreatment with phalloidin-oleate which is known to stabilize F-actin does not lead to increase in viability of PFWT treated cells (Figure 24). The lack of effect of an actin stabilizing drug confirms that depolymerization of actin is not the primary cause of PFWT-induced cell death.

Several studies in the literature suggest that compounds that promote actin polymerization or depolymerization lead to apoptosis in leukemic cells. For instance, Jasplakinolide, an actin polymerizing drug, is shown to induce apoptosis in T cell leukemia (Rao et al., 1999) and cytochalasin B, an actin depolymerization agent enhances apoptosis in growth factor deprived HL-60 cells (pro-myleocytic leukemic cells) (Morley et al., 2003; Desouza et al., 2012; White et al., 2001). We have already established that the AF4 mimetic peptide induces necrosis. Hence it is less likely that PFWT induces necrosis by direct depolymerization of the actin cytoskeleton.

AF9 has a predicted molecular weight of 63 kDa. However, its apparent molecular weight is 58 kDa after electrophoretic separation on a 4-12% gradient gel containing SDS. An efficient transduction of K562 cells with lentivirus expressing AF9

resulted in the identification of a previously undocumented AF9 moiety with the apparent mass of 68 kDa in addition to the commonly observed 58kDa AF9 moiety (Figure 25). The transduced (modified) K562 maintain the expression of both these AF9 moieties on freeze-thawing. The same expression is also maintained through 20 or more passages. One possible reason for detection of both species of AF9 could be that enforced expression of AF9 leads to an increase in AF9 protein levels and hence the identification of the less abundant 68 kDa AF9. To test this hypothesis in the future, wild type (untransduced) K562 cells can be treated with the proteasome inhibitor MG132, to determine if inhibition of protein degradation leads to the accumulation of the less abundant 68 kDa AF9.

Post translational proteolytic processing often decreases the apparent molecular weight of a protein. However, the observed difference in molecular weight of the two AF9 moieties does not involve a proteolytic processing event as antibodies specific to both the amino and the carboxyl terminus of AF9 can identify both the moieties. A FLAG antibody recognizes the N-terminal FLAG tagged AF9 and C-terminal specific AF9 antibody novus 1566 bind AF9 carboxyl terminus. Both of these antibodies are shown to recognize the 58 kDa and the 68 kDa AF9 proteins (Figure 25 A and Figure 28 A). We next performed experiments to determine if AF9 was post translationally modified by monoubiquitinated or O-glycosylation. Both of these modifications are known to occur on transcription factors such as Stat5 and p53 on nuclear localization. The localization is important as the 68 kDa AF9 was shown to concentrate in nuclear fractions (Figure 25). Immunoprecipitation experiments after co-transfection with HA-

UB and FLAGAF9 showed the absence of monoubiqutination (Figure 27). Next we used several different tests to identify O-glycosylation. Enzymatic de-glycosylation using a commercially available O-glycosidase kit did not lead to decrease in 68 kDa AF9 protein (Figure 26). This suggests absence of O-glycosylation. However, a deglycosylation reaction using a known O-glycosylated protein as a positive control can be used in the future to strengthen the results of this assay.

Treatment with mild alkali (0.1N NaOH) at room temperature led to the identification of a 55 kDa protein by an AF9 specific antibody that recognizes the C-terminus. This 55 kDa AF9 is also detected in untreated cells (Figure 26). Further, experiments can be performed to determine if the 55 kDa band identified by the AF9 antibody is a proteolytic degradation product or a full length AF9 protein. If the 55 kDa AF9 band is a full length protein then it should be identified with an antibody that recognizes its N-terminus similar to its identification with a C-terminus specific AF9 antibody. HEK293T cells transfected with vector encoding a N-terminal FLAG tagged AF9 can be treated with mild alkali followed by detection of the 55 kDa AF9 using anti-FLAG antibody. Recognition of AF9 N-terminus confirms that the 55 kDa AF9 is full length. However if the FLAG tag fails to identify the tagged AF9 55 kDa band then it is likely to be a proteolytic degradation product.

The sugar residue of the O-glycosylated protein specifically binds the lectin Wheat germ agglutinin (WGA). Further, this specificity can be confirmed by competing away the bound o-glycosylated protein using N-acetylglucosamine sugar. The 68 kDa AF9 was immunoprecipitated with WGA and could not be competed away with 1M N-

acetyl glucosamine, which suggests nonspecific binding (Figure 26 A). The positive charge on WGA interacts with the negative charge on the sugar moiety of the glycosylated proteins, promoting binding (Monsigny et al., 1980). However, other negative charges on a protein may promote non-specific binding. As the 68 kDa AF9 precipitated with WGA and the 58 kDa AF9 does not, it is possible that the modification present on AF9 imparts a negative charge to it.

Initial mass spectroscopy analysis of AF9 post translational modifications identified a possible acetylation on lysine 297. Two point mutations at this site were generated (K297A and K297Q). The alanine mutation was made to test for loss of acetylation function and the glutamine substitution is known to act as mimetic of acetylation function (Wang and Hayes, 2008). A western blot shown in Figure 28 suggests that the K297 mutant proteins are expressed at a higher level compared to the Flag AF9. Future experiments need to be done to determine if the K297 mutation confers increased stability to AF9, or whether the observed protein level is due to a difference in transfection efficiency. Promoter reporter assays (firefly luciferase reporter assays) often use a secondary reporter plasmid to normalize for transfection efficiency (renilla luciferase). Similarly, we could co-transfect GFP expressing vector along with FLAGAF9K297A, FLAGAF9K297Q and FLAGAF9 and use the expressed levels of GFP in each lysate to normalize for transfection efficiency. After normalization for transfection efficiency, if the protein levels are higher in the mutants then that would suggest that a modification on lysine 297 influences the stability of the AF9 protein.

GFPAF9 transfected in epithelial cells appears to be nuclear (Figure 28B) (Lin and Hemenway, 2010; Srinivasan et al., 2004b). Fluorescent microscopy using EGFPAF9$_{K297A}$ showed its presence in the cytoplasm and the nucleus. This suggests that the modification present on the lysine 297 plays a critical role in the nuclear localization of the protein. Hence, a mutation of this site may lead to its appearance in the cytoplasm. However, from the pattern of AF9 localization in modified K562 cells, we know that forced expression of AF9 leads to the accumulation of 68 kDa AF9 in the nucleus and 58 kDa AF9 in the cytoplasm (Figure 25). Hence, it is also possible that an increased stability of the AF9 $_{K297A}$ mutant protein leads to identification of both cytoplasmic and nuclear AF9.

In summary, our results show the absence of Monoubiqutination or O-glycosylation of AF9. Further experiments will identify if the 68 kDa AF9 accumulates in the nucleus on forced expression due to increased expression of the AF9 protein. Similarly further investigation will determine if lysine 297 is important for nuclear localization and AF9 turn over.

Our second round of mass spectroscopy analysis on FLAGAF9 immunoprecipitates identified the presence of multiple phosphorylation sites (serine 364, 405, 412,448 and 452). However, a western blot analysis of the immunoprecipitated 68 kDa AF9 using an anti-serine phospho antibody is needed to confirm the presence of phosphorylation on AF9. Alternatively the radioisotope P^{32} can be used for identification of phosphorylation sites. Additionally, evidence for AF9 phosphorylation is found in several global scale proteomic studies that determine changes in total cellular

phosphorylation related to mitosis or T- cell activation. These studies have also identified multiple possible phosphorylated forms of AF9 (Daub et al., 2008; Dephoure et al., 2008; Oppermann et al., 2009).

AF9 interacts with several proteins such as AF4, CBX8, BCoR and DOT1L. It is tempting to speculate that the multiple phosphorylation sites on AF9 may singularly or in combination regulate the protein interactions of AF9.

CHAPTER 5

SUMMARY, CONCLUSION AND FUTURE DIRECTIONS

Summary of results

Chromosomal translocations of the *MLL* gene give rise to acute leukemias. Pediatric ALL and therapy-associated MLL leukemias are categorized as high-risk (Pui et al., 2002; Pui and Relling, 2000). Current treatments for MLL leukemia include a combination of cytotoxic drugs and/or allogeneic bone marrow transplants after high dose chemotherapy. However, the event free survival of MLL leukemia patients is low in spite of these advances (Biondi et al., 2000; Mann et al., 2010). Hence there is a need for development of targeted therapies.

A widely accepted mechanistic model of MLL leukemogenesis suggests that MLL fusion proteins aberrantly recruit the super elongation complex (SEC) promoting the transcription of a subset of MLL target genes whose gene products initiate and sustain leukemogenesis (Lin et al., 2010a; Zeisig et al., 2004b). Thus, our therapeutic strategy is to inhibit the activity of the aberrantly recruited SEC. In this study, we evaluated the therapeutic potential of inhibiting the protein-protein interaction between AF4 and AF9, which are constituent components of the super elongation complex, using the AF4 mimetic peptide SPK111.

In summary, our results show that coimmunoprecipitation of AF4 and AF9 in the presence of SPK111 competitively inhibits the AF4-AF9 interaction. SPK111 exposure

also leads to a decrease in transcriptional activity of the SEC-dependent HIV-LTR driven luciferase reporter. This observation suggests that SPK111 decreases the transcriptional output of the SEC by inhibiting the AF4-AF9 protein-protein interaction. Additionally, studies performed in our laboratory have shown that exposure of MLL leukemia cell lines MV4-11 and MOLM13 to SPK111 leads to a decrease in the expression of *MEIS1,* a gene regulated by MLL fusion protein (Bhavana Malik, Dissertation). This observation confirms that the disruption of the AF4-AF9 interaction is effective at inhibiting the transcriptional elongation activity of SEC.

SPK111 exposure leads to necrotic cell death of MLL leukemia cell lines. Further, the MLL leukemia cell lines exhibit relatively higher sensitivity to SPK111 compared to other leukemia cell lines. This sensitivity can be attributed to the increased dependence of these cell lines on the aberrantly recruited SEC.

MV4-11 and MOLM13 MLL leukemia cells fail to engraft after *in vitro* exposure to SPK111. Hence, we conclude that SPK111 is toxic to leukemic initiating cells. This effectiveness, however, was not observed on treatment of mice with an established leukemia xenograft, which may be due to limited bioavailability of the peptide after subcutaneous injections. A standard curve for ELISA was established to determine the levels of SPK111 in mouse serum and it can be further optimized for bio-distribution studies.

Another AF4 mimetic peptide, PFWT, was tested in earlier studies, all of which were performed *in vitro*. These earlier studies suggested that PFWT possibly induces a depolymerization of the actin cytoskeleton. However, our investigations determined that

PFWT exposure does not induce any significant changes in the filamentous actin content. Additionally, pretreatment with filamentous actin stabilizing drugs does not protect against PFWT mediated cell death.

The wild type AF9 protein is observed as a 58 kDa molecule on a western blot using AF9 specific antibody. However, a 68 kDa AF9 molecule was identified in the cell lysates of leukemic cells incubated with PFWT (Amanda Winters, dissertation). Further, we also observed the presence of the 68 kDa AF9 molecules in cell lysates of K562 leukemic cells transduced with AF9 expressing lentivirus. This increase in molecular weight is likely due to a post translational modification. Our attempts to identify a post-translational modification show the absence of O-glycosylation or monoubiquitination. Finally, mass spectroscopy analysis suggested the presence of several phosphorylation sites on AF9 protein and an acetylation site at lysine 297. Mutants of AF9 lysine 297 result in increased expression of the AF9 protein suggesting that this amino acid may play a significant role in AF9 protein turnover. However, as discussed in chapter 4, further experiments need to be performed to confirm the acetylation and phosphorylation of AF9.

The results described here suggest that AF9 is post translationally modified which affects its protein levels and localization. Further we show that the AF4 mimetic peptide SPK111 reduces the viability of MLL leukemia cells and MLL leukemia stem cells. It also effectively reduces the transcriptional activity of the SEC, whose deregulated activity is the underlying cause of MLL leukemias. Thus SPK111 is an effective potential therapy for MLL leukemias.

Model

A
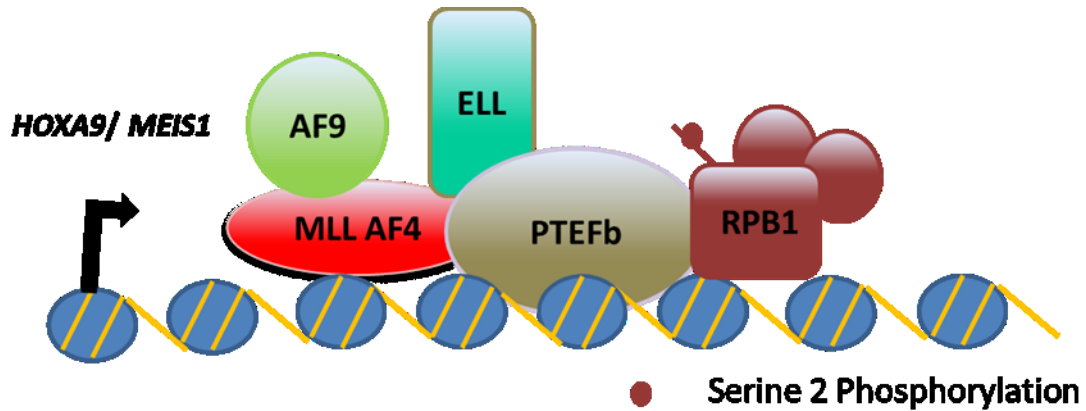
B
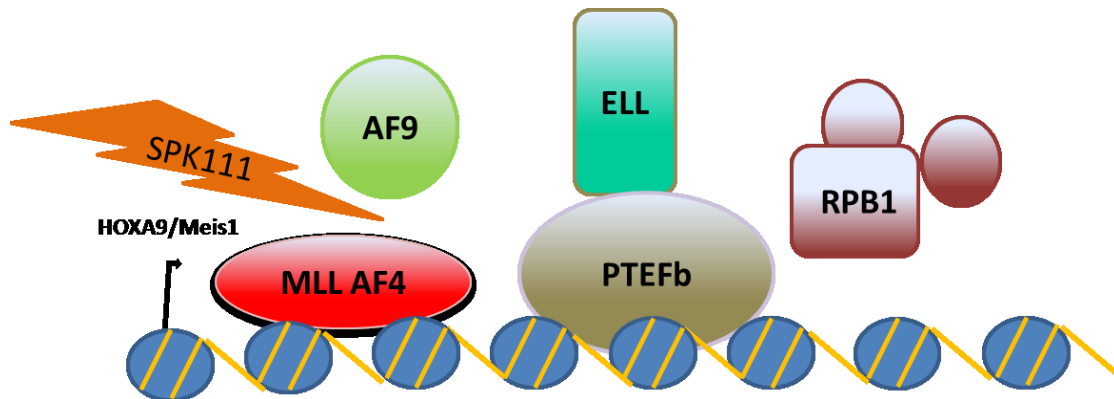
Figure 29 Mechanism of SPK111

(A) MLL fusion proteins aberrantly recruit the super elongation complex by protein-protein interactions. The recruited complex permits the productive transcription of genes that are known to sustain leukemogenesis.

(B) The AF4 mimetic peptide SPK111 disrupts the interaction between AF4 and AF9, two of the constituent components of the super elongation complex. This disruption results in destabilization of the complex, decreases stability of RNA polymerase subunit RPB1 and decrease in transcription of the leukemia sustaining genes.

Future Investigations

SPK111 is effective *in vitro;* however, we cannot detect its presence in the serum a few hours following subcutaneous injection. The ELISA described in chapter 2 can be used to detect the accumulation of SPK111 in an untargeted organs. It is essential to know the bio-distribution of SPK111 in order to determine its clearance rate and accumulation in an untargeted organ. Fluorescence molecular tomography (FMT) can be used to non-invasively image and quantify time dependent increase and decrease in fluorescence intensity throughout the major organs of mice (Vasquez et al., 2011). Thus, a fluorophore conjugated SPK111 can be used in the future for the monitoring of its *in vivo* distribution.

An efficient packaging and delivery system can also be used to improve the *in vivo* efficacy of SPK111. Nanoparticles that effectively target the leukemic blast can be developed. For instance, acute myeloid leukemia stem cells were found to express C-type lectin-like molecule-1 (CLL1) which was used to distinguish between leukemic stem cells (LSC) and hematopoietic stem cells (HSC). Nanoparticles carrying chemotherapeutic drugs were coated with CLL1 binding ligands. The coated nanoparticles specifically and effectively delivered drugs to the AML LSC (Zhang H et

al., 2012). Similarly, MLL leukemic blasts can be evaluated for expression of antigens such as CD44, CD47, and IL-3 R alpha that are known to be highly expressed on leukemic stem cells. This will help single out an antigen that can be used for targeting nanoparticles to MLL leukemia cells. These targeted nanoparticles can be loaded with SPK111 for more effective therapy.

The AF4 mimetic sequence can be packed in liposome. Liposomes are small synthetic lipid bilayers that can carry chemotherapeutics. The liposomes are often attached to antibodies or receptor ligands to improve targeting specificity (Harata et al., 2004). Liposomes coated with antibody that recognize leukemic blast may improve the targeting specificity.

The molecular weight of SPK111 is 2.5 kDa. Peptides smaller than 12 kDa are rapidly cleared by glomerular filtration resulting in decreased serum levels (Vegt et al., 2010). Hence, chemical alterations that reduce glomerular filtration rate can be considered. Several small therapeutic peptides are conjugated to polyethylene glycol (PEG) in order to decrease renal filtration rate and improve their bioavailability. The PEG can be attached to end of a linker peptide that can be cleavage for slow release of the peptide for cellular uptake (Santi et al., 2012). Hence, a reversible pegylation tag may improve the serum half-life of SPK111.

Small molecule inhibitor drugs are preferred over peptide drugs due to stability of the drug, ease of storage, and drug administration. The AF9 C-terminus is unstructured but the presence of an interacting protein such as AF4 results in an induced structure. Hence, it may be difficult to design small molecular inhibitor that can bind the AF9 C-

terminus and inhibit the induction of structural changes. However, a high-throughput assay based on protein-protein interaction has been designed to screen for molecules that preferentially inhibit the AF4-AF9 interaction (Watson et al., 2013). Further screening of compound libraries with this assay may potentially identify a small molecular inhibitor.

As described in chapter 4, we need additional experiments to confirm the multiple phosphorylation sites (serine 364, 405, 412, 448, and 452) on AF9 identified by mass spectroscopy. Previous studies have shown that Af9 is phosphorylated on serine 435 by serum glucocorticoid induced kinase-1 (Sgk1) (Zhang et al., 2007). This phosphorylation results in reduced Af9-Dot1a interaction promoting ENaCα derepression. Based on this example, we speculate that the phosphorylation sites identified by mass spectroscopy are likely to regulate the many protein-protein interactions of AF9. Hence, the identified serine phosphorylation sites can be mutated to alanine. These mutations can be generated as a single site mutation or as a combination of multiple sites. These mutants can then be used to study how phosphorylation affects protein interactions of AF9. The functional effects of AF9 protein-protein interactions in in the hematopoietic regulation include H3K79 methylation, and transcriptional elongation. Additionally, it also regulates ENaCα expression in kidney epithelium. Hence, the effect of AF9 phosphorylation on these functions can be investigated.

Conclusion

From our *in vitro* and *in vivo* studies, we conclude that inhibition of the AF4-AF9 protein-protein interaction effectively reduces the viability of MLL leukemia cells and

can be used for *ex vivo* purging of leukemic stem cells. We also demonstrate that inhibition of this interaction reduces the transcriptional activity of the SEC which is known to be deregulated in MLL leukemias. Hence, further development of small molecular inhibitors that inhibit the AF4-AF9 interaction or further optimization of the AF4 mimetic peptide to improve its systemic bioavailability may lead to effective therapy for MLL leukemias.

APPENDIX A:

ESTABLISHMENT OF XENOGRAFT MODELS FOR MLL LEUKEMIA

Establishment of xenograft models of MLL leukemia

In order to achieve disseminated systemic leukemic mice model, $2x10^6$ MOLM13 cells were injected into tail vein of sublethally irradiated NOD/SCID mice. The injected mice developed disease symptoms such as poor grooming, extreme lethargy or hind limb paralysis, approximately 21 days after transplant. These were sacrificed and their bone marrow analyzed for the presence of human CD45 antigen. CD45 is a ubiquitous antigen present on all hematopoietic cells except erythrocytes and plasma cells. Antibodies to this antigen can help distinguish the species of origin. In our xenograft model, we use it to identify the human leukemic cells. 41% of the cell collected from bone marrow showed the presence of hCD45 antigen confirming engraftment (Figure 30). KOPN8, a cell line carrying MLL-ENL fusion gene, also successfully engrafted following tail vein injection of $2x10^6$ cells (Figure 30). Further, hematoxilin and eosin (H&E) staining showed diffused infiltration of leukemic cells in kidney, liver and blood harvested from the MOLM13 xenografted mice (Figure 30E).

We also performed tail vein injection of $2x10^6$ K562 cells into NOD/SCID mice after sublethal irradiation. Eight weeks after injection, the mice showed no signs of a disease. Hence we sacrificed some of these mice and analyzed their bone marrow for the presence of the human CD45 antigen. As shown in Figure 31, we find that hCD45 labeled cells represents less than 3% of the total population, suggesting inefficient engraftment. Similarly, tail vein injections of MV4-11 cells in NOD/SCID mice failed to establish a xenograft (Figure 31). The successfully established MOLM13 and KOPN8 xenografts were further used to test the efficacy of SPK111.
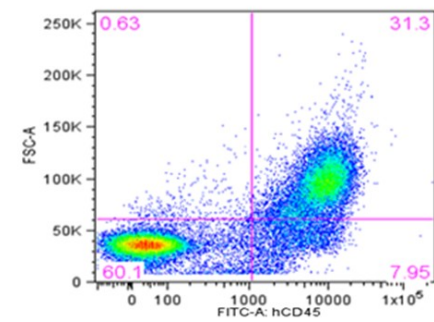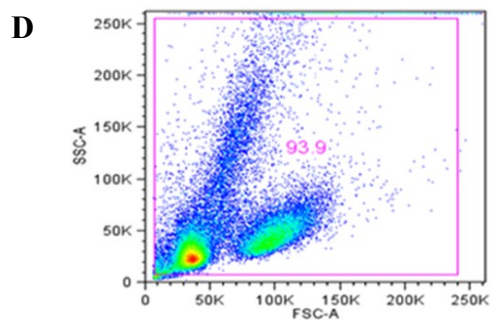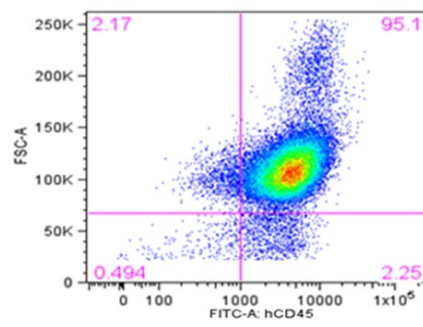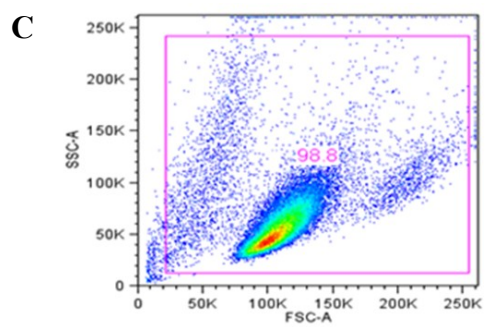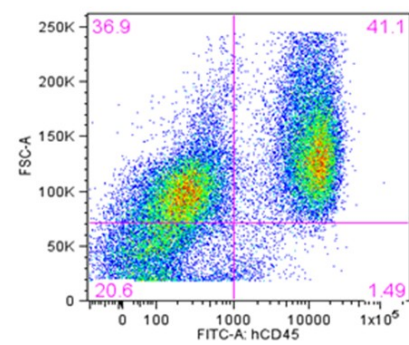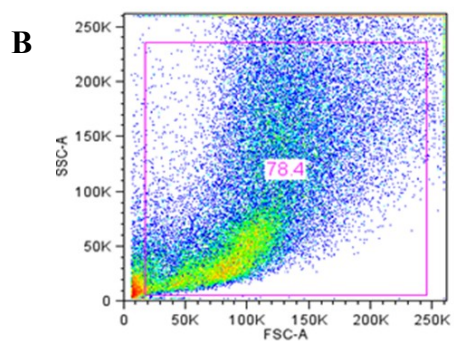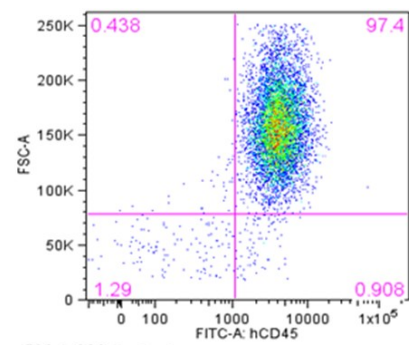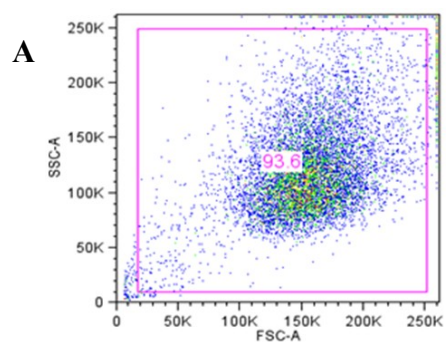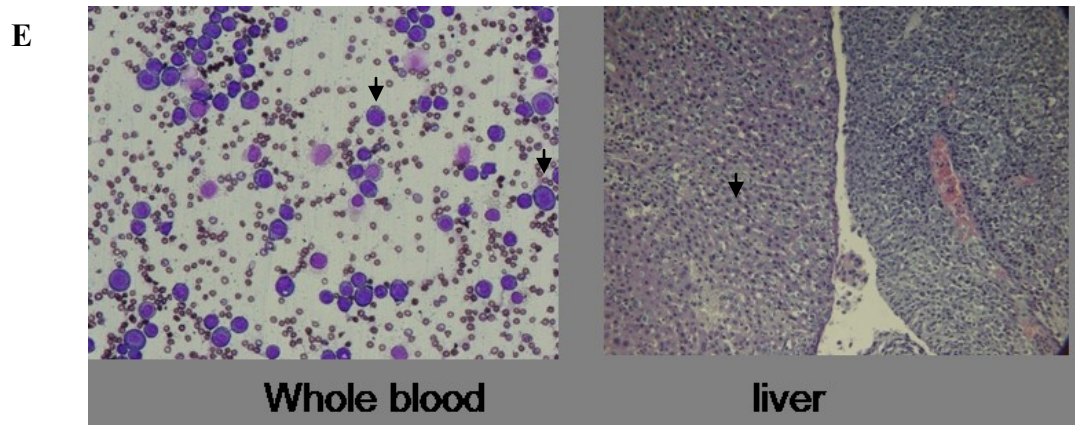
Figure 30 MOLM13 and KOPN8 leukemia xenografts established by tail vein injections

A) Tissue culture MOLM13 cells labeled with anti hCD45 FITC. B) Bone marrow from NOD/SCID mice that received tail vein injection of MOLM13 cells was labelled with anti hCD45 FITC. 41.1% of the total cell population were hCD45 positive. C) Tissue cultured KOPN8 cells labeled with anti hCD45 FITC were used as positive control.D) Bone marrow from NOD/SCID mice that received tail vein injection of KOPN8 cells was labeled with hCD45 FITC. 31.1% of the total population were hCD45 positive. E) H&E staining of liver derived from MOLM13 xenografts shows diffused infiltration of leukemic blast. Their presence is also indicated by arrow heads in the stained blood smears.
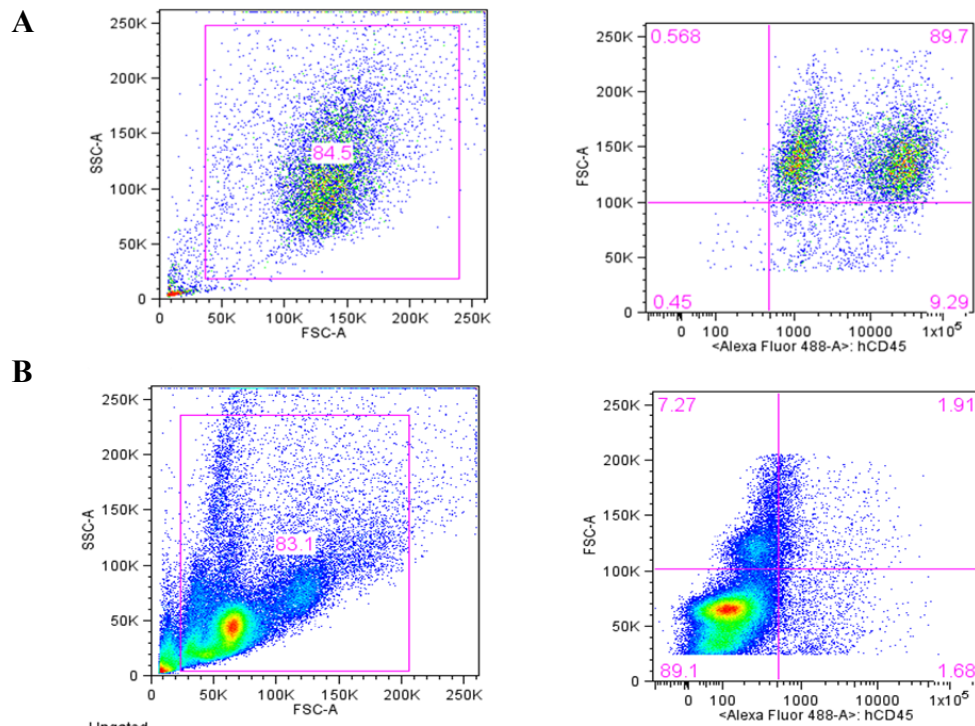
Figure 31 K562 cells fail to engraft in NOD/SCID mice after tail vein injections

A) Tissue cultured K562 cells labeled with anti hCD45 FITC. B) Bone marrow from NOD/SCID mice that received tail vein injection of K562 cells was labeled with anti hCD45 FITC. Less than 3% of the total cell population were hCD45 positive. A total of 16 mice were injected. Viability count using tryphan blue was performed prior to tail vein injections in order to suspend the cells at a density of 2 million cells per 100µl for tail vein injections.

REFERENCES

Andersen, M.K., Christiansen, D.H., Jensen, B.A., Ernst, P., Hauge, G., and Pedersen-Bjergaard, J. (2001). Therapy-related acute lymphoblastic leukaemia with MLL rearrangements following DNA topoisomerase II inhibitors, an increasing problem: report on two new cases and review of the literature since 1992. British journal of haematology *114*, 539-543.

Andrade, J., Ge, S., Symbatyan, G., Rosol, M.S., Olch, A.J., and Crooks, G.M. (2011). Effects of sublethal irradiation on patterns of engraftment after murine bone marrow transplantation. Biology of blood and marrow transplantation : journal of the American Society for Blood and Marrow Transplantation *17*, 608-619.

Argiropoulos, B., and Humphries, R.K. (2007). Hox genes in hematopoiesis and leukemogenesis. Oncogene *26*, 6766-6776.

Armstrong, S.A., Staunton, J.E., Silverman, L.B., Pieters, R., den Boer, M.L., Minden, M.D., Sallan, S.E., Lander, E.S., Golub, T.R., and Korsmeyer, S.J. (2002). MLL translocations specify a distinct gene expression profile that distinguishes a unique leukemia. Nature genetics *30*, 41-47.

Atkinson, S.J., Hosford, M.A., and Molitoris, B.A. (2004). Mechanism of actin polymerization in cellular ATP depletion. J Biol Chem *279*, 5194-5199.

Auffray, I., Dubart, A., Izac, B., Vainchenker, W., and Coulombel, L. (1994). A murine stromal cell line promotes the proliferation of the human factor-dependent leukemic cell line UT-7. Exp Hematol *22*, 417-424.

Ayton, P.M., Chen, E.H., and Cleary, M.L. (2004). Binding to nonmethylated CpG DNA is essential for target recognition, transactivation, and myeloid transformation by an MLL oncoprotein. Mol Cell Biol *24*, 10470-10478.

Ayton, P.M., and Cleary, M.L. (2003). Transformation of myeloid progenitors by MLL oncoproteins is dependent on Hoxa7 and Hoxa9. Genes Dev *17*, 2298-2307.

Bennett, C.A., Winters, A.C., Barretto, N.N., and Hemenway, C.S. (2009). Molecular targeting of MLL-rearranged leukemia cell lines with the synthetic peptide PFWT

synergistically enhances the cytotoxic effect of established chemotherapeutic agents. Leukemia research *33*, 937-947.

Biondi, A., Cimino, G., Pieters, R., and Pui, C.H. (2000). Biological and therapeutic aspects of infant leukemia. Blood *96*, 24-33.

Biswas, D., Milne, T.A., Basrur, V., Kim, J., Elenitoba-Johnson, K.S., Allis, C.D., and Roeder, R.G. (2011). Function of leukemogenic mixed lineage leukemia 1 (MLL) fusion proteins through distinct partner protein complexes. Proceedings of the National Academy of Sciences of the United States of America *108*, 15751-15756.

Bitoun, E., and Davies, K.E. (2005). The robotic mouse: unravelling the function of AF4 in the cerebellum. Cerebellum *4*, 250-260.

Bitoun, E., Finelli, M.J., Oliver, P.L., Lee, S., and Davies, K.E. (2009). AF4 is a critical regulator of the IGF-1 signaling pathway during Purkinje cell development. The Journal of neuroscience : the official journal of the Society for Neuroscience *29*, 15366-15374.

Bitoun, E., Oliver, P.L., and Davies, K.E. (2007a). The mixed-lineage leukemia fusion partner AF4 stimulates RNA polymerase II transcriptional elongation and mediates coordinated chromatin remodeling. Hum Mol Genet *16*, 92-106.

Bitoun, E., Oliver, P.L., and Davies, K.E. (2007b). The mixed-lineage leukemia fusion partner AF4 stimulates RNA polymerase II transcriptional elongation and mediates coordinated chromatin remodeling. Human molecular genetics *16*, 92-106.

Broeker, P.L., Super, H.G., Thirman, M.J., Pomykala, H., Yonebayashi, Y., Tanabe, S., Zeleznik-Le, N., and Rowley, J.D. (1996). Distribution of 11q23 breakpoints within the MLL breakpoint cluster region in de novo acute leukemia and in treatment-related acute myeloid leukemia: correlation with scaffold attachment regions and topoisomerase II consensus binding sites. Blood *87*, 1912-1922.

Broske, A.M., Vockentanz, L., Kharazi, S., Huska, M.R., Mancini, E., Scheller, M., Kuhl, C., Enns, A., Prinz, M., Jaenisch, R.*, et al.* (2009). DNA methylation protects hematopoietic stem cell multipotency from myeloerythroid restriction. Nature genetics *41*, 1207-1215.

Bueno, C., Montes, R., Melen, G.J., Ramos-Mejia, V., Real, P.J., Ayllon, V., Sanchez, L., Ligero, G., Gutierrez-Aranda, I., Fernandez, A.F.*, et al.* (2012). A human ESC model for MLL-AF4 leukemic fusion gene reveals an impaired early hematopoietic-endothelial specification. Cell research *22*, 986-1002.

Butler, L.H., Slany, R., Cui, X., Cleary, M.L., and Mason, D.Y. (1997). The HRX proto-oncogene product is widely expressed in human tissues and localizes to nuclear structures. Blood *89*, 3361-3370.

Buttner, N., Johnsen, S.A., Kugler, S., and Vogel, T. (2010). Af9/Mllt3 interferes with Tbr1 expression through epigenetic modification of histone H3K79 during development of the cerebral cortex. Proceedings of the National Academy of Sciences of the United States of America *107*, 7042-7047.

Cao, F., Chen, Y., Cierpicki, T., Liu, Y., Basrur, V., Lei, M., and Dou, Y. (2010). An Ash2L/RbBP5 heterodimer stimulates the MLL1 methyltransferase activity through coordinated substrate interactions with the MLL1 SET domain. PloS one *5*, e14102.

Carlsson, L., Nystrom, L.E., Sundkvist, I., Markey, F., and Lindberg, U. (1977). Actin polymerizability is influenced by profilin, a low molecular weight protein in non-muscle cells. Journal of molecular biology *115*, 465-483.

Caslini, C., Connelly, J.A., Serna, A., Broccoli, D., and Hess, J.L. (2009). MLL associates with telomeres and regulates telomeric repeat-containing RNA transcription. Mol Cell Biol *29*, 4519-4526.

Celeste Morley, S., Sun, G.P., and Bierer, B.E. (2003). Inhibition of actin polymerization enhances commitment to and execution of apoptosis induced by withdrawal of trophic support. Journal of cellular biochemistry *88*, 1066-1076.

Chang, M.J., Wu, H., Achille, N.J., Reisenauer, M.R., Chou, C.W., Zeleznik-Le, N.J., Hemenway, C.S., and Zhang, W. (2010a). Histone H3 lysine 79 methyltransferase Dot1 is required for immortalization by MLL oncogenes. Cancer research *70*, 10234-10242.

Chang, P.Y., Hom, R.A., Musselman, C.A., Zhu, L., Kuo, A., Gozani, O., Kutateladze, T.G., and Cleary, M.L. (2010b). Binding of the MLL PHD3 finger to histone H3K4me3 is required for MLL-dependent gene transcription. Journal of molecular biology *400*, 137-144.

Chaudhuri, A.A., So, A.Y., Mehta, A., Minisandram, A., Sinha, N., Jonsson, V.D., Rao, D.S., O'Connell, R.M., and Baltimore, D. (2012). Oncomir miR-125b regulates hematopoiesis by targeting the gene Lin28A. Proc Natl Acad Sci U S A *109*, 4233-4238.

Chen, J., Santillan, D.A., Koonce, M., Wei, W., Luo, R., Thirman, M.J., Zeleznik-Le, N.J., and Diaz, M.O. (2008a). Loss of MLL PHD finger 3 is necessary for MLL-ENL-induced hematopoietic stem cell immortalization. Cancer Res *68*, 6199-6207.

Chen, W., Kumar, A.R., Hudson, W.A., Li, Q., Wu, B., Staggs, R.A., Lund, E.A., Sam, T.N., and Kersey, J.H. (2008b). Malignant transformation initiated by Mll-AF9: gene dosage and critical target cells. Cancer cell *13*, 432-440.

Chou, S., Upton, H., Bao, K., Schulze-Gahmen, U., Samelson, A.J., He, N., Nowak, A., Lu, H., Krogan, N.J., Zhou, Q.*, et al.* (2013). HIV-1 Tat recruits transcription elongation factors dispersed along a flexible AFF4 scaffold. Proc Natl Acad Sci U S A *110*, E123-131.

Chowdhury, T., and Brady, H.J. (2008). Insights from clinical studies into the role of the MLL gene in infant and childhood leukemia. Blood cells, molecules & diseases *40*, 192-199.

Cierpicki, T., Risner, L.E., Grembecka, J., Lukasik, S.M., Popovic, R., Omonkowska, M., Shultis, D.D., Zeleznik-Le, N.J., and Bushweller, J.H. (2010). Structure of the MLL CXXC domain-DNA complex and its functional role in MLL-AF9 leukemia. Nature structural & molecular biology *17*, 62-68.

Clevers, H. (2011). The cancer stem cell: premises, promises and challenges. Nature medicine *17*, 313-319.

Collins, E.C., Appert, A., Ariza-McNaughton, L., Pannell, R., Yamada, Y., and Rabbitts, T.H. (2002). Mouse Af9 is a controller of embryo patterning, like Mll, whose human homologue fuses with Af9 after chromosomal translocation in leukemia. Molecular and cellular biology *22*, 7313-7324.

Daigle, S.R., Olhava, E.J., Therkelsen, C.A., Majer, C.R., Sneeringer, C.J., Song, J., Johnston, L.D., Scott, M.P., Smith, J.J., Xiao, Y.*, et al.* (2011). Selective killing of mixed lineage leukemia cells by a potent small-molecule DOT1L inhibitor. Cancer cell *20*, 53-65.

Daser, A., and Rabbitts, T.H. (2004). Extending the repertoire of the mixed-lineage leukemia gene MLL in leukemogenesis. Genes Dev *18*, 965-974.

Daub, H., Olsen, J.V., Bairlein, M., Gnad, F., Oppermann, F.S., Korner, R., Greff, Z., Keri, G., Stemmann, O., and Mann, M. (2008). Kinase-selective enrichment enables quantitative phosphoproteomics of the kinome across the cell cycle. Mol Cell *31*, 438-448.

Dawson, M.A., Prinjha, R.K., Dittmann, A., Giotopoulos, G., Bantscheff, M., Chan, W.I., Robson, S.C., Chung, C.W., Hopf, C., Savitski, M.M.*, et al.* (2011). Inhibition of BET recruitment to chromatin as an effective treatment for MLL-fusion leukaemia. Nature *478*, 529-533.

Delmore, J.E., Issa, G.C., Lemieux, M.E., Rahl, P.B., Shi, J., Jacobs, H.M., Kastritis, E., Gilpatrick, T., Paranal, R.M., Qi, J.*, et al.* (2011). BET bromodomain inhibition as a therapeutic strategy to target c-Myc. Cell *146*, 904-917.

Dephoure, N., Zhou, C., Villen, J., Beausoleil, S.A., Bakalarski, C.E., Elledge, S.J., and Gygi, S.P. (2008). A quantitative atlas of mitotic phosphorylation. Proc Natl Acad Sci U S A *105*, 10762-10767.

Desouza, M., Gunning, P.W., and Stehn, J.R. (2012). The actin cytoskeleton as a sensor and mediator of apoptosis. Bioarchitecture *2*, 75-87.

Diamanti, P., Cox, C.V., Moppett, J.P., and Blair, A. (2013). Parthenolide eliminates leukemia-initiating cell populations and improves survival in xenografts of childhood acute lymphoblastic leukemia. Blood *121*, 1384-1393.

Dobson, C.L., Warren, A.J., Pannell, R., Forster, A., Lavenir, I., Corral, J., Smith, A.J., and Rabbitts, T.H. (1999). The mll-AF9 gene fusion in mice controls myeloproliferation and specifies acute myeloid leukaemogenesis. The EMBO journal *18*, 3564-3574.

Dobson, C.L., Warren, A.J., Pannell, R., Forster, A., and Rabbitts, T.H. (2000). Tumorigenesis in mice with a fusion of the leukaemia oncogene Mll and the bacterial lacZ gene. The EMBO journal *19*, 843-851.

Dou, Y., Milne, T.A., Ruthenburg, A.J., Lee, S., Lee, J.W., Verdine, G.L., Allis, C.D., and Roeder, R.G. (2006). Regulation of MLL1 H3K4 methyltransferase activity by its core components. Nature structural & molecular biology *13*, 713-719.

Dou, Y., Milne, T.A., Tackett, A.J., Smith, E.R., Fukuda, A., Wysocka, J., Allis, C.D., Chait, B.T., Hess, J.L., and Roeder, R.G. (2005). Physical association and coordinate function of the H3 K4 methyltransferase MLL1 and the H4 K16 acetyltransferase MOF. Cell *121*, 873-885.

Drake, A.C., Chen, Q., and Chen, J. (2012). Engineering humanized mice for improved hematopoietic reconstitution. Cellular & molecular immunology *9*, 215-224.

Emambokus, N., Vegiopoulos, A., Harman, B., Jenkinson, E., Anderson, G., and Frampton, J. (2003). Progression through key stages of haemopoiesis is dependent on distinct threshold levels of c-Myb. The EMBO journal *22*, 4478-4488.

Erfurth, F., Hemenway, C.S., de Erkenez, A.C., and Domer, P.H. (2004). MLL fusion partners AF4 and AF9 interact at subnuclear foci. Leukemia *18*, 92-102.

Erfurth, F.E., Popovic, R., Grembecka, J., Cierpicki, T., Theisler, C., Xia, Z.B., Stuart, T., Diaz, M.O., Bushweller, J.H., and Zeleznik-Le, N.J. (2008). MLL protects CpG clusters from methylation within the Hoxa9 gene, maintaining transcript expression. Proc Natl Acad Sci U S A *105*, 7517-7522.

Ernst, P., Wang, J., Huang, M., Goodman, R.H., and Korsmeyer, S.J. (2001). MLL and CREB bind cooperatively to the nuclear coactivator CREB-binding protein. Mol Cell Biol *21*, 2249-2258.

Esposito, G., Cevenini, A., Cuomo, A., de Falco, F., Sabbatino, D., Pane, F., Ruoppolo, M., and Salvatore, F. (2011). Protein network study of human AF4 reveals its central role in RNA Pol II-mediated transcription and in phosphorylation-dependent regulatory mechanisms. The Biochemical journal *438*, 121-131.

Faber, J., Krivtsov, A.V., Stubbs, M.C., Wright, R., Davis, T.N., van den Heuvel-Eibrink, M., Zwaan, C.M., Kung, A.L., and Armstrong, S.A. (2009). HOXA9 is required for survival in human MLL-rearranged acute leukemias. Blood *113*, 2375-2385.

Felix, C.A. (1998). Secondary leukemias induced by topoisomerase-targeted drugs. Biochim Biophys Acta *1400*, 233-255.

Fuda, N.J., Ardehali, M.B., and Lis, J.T. (2009). Defining mechanisms that regulate RNA polymerase II transcription in vivo. Nature *461*, 186-192.

Gaussmann, A., Wenger, T., Eberle, I., Bursen, A., Bracharz, S., Herr, I., Dingermann, T., and Marschalek, R. (2007). Combined effects of the two reciprocal t(4;11) fusion proteins MLL.AF4 and AF4.MLL confer resistance to apoptosis, cell cycling capacity and growth transformation. Oncogene *26*, 3352-3363.

Gilmour, D.S. (2009). Promoter proximal pausing on genes in metazoans. Chromosoma *118*, 1-10.

Gu, Y., Nakamura, T., Alder, H., Prasad, R., Canaani, O., Cimino, G., Croce, C.M., and Canaani, E. (1992). The t(4;11) chromosome translocation of human acute leukemias fuses the ALL-1 gene, related to Drosophila trithorax, to the AF-4 gene. Cell *71*, 701-708.

Gu, Y., and Nelson, D.L. (2003). FMR2 function: insight from a mouse knockout model. Cytogenetic and genome research *100*, 129-139.

Gu, Y., Shen, Y., Gibbs, R.A., and Nelson, D.L. (1996). Identification of FMR2, a novel gene associated with the FRAXE CCG repeat and CpG island. Nature genetics *13*, 109-113.

Guenther, M.G., Jenner, R.G., Chevalier, B., Nakamura, T., Croce, C.M., Canaani, E., and Young, R.A. (2005). Global and Hox-specific roles for the MLL1 methyltransferase. Proc Natl Acad Sci U S A *102*, 8603-8608.

Guinez, C., Morelle, W., Michalski, J.C., and Lefebvre, T. (2005). O-GlcNAc glycosylation: a signal for the nuclear transport of cytosolic proteins? The international journal of biochemistry & cell biology *37*, 765-774.

Hallbrink, M., Floren, A., Elmquist, A., Pooga, M., Bartfai, T., and Langel, U. (2001). Cargo delivery kinetics of cell-penetrating peptides. Biochim Biophys Acta *1515*, 101-109.

Hanson, R.D., Hess, J.L., Yu, B.D., Ernst, P., van Lohuizen, M., Berns, A., van der Lugt, N.M., Shashikant, C.S., Ruddle, F.H., Seto, M.*, et al.* (1999). Mammalian Trithorax and polycomb-group homologues are antagonistic regulators of homeotic development. Proc Natl Acad Sci U S A *96*, 14372-14377.

Harata, M., Soda, Y., Tani, K., Ooi, J., Takizawa, T., Chen, M., Bai, Y., Izawa, K., Kobayashi, S., Tomonari, A.*, et al.* (2004). CD19-targeting liposomes containing

imatinib efficiently kill Philadelphia chromosome-positive acute lymphoblastic leukemia cells. Blood *104*, 1442-1449.

Haribaskar, R., Putz, M., Schupp, B., Skouloudaki, K., Bietenbeck, A., Walz, G., and Schafer, T. (2009). The planar cell polarity (PCP) protein Diversin translocates to the nucleus to interact with the transcription factor AF9. Biochemical and biophysical research communications *387*, 212-217.

Harris, W.J., Huang, X., Lynch, J.T., Spencer, G.J., Hitchin, J.R., Li, Y., Ciceri, F., Blaser, J.G., Greystoke, B.F., Jordan, A.M.*, et al.* (2012). The histone demethylase KDM1A sustains the oncogenic potential of MLL-AF9 leukemia stem cells. Cancer cell *21*, 473-487.

He, N., Chan, C.K., Sobhian, B., Chou, S., Xue, Y., Liu, M., Alber, T., Benkirane, M., and Zhou, Q. (2011). Human Polymerase-Associated Factor complex (PAFc) connects the Super Elongation Complex (SEC) to RNA polymerase II on chromatin. Proc Natl Acad Sci U S A *108*, E636-645.

He, N., Liu, M., Hsu, J., Xue, Y., Chou, S., Burlingame, A., Krogan, N.J., Alber, T., and Zhou, Q. (2010). HIV-1 Tat and host AFF4 recruit two transcription elongation factors into a bifunctional complex for coordinated activation of HIV-1 transcription. Mol Cell *38*, 428-438.

Heerema, N.A., Sather, H.N., Ge, J., Arthur, D.C., Hilden, J.M., Trigg, M.E., and Reaman, G.H. (1999). Cytogenetic studies of infant acute lymphoblastic leukemia: poor prognosis of infants with t(4;11) - a report of the Children's Cancer Group. Leukemia *13*, 679-686.

Hemenway, C.S., de Erkenez, A.C., and Gould, G.C. (2001). The polycomb protein MPc3 interacts with AF9, an MLL fusion partner in t(9;11)(p22;q23) acute leukemias. Oncogene *20*, 3798-3805.

Hisa, T., Spence, S.E., Rachel, R.A., Fujita, M., Nakamura, T., Ward, J.M., Devor-Henneman, D.E., Saiki, Y., Kutsuna, H., Tessarollo, L.*, et al.* (2004). Hematopoietic, angiogenic and eye defects in Meis1 mutant animals. The EMBO journal *23*, 450-459.

Ho, A., Schwarze, S.R., Mermelstein, S.J., Waksman, G., and Dowdy, S.F. (2001). Synthetic protein transduction domains: enhanced transduction potential in vitro and in vivo. Cancer research *61*, 474-477.

Hofmann, W.A., Stojiljkovic, L., Fuchsova, B., Vargas, G.M., Mavrommatis, E., Philimonenko, V., Kysela, K., Goodrich, J.A., Lessard, J.L., Hope, T.J.*, et al.* (2004). Actin is part of pre-initiation complexes and is necessary for transcription by RNA polymerase II. Nature cell biology *6*, 1094-1101.

Horton, S.J., Grier, D.G., McGonigle, G.J., Thompson, A., Morrow, M., De Silva, I., Moulding, D.A., Kioussis, D., Lappin, T.R., Brady, H.J.*, et al.* (2005). Continuous MLL-ENL expression is necessary to establish a "Hox Code" and maintain immortalization of hematopoietic progenitor cells. Cancer Res *65*, 9245-9252.

Horton, S.J., Jaques, J., Woolthuis, C., van Dijk, J., Mesuraca, M., Huls, G., Morrone, G., Vellenga, E., and Schuringa, J.J. (2012). MLL-AF9-mediated immortalization of human hematopoietic cells along different lineages changes during ontogeny. Leukemia.

Hsieh, J.J., Cheng, E.H., and Korsmeyer, S.J. (2003a). Taspase1: a threonine aspartase required for cleavage of MLL and proper HOX gene expression. Cell *115*, 293-303.

Hsieh, J.J., Ernst, P., Erdjument-Bromage, H., Tempst, P., and Korsmeyer, S.J. (2003b). Proteolytic cleavage of MLL generates a complex of N- and C-terminal fragments that confers protein stability and subnuclear localization. Mol Cell Biol *23*, 186-194.

Hu, P., Wu, S., and Hernandez, N. (2004). A role for beta-actin in RNA polymerase III transcription. Genes Dev *18*, 3010-3015.

Iida, S., Seto, M., Yamamoto, K., Komatsu, H., Tojo, A., Asano, S., Kamada, N., Ariyoshi, Y., Takahashi, T., and Ueda, R. (1993). MLLT3 gene on 9p22 involved in t(9;11) leukemia encodes a serine/proline rich protein homologous to MLLT1 on 19p13. Oncogene *8*, 3085-3092.

Irobi, E., Aguda, A.H., Larsson, M., Guerin, C., Yin, H.L., Burtnick, L.D., Blanchoin, L., and Robinson, R.C. (2004). Structural basis of actin sequestration by thymosin-beta4: implications for WH2 proteins. The EMBO journal *23*, 3599-3608.

Isel, C., and Karn, J. (1999). Direct evidence that HIV-1 Tat stimulates RNA polymerase II carboxyl-terminal domain hyperphosphorylation during transcriptional elongation. Journal of molecular biology *290*, 929-941.

Isnard, P., Core, N., Naquet, P., and Djabali, M. (2000). Altered lymphoid development in mice deficient for the mAF4 proto-oncogene. Blood *96*, 705-710.

Jang, M.K., Mochizuki, K., Zhou, M., Jeong, H.S., Brady, J.N., and Ozato, K. (2005). The bromodomain protein Brd4 is a positive regulatory component of P-TEFb and stimulates RNA polymerase II-dependent transcription. Mol Cell *19*, 523-534.

Jeanmougin, F., Wurtz, J.M., Le Douarin, B., Chambon, P., and Losson, R. (1997). The bromodomain revisited. Trends in biochemical sciences *22*, 151-153.

Jiang, X., Huang, H., Li, Z., He, C., Li, Y., Chen, P., Gurbuxani, S., Arnovitz, S., Hong, G.M., Price, C.*, et al.* (2012). MiR-495 is a tumor-suppressor microRNA down-regulated in MLL-rearranged leukemia. Proc Natl Acad Sci U S A *109*, 19397-19402.

Jin, S., Zhao, H., Yi, Y., Nakata, Y., Kalota, A., and Gewirtz, A.M. (2010). c-Myb binds MLL through menin in human leukemia cells and is an important driver of MLL-associated leukemogenesis. The Journal of clinical investigation *120*, 593-606.

Jo, S.Y., Granowicz, E.M., Maillard, I., Thomas, D., and Hess, J.L. (2011). Requirement for Dot1l in murine postnatal hematopoiesis and leukemogenesis by MLL translocation. Blood *117*, 4759-4768.

Jude, C.D., Climer, L., Xu, D., Artinger, E., Fisher, J.K., and Ernst, P. (2007). Unique and independent roles for MLL in adult hematopoietic stem cells and progenitors. Cell stem cell *1*, 324-337.

Kasamon, Y.L., Jones, R.J., Gocke, C.D., Blackford, A.L., Seifter, E.J., Davis-Sproul, J.M., Gore, S.D., and Ambinder, R.F. (2011). Extended follow-up of autologous bone marrow transplantation with 4-hydroperoxycyclophosphamide (4-HC) purging for indolent or transformed non-Hodgkin lymphomas. Biology of blood and marrow transplantation : journal of the American Society for Blood and Marrow Transplantation *17*, 365-373.

Kawagoe, H., Humphries, R.K., Blair, A., Sutherland, H.J., and Hogge, D.E. (1999). Expression of HOX genes, HOX cofactors, and MLL in phenotypically and functionally defined subpopulations of leukemic and normal human hematopoietic cells. Leukemia *13*, 687-698.

Kim, H.R., Gallant, C., Leavis, P.C., Gunst, S.J., and Morgan, K.G. (2008). Cytoskeletal remodeling in differentiated vascular smooth muscle is actin isoform dependent and stimulus dependent. American journal of physiology Cell physiology *295*, C768-778.

Kim, S.J., Hwang, S.G., Kim, I.C., and Chun, J.S. (2003). Actin cytoskeletal architecture regulates nitric oxide-induced apoptosis, dedifferentiation, and cyclooxygenase-2 expression in articular chondrocytes via mitogen-activated protein kinase and protein kinase C pathways. J Biol Chem *278*, 42448-42456.

Klose, R.J., and Bird, A.P. (2006). Genomic DNA methylation: the mark and its mediators. Trends in biochemical sciences *31*, 89-97.

Kouzarides, T. (2002). Histone methylation in transcriptional control. Current opinion in genetics & development *12*, 198-209.

Kozuka, T., Sugita, M., Shetzline, S., Gewirtz, A.M., and Nakata, Y. (2011). c-Myb and GATA-3 cooperatively regulate IL-13 expression via conserved GATA-3 response element and recruit mixed lineage leukemia (MLL) for histone modification of the IL-13 locus. J Immunol *187*, 5974-5982.

Krivtsov, A.V., and Armstrong, S.A. (2007). MLL translocations, histone modifications and leukaemia stem-cell development. Nature reviews Cancer *7*, 823-833.

Kroon, E., Krosl, J., Thorsteinsdottir, U., Baban, S., Buchberg, A.M., and Sauvageau, G. (1998). Hoxa9 transforms primary bone marrow cells through specific collaboration with Meis1a but not Pbx1b. The EMBO journal *17*, 3714-3725.

Kumar, A.R., Hudson, W.A., Chen, W., Nishiuchi, R., Yao, Q., and Kersey, J.H. (2004). Hoxa9 influences the phenotype but not the incidence of Mll-AF9 fusion gene leukemia. Blood *103*, 1823-1828.

Laudadio, R.E., Millet, E.J., Fabry, B., An, S.S., Butler, J.P., and Fredberg, J.J. (2005). Rat airway smooth muscle cell during actin modulation: rheology and glassy dynamics. American journal of physiology Cell physiology *289*, C1388-1395.

Lavau, C., Szilvassy, S.J., Slany, R., and Cleary, M.L. (1997). Immortalization and leukemic transformation of a myelomonocytic precursor by retrovirally transduced HRX-ENL. The EMBO journal *16*, 4226-4237.

Lawrence, H.J., Helgason, C.D., Sauvageau, G., Fong, S., Izon, D.J., Humphries, R.K., and Largman, C. (1997). Mice bearing a targeted interruption of the homeobox gene HOXA9 have defects in myeloid, erythroid, and lymphoid hematopoiesis. Blood *89*, 1922-1930.

Leach, B.I., Kuntimaddi, A., Schmidt, C.R., Cierpicki, T., Johnson, S.A., and Bushweller, J.H. (2013). Leukemia fusion target AF9 is an intrinsically disordered transcriptional regulator that recruits multiple partners via coupled folding and binding. Structure (London, England : 1993) *21*, 176-183.

Li, J., Li, Q., Xie, C., Zhou, H., Wang, Y., Zhang, N., Shao, H., Chan, S.C., Peng, X., Lin, S.C.*, et al.* (2004). Beta-actin is required for mitochondria clustering and ROS generation in TNF-induced, caspase-independent cell death. Journal of cell science *117*, 4673-4680.

Li, X., Wu, L., Corsa, C.A., Kunkel, S., and Dou, Y. (2009). Two mammalian MOF complexes regulate transcription activation by distinct mechanisms. Mol Cell *36*, 290-301.

Li, Z., Zhang, Z., Li, Y., Arnovitz, S., Chen, P., Huang, H., Jiang, X., Hong, G.M., Kunjamma, R.B., Ren, H.*, et al.* (2013). PBX3 is an important cofactor of HOXA9 in leukemogenesis. Blood *121*, 1422-1431.

Lin, C., Garrett, A.S., De Kumar, B., Smith, E.R., Gogol, M., Seidel, C., Krumlauf, R., and Shilatifard, A. (2011). Dynamic transcriptional events in embryonic stem cells mediated by the super elongation complex (SEC). Genes Dev *25*, 1486-1498.

Lin, C., Smith, E.R., Takahashi, H., Lai, K.C., Martin-Brown, S., Florens, L., Washburn, M.P., Conaway, J.W., Conaway, R.C., and Shilatifard, A. (2010a). AFF4, a component of the ELL/P-TEFb elongation complex and a shared subunit of MLL chimeras, can link transcription elongation to leukemia. Mol Cell *37*, 429-437.

Lin, C., Smith, E.R., Takahashi, H., Lai, K.C., Martin-Brown, S., Florens, L., Washburn, M.P., Conaway, J.W., Conaway, R.C., and Shilatifard, A. (2010b). AFF4, a component of the ELL/P-TEFb elongation complex and a shared subunit of MLL chimeras, can link transcription elongation to leukemia. Molecular cell *37*, 429-437.

Lin, J.H. (2009). Pharmacokinetics of biotech drugs: peptides, proteins and monoclonal antibodies. Current drug metabolism *10*, 661-691.

Lin, J.J., and Hemenway, C.S. (2010). Hsp90 directly modulates the spatial distribution of AF9/MLLT3 and affects target gene expression. J Biol Chem *285*, 11966-11973.

Liu, H., Cheng, E.H., and Hsieh, J.J. (2007). Bimodal degradation of MLL by SCFSkp2 and APCCdc20 assures cell cycle execution: a critical regulatory circuit lost in leukemogenic MLL fusions. Genes Dev *21*, 2385-2398.

Liu, H., Takeda, S., Cheng, E.H., and Hsieh, J.J. (2008). Biphasic MLL takes helm at cell cycle control: implications in human mixed lineage leukemia. Cell Cycle *7*, 428-435.

Liu, H., Takeda, S., Kumar, R., Westergard, T.D., Brown, E.J., Pandita, T.K., Cheng, E.H., and Hsieh, J.J. (2010). Phosphorylation of MLL by ATR is required for execution of mammalian S-phase checkpoint. Nature *467*, 343-346.

Liu, M., Hsu, J., Chan, C., Li, Z., and Zhou, Q. (2012). The ubiquitin ligase Siah1 controls ELL2 stability and formation of super elongation complexes to modulate gene transcription. Mol Cell *46*, 325-334.

Ma, C., and Staudt, L.M. (1996). LAF-4 encodes a lymphoid nuclear protein with transactivation potential that is homologous to AF-4, the gene fused to MLL in t(4;11) leukemias. Blood *87*, 734-745.

Mann, G., Attarbaschi, A., Schrappe, M., De Lorenzo, P., Peters, C., Hann, I., De Rossi, G., Felice, M., Lausen, B., Leblanc, T.*, et al.* (2010). Improved outcome with hematopoietic stem cell transplantation in a poor prognostic subgroup of infants with mixed-lineage-leukemia (MLL)-rearranged acute lymphoblastic leukemia: results from the Interfant-99 Study. Blood *116*, 2644-2650.

Martin, M.E., Milne, T.A., Bloyer, S., Galoian, K., Shen, W., Gibbs, D., Brock, H.W., Slany, R., and Hess, J.L. (2003). Dimerization of MLL fusion proteins immortalizes hematopoietic cells. Cancer cell *4*, 197-207.

Melko, M., Douguet, D., Bensaid, M., Zongaro, S., Verheggen, C., Gecz, J., and Bardoni, B. (2011). Functional characterization of the AFF (AF4/FMR2) family of RNA-

binding proteins: insights into the molecular pathology of FRAXE intellectual disability. Hum Mol Genet *20*, 1873-1885.

Menendez, P., Catalina, P., Rodriguez, R., Melen, G.J., Bueno, C., Arriero, M., Garcia-Sanchez, F., Lassaletta, A., Garcia-Sanz, R., and Garcia-Castro, J. (2009). Bone marrow mesenchymal stem cells from infants with MLL-AF4+ acute leukemia harbor and express the MLL-AF4 fusion gene. The Journal of experimental medicine *206*, 3131-3141.

Meyer, C., Kowarz, E., Hofmann, J., Renneville, A., Zuna, J., Trka, J., Ben Abdelali, R., Macintyre, E., De Braekeleer, E., De Braekeleer, M.*, et al.* (2009). New insights to the MLL recombinome of acute leukemias. Leukemia *23*, 1490-1499.

Mi, Z., Mai, J., Lu, X., and Robbins, P.D. (2000). Characterization of a class of cationic peptides able to facilitate efficient protein transduction in vitro and in vivo. Molecular therapy : the journal of the American Society of Gene Therapy *2*, 339-347.

Milne, T.A., Briggs, S.D., Brock, H.W., Martin, M.E., Gibbs, D., Allis, C.D., and Hess, J.L. (2002). MLL targets SET domain methyltransferase activity to Hox gene promoters. Mol Cell *10*, 1107-1117.

Milne, T.A., Dou, Y., Martin, M.E., Brock, H.W., Roeder, R.G., and Hess, J.L. (2005a). MLL associates specifically with a subset of transcriptionally active target genes. Proc Natl Acad Sci U S A *102*, 14765-14770.

Milne, T.A., Hughes, C.M., Lloyd, R., Yang, Z., Rozenblatt-Rosen, O., Dou, Y., Schnepp, R.W., Krankel, C., Livolsi, V.A., Gibbs, D.*, et al.* (2005b). Menin and MLL cooperatively regulate expression of cyclin-dependent kinase inhibitors. Proc Natl Acad Sci U S A *102*, 749-754.

Mohan, M., Herz, H.M., Takahashi, Y.H., Lin, C., Lai, K.C., Zhang, Y., Washburn, M.P., Florens, L., and Shilatifard, A. (2010a). Linking H3K79 trimethylation to Wnt signaling through a novel Dot1-containing complex (DotCom). Genes Dev *24*, 574-589.

Mohan, M., Lin, C., Guest, E., and Shilatifard, A. (2010b). Licensed to elongate: a molecular mechanism for MLL-based leukaemogenesis. Nature reviews Cancer *10*, 721-728.

Monroe, S.C., Jo, S.Y., Sanders, D.S., Basrur, V., Elenitoba-Johnson, K.S., Slany, R.K., and Hess, J.L. (2011). MLL-AF9 and MLL-ENL alter the dynamic association of transcriptional regulators with genes critical for leukemia. Experimental hematology *39*, 77-86.e71-75.

Monsigny, M., Roche, A.C., Sene, C., Maget-Dana, R., and Delmotte, F. (1980). Sugar-lectin interactions: how does wheat-germ agglutinin bind sialoglycoconjugates? European journal of biochemistry / FEBS *104*, 147-153.

Montes, R., Ayllon, V., Gutierrez-Aranda, I., Prat, I., Hernandez-Lamas, M.C., Ponce, L., Bresolin, S., Te Kronnie, G., Greaves, M., Bueno, C.*, et al.* (2011). Enforced expression of MLL-AF4 fusion in cord blood CD34+ cells enhances the hematopoietic repopulating cell function and clonogenic potential but is not sufficient to initiate leukemia. Blood *117*, 4746-4758.

Morey, L., and Helin, K. (2010). Polycomb group protein-mediated repression of transcription. Trends in biochemical sciences *35*, 323-332.

Morton, W.M., Ayscough, K.R., and McLaughlin, P.J. (2000). Latrunculin alters the actin-monomer subunit interface to prevent polymerization. Nature cell biology *2*, 376-378.

Mucenski, M.L., McLain, K., Kier, A.B., Swerdlow, S.H., Schreiner, C.M., Miller, T.A., Pietryga, D.W., Scott, W.J., Jr., and Potter, S.S. (1991). A functional c-myb gene is required for normal murine fetal hepatic hematopoiesis. Cell *65*, 677-689.

Mueller, D., Garcia-Cuellar, M.P., Bach, C., Buhl, S., Maethner, E., and Slany, R.K. (2009). Misguided transcriptional elongation causes mixed lineage leukemia. PLoS Biol *7*, e1000249.

Muntean, A.G., Giannola, D., Udager, A.M., and Hess, J.L. (2008). The PHD fingers of MLL block MLL fusion protein-mediated transformation. Blood *112*, 4690-4693.

Muntean, A.G., Tan, J., Sitwala, K., Huang, Y., Bronstein, J., Connelly, J.A., Basrur, V., Elenitoba-Johnson, K.S., and Hess, J.L. (2010). The PAF complex synergizes with MLL fusion proteins at HOX loci to promote leukemogenesis. Cancer cell *17*, 609-621.

Muratani, M., and Tansey, W.P. (2003). How the ubiquitin-proteasome system controls transcription. Nature reviews Molecular cell biology *4*, 192-201.

Nakamura, T., Alder, H., Gu, Y., Prasad, R., Canaani, O., Kamada, N., Gale, R.P., Lange, B., Crist, W.M., and Nowell, P.C. (1993). Genes on chromosomes 4, 9, and 19 involved in 11q23 abnormalities in acute leukemia share sequence homology and/or common motifs. Proceedings of the National Academy of Sciences of the United States of America *90*, 4631-4635.

Neff, T., Sinha, A.U., Kluk, M.J., Zhu, N., Khattab, M.H., Stein, L., Xie, H., Orkin, S.H., and Armstrong, S.A. (2012). Polycomb repressive complex 2 is required for MLL-AF9 leukemia. Proc Natl Acad Sci U S A *109*, 5028-5033.

Nguyen, A.T., Taranova, O., He, J., and Zhang, Y. (2011). DOT1L, the H3K79 methyltransferase, is required for MLL-AF9-mediated leukemogenesis. Blood *117*, 6912-6922.

Nie, L., Sasaki, M., and Maki, C.G. (2007). Regulation of p53 nuclear export through sequential changes in conformation and ubiquitination. J Biol Chem *282*, 14616-14625.

Okada, Y., Feng, Q., Lin, Y., Jiang, Q., Li, Y., Coffield, V.M., Su, L., Xu, G., and Zhang, Y. (2005). hDOT1L links histone methylation to leukemogenesis. Cell *121*, 167-178.

Oliver, P.L., Bitoun, E., Clark, J., Jones, E.L., and Davies, K.E. (2004). Mediation of Af4 protein function in the cerebellum by Siah proteins. Proc Natl Acad Sci U S A *101*, 14901-14906.

Olsen, J.V., Vermeulen, M., Santamaria, A., Kumar, C., Miller, M.L., Jensen, L.J., Gnad, F., Cox, J., Jensen, T.S., Nigg, E.A.*, et al.* (2010). Quantitative phosphoproteomics reveals widespread full phosphorylation site occupancy during mitosis. Science signaling *3*, ra3.

Oppermann, F.S., Gnad, F., Olsen, J.V., Hornberger, R., Greff, Z., Keri, G., Mann, M., and Daub, H. (2009). Large-scale proteomics analysis of the human kinome. Molecular & cellular proteomics : MCP *8*, 1751-1764.

Palermo, C.M., Bennett, C.A., Winters, A.C., and Hemenway, C.S. (2008). The AF4-mimetic peptide, PFWT, induces necrotic cell death in MV4-11 leukemia cells. Leukemia research *32*, 633-642.

Papakonstanti, E.A., and Stournaras, C. (2008). Cell responses regulated by early reorganization of actin cytoskeleton. FEBS letters *582*, 2120-2127.

Park, S., Osmers, U., Raman, G., Schwantes, R.H., Diaz, M.O., and Bushweller, J.H. (2010). The PHD3 domain of MLL acts as a CYP33-regulated switch between MLL-mediated activation and repression. Biochemistry *49*, 6576-6586.

Peloponese, J.M., Jr., Iha, H., Yedavalli, V.R., Miyazato, A., Li, Y., Haller, K., Benkirane, M., and Jeang, K.T. (2004). Ubiquitination of human T-cell leukemia virus type 1 tax modulates its activity. Journal of virology *78*, 11686-11695.

Peterlin, B.M., and Price, D.H. (2006). Controlling the elongation phase of transcription with P-TEFb. Mol Cell *23*, 297-305.

Peterson, C.L., and Laniel, M.A. (2004). Histones and histone modifications. Current biology : CB *14*, R546-551.

Philimonenko, V.V., Zhao, J., Iben, S., Dingova, H., Kysela, K., Kahle, M., Zentgraf, H., Hofmann, W.A., de Lanerolle, P., Hozak, P.*, et al.* (2004). Nuclear actin and myosin I are required for RNA polymerase I transcription. Nature cell biology *6*, 1165-1172.

Pina, C., May, G., Soneji, S., Hong, D., and Enver, T. (2008). MLLT3 regulates early human erythroid and megakaryocytic cell fate. Cell stem cell *2*, 264-273.

Popovic, R., Riesbeck, L.E., Velu, C.S., Chaubey, A., Zhang, J., Achille, N.J., Erfurth, F.E., Eaton, K., Lu, J., Grimes, H.L.*, et al.* (2009). Regulation of mir-196b by MLL and its overexpression by MLL fusions contributes to immortalization. Blood *113*, 3314-3322.

Pramparo, T., Grosso, S., Messa, J., Zatterale, A., Bonaglia, M.C., Chessa, L., Balestri, P., Rocchi, M., Zuffardi, O., and Giorda, R. (2005). Loss-of-function mutation of the AF9/MLLT3 gene in a girl with neuromotor development delay, cerebellar ataxia, and epilepsy. Human genetics *118*, 76-81.

Prasad, R., Yano, T., Sorio, C., Nakamura, T., Rallapalli, R., Gu, Y., Leshkowitz, D., Croce, C.M., and Canaani, E. (1995). Domains with transcriptional regulatory activity within the ALL1 and AF4 proteins involved in acute leukemia. Proc Natl Acad Sci U S A *92*, 12160-12164.

Pui, C.H., Gaynon, P.S., Boyett, J.M., Chessells, J.M., Baruchel, A., Kamps, W., Silverman, L.B., Biondi, A., Harms, D.O., Vilmer, E.*, et al.* (2002). Outcome of treatment in childhood acute lymphoblastic leukaemia with rearrangements of the 11q23 chromosomal region. Lancet *359*, 1909-1915.

Pui, C.H., and Relling, M.V. (2000). Topoisomerase II inhibitor-related acute myeloid leukaemia. British journal of haematology *109*, 13-23.

Rao, J.Y., Jin, Y.S., Zheng, Q., Cheng, J., Tai, J., and Hemstreet, G.P., 3rd (1999). Alterations of the actin polymerization status as an apoptotic morphological effector in HL-60 cells. Journal of cellular biochemistry *75*, 686-697.

Reisenauer, M.R., Anderson, M., Huang, L., Zhang, Z., Zhou, Q., Kone, B.C., Morris, A.P., Lesage, G.D., Dryer, S.E., and Zhang, W. (2009). AF17 competes with AF9 for binding to Dot1a to up-regulate transcription of epithelial Na+ channel alpha. J Biol Chem *284*, 35659-35669.

Ren, J.G., Seth, P., Everett, P., Clish, C.B., and Sukhatme, V.P. (2010). Induction of erythroid differentiation in human erythroleukemia cells by depletion of malic enzyme 2. PloS one *5*.

Ross, M.E., Mahfouz, R., Onciu, M., Liu, H.C., Zhou, X., Song, G., Shurtleff, S.A., Pounds, S., Cheng, C., Ma, J.*, et al.* (2004). Gene expression profiling of pediatric acute myelogenous leukemia. Blood *104*, 3679-3687.

Rozovskaia, T., Feinstein, E., Mor, O., Foa, R., Blechman, J., Nakamura, T., Croce, C.M., Cimino, G., and Canaani, E. (2001). Upregulation of Meis1 and HoxA9 in acute lymphocytic leukemias with the t(4 : 11) abnormality. Oncogene *20*, 874-878.

Rozovskaia, T., Ravid-Amir, O., Tillib, S., Getz, G., Feinstein, E., Agrawal, H., Nagler, A., Rappaport, E.F., Issaeva, I., Matsuo, Y.*, et al.* (2003). Expression profiles of acute lymphoblastic and myeloblastic leukemias with ALL-1 rearrangements. Proc Natl Acad Sci U S A *100*, 7853-7858.

Rubnitz, J.E., Morrissey, J., Savage, P.A., and Cleary, M.L. (1994). ENL, the gene fused with HRX in t(11;19) leukemias, encodes a nuclear protein with transcriptional activation potential in lymphoid and myeloid cells. Blood *84*, 1747-1752.

Salghetti, S.E., Muratani, M., Wijnen, H., Futcher, B., and Tansey, W.P. (2000). Functional overlap of sequences that activate transcription and signal ubiquitin-mediated proteolysis. Proc Natl Acad Sci U S A *97*, 3118-3123.

Santi, D.V., Schneider, E.L., Reid, R., Robinson, L., and Ashley, G.W. (2012). Predictable and tunable half-life extension of therapeutic agents by controlled chemical release from macromolecular conjugates. Proc Natl Acad Sci U S A *109*, 6211-6216.

Schnabel, C.A., Jacobs, Y., and Cleary, M.L. (2000). HoxA9-mediated immortalization of myeloid progenitors requires functional interactions with TALE cofactors Pbx and Meis. Oncogene *19*, 608-616.

Schoch, C., Schnittger, S., Klaus, M., Kern, W., Hiddemann, W., and Haferlach, T. (2003). AML with 11q23/MLL abnormalities as defined by the WHO classification: incidence, partner chromosomes, FAB subtype, age distribution, and prognostic impact in an unselected series of 1897 cytogenetically analyzed AML cases. Blood *102*, 2395-2402.

Schulze, J.M., Jackson, J., Nakanishi, S., Gardner, J.M., Hentrich, T., Haug, J., Johnston, M., Jaspersen, S.L., Kobor, M.S., and Shilatifard, A. (2009a). Linking cell cycle to histone modifications: SBF and H2B monoubiquitination machinery and cell-cycle regulation of H3K79 dimethylation. Mol Cell *35*, 626-641.

Schulze, J.M., Wang, A.Y., and Kobor, M.S. (2009b). YEATS domain proteins: a diverse family with many links to chromatin modification and transcription. Biochemistry and cell biology = Biochimie et biologie cellulaire *87*, 65-75.

Selvaggi, K.J., Wilson, J.W., Mills, L.E., Cornwell, G.G., 3rd, Hurd, D., Dodge, W., Gingrich, R., Martin, S.E., McMillan, R., Miller, W.*, et al.* (1994). Improved outcome for high-risk acute myeloid leukemia patients using autologous bone marrow transplantation and monoclonal antibody-purged bone marrow. Blood *83*, 1698-1705.

Shi, J., Wang, E., Zuber, J., Rappaport, A., Taylor, M., Johns, C., Lowe, S.W., and Vakoc, C.R. (2013). The Polycomb complex PRC2 supports aberrant self-renewal in a mouse model of MLL-AF9;Nras(G12D) acute myeloid leukemia. Oncogene *32*, 930-938.

Shi, Y., Lan, F., Matson, C., Mulligan, P., Whetstine, J.R., Cole, P.A., and Casero, R.A. (2004). Histone demethylation mediated by the nuclear amine oxidase homolog LSD1. Cell *119*, 941-953.

Sitwala, K.V., Dandekar, M.N., and Hess, J.L. (2008). HOX proteins and leukemia. International journal of clinical and experimental pathology *1*, 461-474.

Slany, R.K., Lavau, C., and Cleary, M.L. (1998). The oncogenic capacity of HRX-ENL requires the transcriptional transactivation activity of ENL and the DNA binding motifs of HRX. Mol Cell Biol *18*, 122-129.

So, C.W., Karsunky, H., Wong, P., Weissman, I.L., and Cleary, M.L. (2004). Leukemic transformation of hematopoietic progenitors by MLL-GAS7 in the absence of Hoxa7 or Hoxa9. Blood *103*, 3192-3199.

So, C.W., Lin, M., Ayton, P.M., Chen, E.H., and Cleary, M.L. (2003). Dimerization contributes to oncogenic activation of MLL chimeras in acute leukemias. Cancer cell *4*, 99-110.

Sobhian, B., Laguette, N., Yatim, A., Nakamura, M., Levy, Y., Kiernan, R., and Benkirane, M. (2010). HIV-1 Tat assembles a multifunctional transcription elongation complex and stably associates with the 7SK snRNP. Molecular cell *38*, 439-451.

Somervaille, T.C., Matheny, C.J., Spencer, G.J., Iwasaki, M., Rinn, J.L., Witten, D.M., Chang, H.Y., Shurtleff, S.A., Downing, J.R., and Cleary, M.L. (2009). Hierarchical maintenance of MLL myeloid leukemia stem cells employs a transcriptional program shared with embryonic rather than adult stem cells. Cell stem cell *4*, 129-140.

Srinivasan, R.S., de Erkenez, A.C., and Hemenway, C.S. (2003). The mixed lineage leukemia fusion partner AF9 binds specific isoforms of the BCL-6 corepressor. Oncogene *22*, 3395-3406.

Srinivasan, R.S., Nesbit, J.B., Marrero, L., Erfurth, F., LaRussa, V.F., and Hemenway, C.S. (2004a). The synthetic peptide PFWT disrupts AF4-AF9 protein complexes and induces apoptosis in t(4;11) leukemia cells. Leukemia : official journal of the Leukemia Society of America, Leukemia Research Fund, UK *18*, 1364-1372.

Srinivasan, R.S., Nesbit, J.B., Marrero, L., Erfurth, F., LaRussa, V.F., and Hemenway, C.S. (2004b). The synthetic peptide PFWT disrupts AF4-AF9 protein complexes and induces apoptosis in t(4;11) leukemia cells. Leukemia *18*, 1364-1372.

Stam, R.W., den Boer, M.L., Passier, M.M., Janka-Schaub, G.E., Sallan, S.E., Armstrong, S.A., and Pieters, R. (2006). Silencing of the tumor suppressor gene FHIT is highly characteristic for MLL gene rearranged infant acute lymphoblastic leukemia. Leukemia *20*, 264-271.

Strout, M.P., Marcucci, G., Bloomfield, C.D., and Caligiuri, M.A. (1998). The partial tandem duplication of ALL1 (MLL) is consistently generated by Alu-mediated homologous recombination in acute myeloid leukemia. Proc Natl Acad Sci U S A *95*, 2390-2395.

Stumpel, D.J., Schneider, P., van Roon, E.H., Boer, J.M., de Lorenzo, P., Valsecchi, M.G., de Menezes, R.X., Pieters, R., and Stam, R.W. (2009). Specific promoter methylation identifies different subgroups of MLL-rearranged infant acute lymphoblastic leukemia, influences clinical outcome, and provides therapeutic options. Blood *114*, 5490-5498.

Stumpel, D.J., Schotte, D., Lange-Turenhout, E.A., Schneider, P., Seslija, L., de Menezes, R.X., Marquez, V.E., Pieters, R., den Boer, M.L., and Stam, R.W. (2011). Hypermethylation of specific microRNA genes in MLL-rearranged infant acute lymphoblastic leukemia: major matters at a micro scale. Leukemia *25*, 429-439.

Super, H.J., McCabe, N.R., Thirman, M.J., Larson, R.A., Le Beau, M.M., Pedersen-Bjergaard, J., Philip, P., Diaz, M.O., and Rowley, J.D. (1993). Rearrangements of the MLL gene in therapy-related acute myeloid leukemia in patients previously treated with agents targeting DNA-topoisomerase II. Blood *82*, 3705-3711.

Takacova, S., Slany, R., Bartkova, J., Stranecky, V., Dolezel, P., Luzna, P., Bartek, J., and Divoky, V. (2012). DNA damage response and inflammatory signaling limit the MLL-ENL-induced leukemogenesis in vivo. Cancer cell *21*, 517-531.

Takahashi, H., Parmely, T.J., Sato, S., Tomomori-Sato, C., Banks, C.A., Kong, S.E., Szutorisz, H., Swanson, S.K., Martin-Brown, S., Washburn, M.P.*, et al.* (2011). Human mediator subunit MED26 functions as a docking site for transcription elongation factors. Cell *146*, 92-104.

Takeda, S., Chen, D.Y., Westergard, T.D., Fisher, J.K., Rubens, J.A., Sasagawa, S., Kan, J.T., Korsmeyer, S.J., Cheng, E.H., and Hsieh, J.J. (2006). Proteolysis of MLL family proteins is essential for taspase1-orchestrated cell cycle progression. Genes Dev *20*, 2397-2409.

Taki, T., Kano, H., Taniwaki, M., Sako, M., Yanagisawa, M., and Hayashi, Y. (1999). AF5q31, a newly identified AF4-related gene, is fused to MLL in infant acute lymphoblastic leukemia with ins(5;11)(q31;q13q23). Proc Natl Acad Sci U S A *96*, 14535-14540.

Tamai, H., Miyake, K., Takatori, M., Miyake, N., Yamaguchi, H., Dan, K., Shimada, T., and Inokuchi, K. (2011). Activated K-Ras protein accelerates human MLL/AF4-induced leukemo-lymphomogenicity in a transgenic mouse model. Leukemia *25*, 888-891.

Tan, J., Jones, M., Koseki, H., Nakayama, M., Muntean, A.G., Maillard, I., and Hess, J.L. (2011). CBX8, a polycomb group protein, is essential for MLL-AF9-induced leukemogenesis. Cancer cell *20*, 563-575.

Tanaka, S., Miyagi, S., Sashida, G., Chiba, T., Yuan, J., Mochizuki-Kashio, M., Suzuki, Y., Sugano, S., Nakaseko, C., Yokote, K.*, et al.* (2012). Ezh2 augments leukemogenicity by reinforcing differentiation blockage in acute myeloid leukemia. Blood *120*, 1107-1117.

Trotman, L.C., Wang, X., Alimonti, A., Chen, Z., Teruya-Feldstein, J., Yang, H., Pavletich, N.P., Carver, B.S., Cordon-Cardo, C., Erdjument-Bromage, H.*, et al.* (2007). Ubiquitination regulates PTEN nuclear import and tumor suppression. Cell *128*, 141-156.

Tunnemann, G., Martin, R.M., Haupt, S., Patsch, C., Edenhofer, F., and Cardoso, M.C. (2006). Cargo-dependent mode of uptake and bioavailability of TAT-containing proteins and peptides in living cells. FASEB journal : official publication of the Federation of American Societies for Experimental Biology *20*, 1775-1784.

Tyagi, S., Chabes, A.L., Wysocka, J., and Herr, W. (2007). E2F activation of S phase promoters via association with HCF-1 and the MLL family of histone H3K4 methyltransferases. Mol Cell *27*, 107-119.

Vasquez, K.O., Casavant, C., and Peterson, J.D. (2011). Quantitative whole body biodistribution of fluorescent-labeled agents by non-invasive tomographic imaging. PloS one *6*, e20594.

Vegt, E., de Jong, M., Wetzels, J.F., Masereeuw, R., Melis, M., Oyen, W.J., Gotthardt, M., and Boerman, O.C. (2010). Renal toxicity of radiolabeled peptides and antibody fragments: mechanisms, impact on radionuclide therapy, and strategies for prevention. Journal of nuclear medicine : official publication, Society of Nuclear Medicine *51*, 1049-1058.

von Bergh, A.R., Beverloo, H.B., Rombout, P., van Wering, E.R., van Weel, M.H., Beverstock, G.C., Kluin, P.M., Slater, R.M., and Schuuring, E. (2002). LAF4, an AF4-related gene, is fused to MLL in infant acute lymphoblastic leukemia. Genes, chromosomes & cancer *35*, 92-96.

Wang, J., Muntean, A.G., and Hess, J.L. (2012a). ECSASB2 mediates MLL degradation during hematopoietic differentiation. Blood *119*, 1151-1161.

Wang, J., Muntean, A.G., Wu, L., and Hess, J.L. (2012b). A subset of mixed lineage leukemia proteins has plant homeodomain (PHD)-mediated E3 ligase activity. J Biol Chem *287*, 43410-43416.

Wang, Q.F., Wu, G., Mi, S., He, F., Wu, J., Dong, J., Luo, R.T., Mattison, R., Kaberlein, J.J., Prabhakar, S.*, et al.* (2011). MLL fusion proteins preferentially regulate a subset of wild-type MLL target genes in the leukemic genome. Blood *117*, 6895-6905.

Wang, X., and Hayes, J.J. (2008). Acetylation mimics within individual core histone tail domains indicate distinct roles in regulating the stability of higher-order chromatin structure. Mol Cell Biol *28*, 227-236.

Wang, Z., Song, J., Milne, T.A., Wang, G.G., Li, H., Allis, C.D., and Patel, D.J. (2010). Pro isomerization in MLL1 PHD3-bromo cassette connects H3K4me readout to CyP33 and HDAC-mediated repression. Cell *141*, 1183-1194.

Wanger, M., Keiser, T., Neuhaus, J.M., and Wegner, A. (1985). The actin treadmill. Canadian journal of biochemistry and cell biology = Revue canadienne de biochimie et biologie cellulaire *63*, 414-421.

Watson, V.G., Drake, K.M., Peng, Y., and Napper, A.D. (2013). Development of a high-throughput screening-compatible assay for the discovery of inhibitors of the AF4-AF9 interaction using AlphaScreen technology. Assay and drug development technologies *11*, 253-268.

Welch, M.D., and Drubin, D.G. (1994). A nuclear protein with sequence similarity to proteins implicated in human acute leukemias is important for cellular morphogenesis and actin cytoskeletal function in Saccharomyces cerevisiae. Molecular biology of the cell *5*, 617-632.

Welch, M.D., Vinh, D.B., Okamura, H.H., and Drubin, D.G. (1993). Screens for extragenic mutations that fail to complement act1 alleles identify genes that are important for actin function in Saccharomyces cerevisiae. Genetics *135*, 265-274.

Wells, L., and Hart, G.W. (2003). O-GlcNAc turns twenty: functional implications for post-translational modification of nuclear and cytosolic proteins with a sugar. FEBS letters *546*, 154-158.

White, S.R., Williams, P., Wojcik, K.R., Sun, S., Hiemstra, P.S., Rabe, K.F., and Dorscheid, D.R. (2001). Initiation of apoptosis by actin cytoskeletal derangement in human airway epithelial cells. American journal of respiratory cell and molecular biology *24*, 282-294.

Wilson, M.D., Harreman, M., and Svejstrup, J.Q. (2013). Ubiquitylation and degradation of elongating RNA polymerase II: the last resort. Biochimica et biophysica acta *1829*, 151-157.

Wittwer, F., van der Straten, A., Keleman, K., Dickson, B.J., and Hafen, E. (2001). Lilliputian: an AF4/FMR2-related protein that controls cell identity and cell growth. Development *128*, 791-800.

Wong, P., Iwasaki, M., Somervaille, T.C., So, C.W., and Cleary, M.L. (2007). Meis1 is an essential and rate-limiting regulator of MLL leukemia stem cell potential. Genes Dev *21*, 2762-2774.

Wu, H., Chen, L., Zhou, Q., and Zhang, W. (2011). AF17 facilitates Dot1a nuclear export and upregulates ENaC-mediated Na+ transport in renal collecting duct cells. PloS one *6*, e27429.

Wu, X., Yoo, Y., Okuhama, N.N., Tucker, P.W., Liu, G., and Guan, J.L. (2006). Regulation of RNA-polymerase-II-dependent transcription by N-WASP and its nuclear-binding partners. Nature cell biology *8*, 756-763.

Wulf, E., Deboben, A., Bautz, F.A., Faulstich, H., and Wieland, T. (1979). Fluorescent phallotoxin, a tool for the visualization of cellular actin. Proc Natl Acad Sci U S A *76*, 4498-4502.

Wysocka, J., Swigut, T., Milne, T.A., Dou, Y., Zhang, X., Burlingame, A.L., Roeder, R.G., Brivanlou, A.H., and Allis, C.D. (2005). WDR5 associates with histone H3 methylated at K4 and is essential for H3 K4 methylation and vertebrate development. Cell *121*, 859-872.

Xia, Z.B., Anderson, M., Diaz, M.O., and Zeleznik-Le, N.J. (2003). MLL repression domain interacts with histone deacetylases, the polycomb group proteins HPC2 and BMI-1, and the corepressor C-terminal-binding protein. Proc Natl Acad Sci U S A *100*, 8342-8347.

Xia, Z.B., Popovic, R., Chen, J., Theisler, C., Stuart, T., Santillan, D.A., Erfurth, F., Diaz, M.O., and Zeleznik-Le, N.J. (2005). The MLL fusion gene, MLL-AF4, regulates cyclin-dependent kinase inhibitor CDKN1B (p27kip1) expression. Proc Natl Acad Sci U S A *102*, 14028-14033.

Yang, Z., Yik, J.H., Chen, R., He, N., Jang, M.K., Ozato, K., and Zhou, Q. (2005). Recruitment of P-TEFb for stimulation of transcriptional elongation by the bromodomain protein Brd4. Mol Cell *19*, 535-545.

Yarmola, E.G., Somasundaram, T., Boring, T.A., Spector, I., and Bubb, M.R. (2000). Actin-latrunculin A structure and function. Differential modulation of actin-binding protein function by latrunculin A. J Biol Chem *275*, 28120-28127.

Yeager, A.M., Kaizer, H., Santos, G.W., Saral, R., Colvin, O.M., Stuart, R.K., Braine, H.G., Burke, P.J., Ambinder, R.F., Burns, W.H.*, et al.* (1986). Autologous bone marrow transplantation in patients with acute nonlymphocytic leukemia, using ex vivo marrow treatment with 4-hydroperoxycyclophosphamide. The New England journal of medicine *315*, 141-147.

Yeoh, E.J., Ross, M.E., Shurtleff, S.A., Williams, W.K., Patel, D., Mahfouz, R., Behm, F.G., Raimondi, S.C., Relling, M.V., Patel, A.*, et al.* (2002). Classification,

subtype discovery, and prediction of outcome in pediatric acute lymphoblastic leukemia by gene expression profiling. Cancer cell *1*, 133-143.

Yokoyama, A., and Cleary, M.L. (2008). Menin critically links MLL proteins with LEDGF on cancer-associated target genes. Cancer cell *14*, 36-46.

Yokoyama, A., Ficara, F., Murphy, M.J., Meisel, C., Naresh, A., Kitabayashi, I., and Cleary, M.L. (2011). Proteolytically cleaved MLL subunits are susceptible to distinct degradation pathways. Journal of cell science *124*, 2208-2219.

Yokoyama, A., Lin, M., Naresh, A., Kitabayashi, I., and Cleary, M.L. (2010). A higher-order complex containing AF4 and ENL family proteins with P-TEFb facilitates oncogenic and physiologic MLL-dependent transcription. Cancer cell *17*, 198-212.

Yokoyama, A., Somervaille, T.C., Smith, K.S., Rozenblatt-Rosen, O., Meyerson, M., and Cleary, M.L. (2005). The menin tumor suppressor protein is an essential oncogenic cofactor for MLL-associated leukemogenesis. Cell *123*, 207-218.

Yokoyama, A., Wang, Z., Wysocka, J., Sanyal, M., Aufiero, D.J., Kitabayashi, I., Herr, W., and Cleary, M.L. (2004). Leukemia proto-oncoprotein MLL forms a SET1-like histone methyltransferase complex with menin to regulate Hox gene expression. Mol Cell Biol *24*, 5639-5649.

Yu, B.D., Hanson, R.D., Hess, J.L., Horning, S.E., and Korsmeyer, S.J. (1998). MLL, a mammalian trithorax-group gene, functions as a transcriptional maintenance factor in morphogenesis. Proc Natl Acad Sci U S A *95*, 10632-10636.

Yu, B.D., Hess, J.L., Horning, S.E., Brown, G.A., and Korsmeyer, S.J. (1995). Altered Hox expression and segmental identity in Mll-mutant mice. Nature *378*, 505-508.

Yu, X.F., Yang, C., Liang, L.H., Liu, B., Zhou, B., Li, B., and Han, Z.C. (2006). Inhibition of human leukemia xenograft in nude mice by adenovirus-mediated tissue inhibitor of metalloproteinase-3. Leukemia *20*, 1-8.

Zeisig, B.B., Milne, T., Garcia-Cuellar, M.P., Schreiner, S., Martin, M.E., Fuchs, U., Borkhardt, A., Chanda, S.K., Walker, J., Soden, R.*, et al.* (2004a). Hoxa9 and Meis1 are key targets for MLL-ENL-mediated cellular immortalization. Molecular and cellular biology *24*, 617-628.

Zeisig, B.B., Milne, T., Garcia-Cuellar, M.P., Schreiner, S., Martin, M.E., Fuchs, U., Borkhardt, A., Chanda, S.K., Walker, J., Soden, R*., et al.* (2004b). Hoxa9 and Meis1 are key targets for MLL-ENL-mediated cellular immortalization. Mol Cell Biol *24*, 617-628.

Zhang, H., Luo, J., Li, Y., Henderson, P.T., Wang, Y., Wachsmann-Hogiu, S., Zhao, W., Lam, K.S., and Pan, C.X. (2012). Characterization of high-affinity peptides and their feasibility for use in nanotherapeutics targeting leukemia stem cells. Nanomedicine : nanotechnology, biology, and medicine *8*, 1116-1124.

Zhang, W., Xia, X., Reisenauer, M.R., Hemenway, C.S., and Kone, B.C. (2006). Dot1a-AF9 complex mediates histone H3 Lys-79 hypermethylation and repression of ENaCalpha in an aldosterone-sensitive manner. J Biol Chem *281*, 18059-18068.

Zhang, W., Xia, X., Reisenauer, M.R., Rieg, T., Lang, F., Kuhl, D., Vallon, V., and Kone, B.C. (2007). Aldosterone-induced Sgk1 relieves Dot1a-Af9-mediated transcriptional repression of epithelial Na+ channel alpha. The Journal of clinical investigation *117*, 773-783.

Zhang, W., Yu, Z., Wu, H., Chen, L., Kong, Q., and Kone, B.C. (2013). An Af9 cis-element directly targets Dot1a to mediate transcriptional repression of the alphaENaC gene. American journal of physiology Renal physiology *304*, F367-375.

Ziemin-van der Poel, S., McCabe, N.R., Gill, H.J., Espinosa, R., 3rd, Patel, Y., Harden, A., Rubinelli, P., Smith, S.D., LeBeau, M.M., Rowley, J.D*., et al.* (1991). Identification of a gene, MLL, that spans the breakpoint in 11q23 translocations associated with human leukemias. Proc Natl Acad Sci U S A *88*, 10735-10739.

Zuber, J., Shi, J., Wang, E., Rappaport, A.R., Herrmann, H., Sison, E.A., Magoon, D., Qi, J., Blatt, K., Wunderlich, M*., et al.* (2011). RNAi screen identifies Brd4 as a therapeutic target in acute myeloid leukaemia. Nature *478*, 524-528.

VITA

The author, Nisha Barretto, was born in Ahmedabad, Gujarat, India to Elizabeth and Nelson Barretto. She has a younger sister Nituna Barretto. She currently resides in Forest Park, Illinois with her husband Gordon Mendonsa.

She received a Bachelor of Science in Biochemistry from Gujarat University (Gujarat, India) in July of 2002 and graduated at the top of her class with Master of Science in Biotechnology from Gujarat University in June of 2004. Soon after graduating, she began work as a BioBulk Production Officer at Intas Biopharmaceuticals Ltd, India. Later, she also served as an instructor in the Biotechnology program at St. Xaviers College, Ahmedabad.

In August of 2007, Nisha joined the Department of Molecular and Cellular Biochemistry at Loyola University Medical Center (Maywood, IL). Shortly thereafter, she joined the laboratory of Dr. Charles Hemenway, where she studied the *in vitro* and in *vivo* effects of the AF4 mimetic peptide, as a possible therapeutic for MLL leukemias. In 2012 she received the Graduate Research Mentoring Award that provided the opportunity to mentor an undergraduate student. In addition, she has also served as a research mentor for summer students and medical residents.

After completing her Ph.D., Nisha intends to pursue research and teaching in the field of oncology